

DYNAMICS AND COEXISTENCE OF MICROBIAL MIXED CULTURES

Thesis by

Brian Henry Davison

In Partial Fulfillment of the Requirements
for the Degree of
Doctor of Philosophy

California Institute of Technology
Pasadena, California

1985

(Submitted March 27, 1985)

• 1985

Brian H. Davison

All Rights Reserved

iii.

Dedicated to all those who have fed me —physically, emotionally and
spiritually, in particular, Mom and Dad, who were first.

An observation:

when I tell laypeople that I am a biochemical engineer
working on the Coexistence of Competing Mixed Cultures,

I have generally gotten one of two responses:

- (1) *Is this going to help people live more peacefully?*
- (2) *Do you make new bugs for germ and chemical warfare?*

This points out our responsibility beyond our research to
educate and protect our fellow man and world.

Acknowledgments

First I must thank Dr. Greg Stephanopoulos for his support, accessibility, inspiration, and the freedom and responsibility he gave me. Through him, I am grateful for the partial financial support of the NSF. My fellow Stephanopoulites (Ron, Nam, and especially Kai Yiu) were invaluable for checking on my reactors for malfunctions, allowing me to survive month-long experiments, and for input on my projects. The typing skills of Kathy and Jan were appreciated in this work.

A special thanks goes to Dr. Bailey and his group (in particular, Martin, Ken, and Pauline) for use of equipment and valuable mutualistic interactions.

Caltech's summer support of four undergraduates (particularly, Dorian and Greg) through the SURF Program was invaluable.

In addition, many made this a good place to work by listening and offering support, jokes, and suggestions including Teri, Murray, Dinah, and Puvín - my officemate for five years. My roommates Carl, Doug, Mike and Phil helped me form a niche to call home. Finally, a praise is made to those truest friends who never doubted: Kathy, John and my parents, Mary Lou and John.

ABSTRACT

Various methods of establishing a persistent mixed culture were examined in continuous culture. A well-defined system consisting of *Escherichia coli* and *Saccharomyces cerevisiae* was used. The primary interaction was competition for glucose, the rate limiting nutrient. When this was the only interaction no coexistence is possible in a well mixed fermentor at constant conditions (i.e., a chemostat).

The two microorganisms while competing for glucose were maintained in a stable cycle of coexistence by alternating the growth advantage between the two organisms by oscillating the pH in a chemostat. Pure culture experiments found *Scerevisiae* to be insensitive to pH between 5 and 4.3 with a maximum specific growth rate (U_{max}) of 0.4/hr; while U_{max} of *E.coli* decreased from 0.6/hr at pH 5 to 0.1/hr at pH 4.3. Steady state and crossinoculation chemostat runs at a dilution rate of 0.17/hr confirmed the expectation that the mixed culture system is unstable at constant pH with *E.coli* dominating at pH 5 and *Scerevisiae* dominating at pH 4.3. Three pH oscillation experiments were performed at $D=0.17/hr$ with 1 gm/l glucose feed. The 16 hr/16 hr cycle was stable for six periods with a stable alternating cycle of *E.coli* and *S. cerevisiae* being quickly established. A 18 hr pH5./14 hr pH4.3 cycle was found to be stable with smaller yeast concentrations. A 6hr/6hr cycle was found unstable with yeast washout. Simulation results were compared with these runs and were used to predict the onset of instability. Oscillations of pH can force stable persistence of a competing mixed culture that is otherwise unstable. Thus time varying conditions are experimentally demonstrated to be one explanation for competitive coexistence.

A mixed culture of *Saccharomyces cerevisiae* and *Escherichia coli* was esta-

blished in a stable coexistence steady state in a chemostat under constant operating conditions at higher feed concentrations. The species competed for glucose, the growth limiting resource, and produced acetate and ethanol. The acetic acid was shown to be very inhibitory to *E. coli* in pure culture at pH 5 while ethanol inhibition was only marginal. No significant inhibition of *S. cerevisiae* growth was observed by either acetate or ethanol. Pure culture parameters were measured and used in the analysis. Linearized stability analysis for the case when both organisms produce the inhibitor showed that a transition through three stable outcomes was possible as the feed concentration is lowered. Experimental studies verified these predictions and successive transitions from a yeast growth steady state, to a coexistence steady state, and to a *E. coli* growth steady state were obtained by lowering the glucose concentration in the feed from 10 to 5 to 2.5 g/l. This dynamic behavior is distinctly different from other competition-inhibition combinations and demonstrates for the first time that coexistence is possible due to substrate competition and product inhibition.

A bioreactor with simultaneous fermentation and cell recycle was investigated. The reactor consisted of a typical fermentor and an attached inclined side-arm that allowed enhanced sedimentation. Due to the enhanced sedimentation in the side-arm settler the cells precipitate quickly and flow back into the reactor. A virtually cell free broth can be withdrawn through the side-arm while maintaining both a high flowrate and a high cell density. Continuous fermentations with *Scerevisiae* demonstrated these features and the possibility of high cell densities at flowrates that ordinarily would lead to washout. Ethanol productivities and yields were high. Increased resistance to contamination was feasible and tested using *E.coli* as the model contaminant.

This new reactor with size-selective properties was found to allow a coexistent mixed culture of *Escherichia coli* and *Saccharomyces cerevisiae*. The larger yeast population was retained and recycled at high efficiencies, while the smaller yet faster growing bacteria were removed preferentially through the side-arm. Stability analysis indicated that the coexistence of this system could be stable only if the yeast removal rate as a function of biomass was concave up. This would occur if growth continued in the side-arm. Another experimental system was devised to measure this removal rate function. A negative removal rate (i.e., a net addition of yeast to the fermentor) was observed at low biomass indicating growth in the settler and explaining the stability of the coexistence steady state.

A mixed culture, that was unstable during pure competition under constant well-mixed conditions as expressed in the Competitive Exclusion Principle, was made to persist indefinitely by the use of time-varying conditions (such as pH oscillations), or the addition of other interactions (such as inhibition), or the design of spatially nonuniform reactors (such as the side-arm settler).

Table of Contents

Acknowledgments	iv
Abstract	v
List of Tables	ix
List of Figures	ix
Chapter 1. Introduction	1
References	5
Chapter 2. Effect of pH Oscillations on a Competing Mixed Culture	6
References	27
Figures	29
Chapter 3. Coexistence of <i>S. cerevisiae</i> and <i>E. coli</i> in a Chemostat under Substrate Competition and Product Inhibition	44
References	66
Figures	69
Chapter 4. A Novel Bioreactor-Cell Precipitation Combination for High Cell Density, High Flow Fermentations	94
References	117
Figures	120
Chapter 5. Coexistence in a Recycle Reactor with Size Selective Properties	128
Figures	146
Chapter 6. Cross-Dominance and Dilution Rate in Two Mixed Culture Pairs	153
References	167
Figures	172
Chapter 7. Conclusions and Future Work	176
Appendices	
A. Coulter Counter Programs and Calibration Equations	179
B. Floquet Analysis	190
C. Additional pH Oscillation Simulations	191
D. Calibration of yeast Dry Weight vs O.D.	193
E. Observations of the Continuous Settler	194

List of Tables

Chapter 2

Table 1.	Coulter Counter Settings.	15
Table 2.	Monod Growth Constants: Estimates for Simulation.	22

Chapter 3.

Table 1.	Kinetic Parameters from Pure Culture Experiments.	68
Table 2.	Stability Results: Summary of Runs.	68

Chapter 4

Table 1.	Media	118
Table 2.	Results of High-feed, High-retention, and High-conversion Experiments.	119

Chapter 6.

Table 1.	Monod Growth Constants from Literature.	159
Table 2.	Summary of Batch Experiments.	168
Table 3.	Summary of Preliminary Continuous Experiments.	170

List of Figure Captions

Chapter 2

Figure 1. Operating Diagrams for a Chemostat in which Two Populations Compete for a Rate-Limiting Substrate.	30
Figure 2a. Particle Size Distribution for <i>E. coli</i>	31
Figure 2b. Particle Size Distribution for <i>S. cerevisiae</i>	32
Figure 3. Maximum Specific Growth Rate vs. pH for <i>E. coli</i> and <i>S. cerevisiae</i> on 1 g/l glucose.	33
Figure 4. Effect of Products on the Maximum Specific Growth Rate on glucose - Inhibition of <i>E. coli</i> by EtOH and of <i>S. cerevisiae</i> by Acetate.	34
Figure 5. Specific growth rate as a function of glucose for <i>E. coli</i> at pH 4.3, 4.5, and 5.0 and for <i>S. cerevisiae</i> .	35
Figure 6. pH Oscillation Experiment - 16 hr. pH5/ 16 hr. pH4.3 - Demonstration of Stability 6a. Cell Number of <i>E. coli</i> and <i>S. cerevisiae</i> 6b. Glucose concentration	36
Figure 7. pH Oscillation Experiment - 18 hr. pH5/ 14 hr. pH4.3 - Demonstration of Stability at Different Cycle Ratio 7a. Cell Number of <i>E. coli</i> and <i>S. cerevisiae</i> 7b. Glucose concentration	38
Figure 8. pH Oscillation Experiment - 16 hr. pH5/ 16 hr. pH4.3 changed to 6 hr pH5/ 6 hr. pH4.3 - Shortened Cycle Period is Unstable 8a. Cell Number of <i>E. coli</i> and <i>S. cerevisiae</i> 8b. Glucose concentration	40
Figure 9. pH Oscillation Computer Simulation - 16 hr. pH5/ 16 hr. pH4.3 - 9a. <i>S. cerevisiae</i> 9b. <i>E. coli</i> 9c. Glucose concentration	42

Chapter 3

Figure 1. Inhibition by Acetic acid of μ_{\max} of <i>S. cerevisiae</i> on 1 g/l glucose at pH 5.	72
Figure 2. Inhibition by ethanol of μ_{\max} of <i>E. coli</i> on 1 g/l glucose at pH 5 and at pH 4.5.	73
Figure 3. Specific growth rate of <i>E. coli</i> in the presence of excess glucose at pH 5 as a function of acetic acid concentration.	74
Figure 4. System of all possible interactions of two species, one substrate and two inhibitory products.	75
Figure 5. Subcases of Fig. 4, theoretically examined by DeFreitas et al. [1978]. 5a. Specific Autoinhibition, 5b. Specific Cross Inhibition.	75
Figure 6. Possible important interactions for <i>E. coli</i> , x_1 , and <i>S. cerevisiae</i> , x_2 .	76

Figure 7. Stability diagrams showing the stable outcomes for different regions of the operating conditions (D , s_f). All figures include the curves $\mu_1(s_f, 0, 0)$ — and $\mu_2(s_f)$ -----.	77
Figure 7a. Stability diagram - only ethanol inhibition is considered, acetate production is neglected.	77
Figure 7b. Stability diagram - only acetate production by <i>E. coli</i> is considered, ethanol and acetate production by <i>S. cerevisiae</i> is neglected.	78
Figure 7c. Stability diagram - acetate production by both <i>E. coli</i> and <i>S. cerevisiae</i> is considered, ethanol production by <i>S. cerevisiae</i> is neglected.	79
Figure 8. Schematics of phase plane diagrams of x_1 vs. x_2 showing three possible outcomes for dual initial trajectory tests and the steady state stability required for each. ● denotes a stable P.W.S.S., ○ denotes an unstable P.W.S.S..	80
Figure 9. Run A1: pure culture S.S. of <i>S. cerevisiae</i> perturbed with <i>E. coli</i> at $D=0.31/\text{hr}$ and $s_f = 10 \text{ g/l}$.	81
Figure 10. Run A2: pure culture S.S. of <i>S. cerevisiae</i> perturbed with <i>E. coli</i> at $D=0.31/\text{hr}$ and $s_f = 10 \text{ g/l}$.	82
Figure 11. Run B1: pure culture S.S. of <i>E. coli</i> perturbed with <i>S. cerevisiae</i> at $D=0.31/\text{hr}$ and $s_f = 10 \text{ g/l}$.	83
Figure 12. Run A3: pure culture S.S. of <i>E. coli</i> perturbed with <i>S. cerevisiae</i> at $D=0.37/\text{hr}$ and $s_f = 5 \text{ g/l}$.	84
Figure 13. Run B2: pure culture S.S. of <i>S. cerevisiae</i> perturbed with <i>E. coli</i> at $D=0.37/\text{hr}$ and $s_f = 5 \text{ g/l}$.	85
Figure 14. Run A4: pure culture S.S. of <i>E. coli</i> perturbed with <i>S. cerevisiae</i> at $D=0.34/\text{hr}$ and $s_f = 5 \text{ g/l}$.	86
Figure 15. Run B3: pure culture S.S. of <i>S. cerevisiae</i> perturbed with <i>E. coli</i> at $D=0.34/\text{hr}$ and $s_f = 5 \text{ g/l}$.	87
Figure 16. Run B4: pure culture S.S. of <i>S. cerevisiae</i> perturbed with <i>E. coli</i> at $D=0.34/\text{hr}$ and $s_f = 2.5 \text{ g/l}$.	88
Figure 17. Run B5: pure culture S.S. of <i>S. cerevisiae</i> perturbed with <i>E. coli</i> at $D=0.34/\text{hr}$ and $s_f = 2.5 \text{ g/l}$.	89
Figure 18. Run B6: pure culture S.S. of <i>S. cerevisiae</i> perturbed with <i>E. coli</i> at $D=0.20/\text{hr}$ and $s_f = 2.5 \text{ g/l}$.	90
Figure 19. Phase Plane of Runs A1, A2, and B1. (arrows denote temporal sequence of readings)	91
Figure 20. Phase Plane of Runs A4 and B3. (arrows denote temporal sequence of readings)	92

Figure 21. Phase Plane of Run B6. (arrows denote temporal sequence of readings)	93
---	----

Chapter 4

Figure 1. Schematic illustration of the phenomenon of enhanced sedimentation.	121
Figure 2. Schematic of the new fermentor design for facilitated cell precipitation and recycle.	122
Figure 3. Experimental Determination of the Stokes velocity of <i>S. cerevisiae</i> cells.	123
Figure 4. Top view of the settler part of the fermentor of Fig. 2.	124
Figure 5. Steady State cell size distributions at the entrance and exit streams of the settler for varying flowrates.	125
Figure 6. Steady State cell densities and product concentrations for the fermentor-precipitator combination as functions of the reactor dilution rate. (●, ▲: biomass, ethanol conc. for $D_p=0.4/\text{hr}$; ○, △: biomass, ethanol conc. for $D_p=0.0/\text{hr}$; $s_f=5$ g/l glucose). $D_p=0$ is an ordinary chemostat.	126
Figure 7. Washout of the smaller-size population from a mixed culture of <i>E. coli</i> and <i>S. cerevisiae</i> occurs at high flow rates. $D_T=0.89/\text{hr}$, $D_p=0.48/\text{hr}$ and $s_f=5$ g/l.	127

Chapter 5.

Figure 1. Schematic of the new reactor design for facilitated cell precipitation and recycle. Reactor also contains probes for pH and temperature with controllers attached to a KOH addition line and a heater.	147
Figure 2. Coexistence at moderate D_R of <i>E. coli</i> and <i>S. cerevisiae</i> with 5 g/l glucose feed, $D_T=0.33/\text{hr}$ and $D_p=0.23/\text{hr}$. Fig. 2a High initial <i>E. coli</i> . Fig. 2b Low initial <i>E. coli</i> .	148
Figure 3. Washout of <i>E. coli</i> at high flow, $D_T=0.89/\text{hr}$, $D_p=0.48/\text{hr}$, and $s_f=5$ g/l.	149
Figure 4. Possible curves for the Net Removal Rate, $f(x_R)$, from transport characteristics.	150
Figure 5. Possible curves for $f(x_R)$ if growth occurs.	150
Figure 6. Schematic of experimental apparatus to determine $f(x_R, Q_p)$.	151

Figure 7. Experimental Net Removal Rate, $f(x_R, Q_P)$.	152
--	-----

Chapter 6

Figure 1a. Typical Batch Run of <i>E. coli</i> - $\ln(\text{Abs})$ and Acetate	173
--	-----

Figure 1b. Typical Batch Run of <i>S. cerevisiae</i> - $\ln(\text{Abs})$ and EtOH	174
---	-----

Figure 2. Mixed Continuous Culture of <i>E. coli</i> and <i>S. cerevisiae</i> at pH 4.3 and various D.	175
--	-----

Appendix

Appendix C. Additional pH Oscillation Simulations: 18 hr pH5/14 hr pH4.3.	191
---	-----

Appendix D. Calibration of yeast Dry Weight vs O.D.	193
---	-----

Appendix E. Continuous Settler: Length of clarified Zone as a Function of Q_P .	194
---	-----

1.

Chapter 1.

Introduction

INTRODUCTION

When microbial pure culture techniques were first developed a century ago, they opened new avenues for isolating and identifying many processes of individual species. Eventually, with this increased knowledge, attempts were begun particularly in the fields of wastewater treatment and ecology to go back and analyze the complex mixed systems from where all pure cultures were derived. For simplicity, most interest has been on simple competition: two populations compete for one resource which is rate-limiting to both. Gause's [1934] demand for analytic study of microbial growth and Monod's [1942] pure culture experiments were combined by Powell [1958] into a theory of competition. Early work on growth in chemostats led to the competitive exclusion principle [1960], which states that, for two populations competing for a nutrient, one population will dominate. With the advent of increased interest by chemical engineers in biological systems, valuable skills of mathematical modeling of kinetics and dynamics were promised to be joined to the biologists' observational expertise. The majority of this first generation of engineering efforts into mixed cultures were theoretical constructs indicating the possibility of many interesting behaviors including coexistence and sustained oscillations while biologists continued observations of selection in the environment. These studies supported Hardin's Competitive Exclusion Principle[1960] that one species will dominate provided that the reactor operates under conditions of spatial uniformity and time invariant inputs. Reviews of the status of mixed culture research are available [Fredrickson, 1977; Harder et al., 1977; Bungay et al., 1980; Veldkamp et al., 1972].

Still it was noted that each stable environmental niche theoretically required at least one interacting substance. But even these could not fully explain the great sustained diversity of the natural environment. From these

3.

considerations, Hutchinson [1961] stated what is known as the 'plankton paradox' or that many apparently stable natural systems can consist of a large number of species competing for a definitely smaller number of nutrients. In addition, experimentation was needed to test, confirm, and elucidate

the interactions in a real system. Considerations of microbial ecology aside, the new field of biotechnology, while still focused on pure culture, has spurred interest in mixed continuous cultures. The ability to predict, a priori, and understand the stability of a mixed culture can lead to establishing the desired stability. This could be a powerful tool, whether considering contamination where washout of the contaminant is desired, or a synergistic process requiring a stable mixed culture, or the maintainence of plasmid containing cell against the wild type revertants.

My thesis focused on various methods of establishing a persistent mixed culture in continuous culture. A well-defined system consisting of *Escherichia coli* and *Saccharomyces cerevisiae* was used. The primary interaction was competition for glucose, the rate limiting nutrient. It was demonstrated that, when this was the only interaction, no coexistence is possible in a well-mixed fermentor at constant conditions (i.e. a chemostat). The approach was to examine the result of removing these constraints experimentally one at a time and to develop and use theory and simulations to explain and justify the observed results.

In Chapter 2 the assumption of constant conditions was removed. Certain pH oscillations were found to give stable cycles of the two populations by alternating the advantage between the two species. These experimental results were compared to a simulation and its Floquet stability analysis.

Next another interaction, namely product inhibition, was added to substrate competition by increasing the feed concentration. In a constant well-mixed

reactor, three different stable outcomes were found when the feed concentration was increased and are reported in Chapter 3. The three outcomes were accurately predicted by using linearized stability analysis and the pure culture data to construct a stability diagram of dilution rate versus feed concentration.

A novel recycle bioreactor combines a chemostat with a side-arm for enhanced sedimentation. Preliminary results on its effectiveness for cell recycle, high cell densities and high productivity are presented in Chapter 4. Chapter 5 takes this reactor with its size-selective cell-retention properties (due to its two sections) and demonstrates that coexistence can occur since the distinct spatial regions within the reactor can be used to exploit the physical differences within the mixed culture. The theoretical stability requirements are justified by additional experimentation on another apparatus to measure the net yeast removal rate from the fermentor proper into the side-arm.

Chapter 6 elucidates some of the experimental difficulties encountered during this work with mixed cultures, notably the search for a good pair of organisms and the problem of species' adaptation.

From this work it can be shown that a mixed culture, which is unstable during pure competition under constant well-mixed conditions as expressed in the Competitive Exclusion Principle, can be made to persist indefinitely by the use of time-varying conditions (such as pH oscillations) or the addition of other interactions (such as inhibition), or the design of spatially nonuniform reactors (such as the side-arm settler).

REFERENCES

- Fredrickson, A.G. (1977). "The Behavior of Mixed Cultures of Microorganisms," *Ann. Rev. Microbiol.*, **31**, 63-87.
- Gause, G.F. (1934). **The Struggle for Existence**. Williams and Williams, Baltimore.
- Haas, C.N., H.R. Bungay, and M. L. Bungay (1981). "Practical Mixed Culture Processes," *Ann. Rep. on Ferment. Proc.*, **4**, 1-29.
- Harder, W., J.G. Kuenen, and A. Matin (1977). "A Review: Microbial Selection in Continuous Culture," *J. Appl. Bacteriol.*, **43**, 1-24.
- Hardin, G. (1960). *Science*, **131**, 1292.
- Hutchinson, G.E. (1961). *Am. Nat.*, **95**, 137.
- Monod, J. (1942). **Recherches sur la Croissance des Cultures Bacteriennes**. Paris, Hermann.
- Powell, E.O. (1958). "Criteria for the Growth of Contaminants and Mutants in Continuous Culture," *J. General Microbiology*, **18**, 259.
- Veldkamp, H., and H.W. Jannasch (1972). "Mixed Culture Studies with the Chemostat," *J. Appl. Chem. Biotechnol.*, **22**, 105-123.

Chapter 2.

Effect of pH Oscillations on a Competing Mixed Culture

originally presented at the AIChE Annual Meeting,

San Francisco, November, 1984.

SUMMARY

Two microorganisms, *E.coli* and *Scerevisiae* competing for glucose, were maintained in a stable cycle of coexistence by alternating the growth advantage between the two organisms by oscillating the pH in a chemostat. Pure culture experiments found *Scerevisiae* to be insensitive to pH between 5 and 4.3 with a maximum specific growth rate (μ_{max}) of 0.4/hr; while μ_{max} of *E.coli* decreased from 0.6/hr at pH 5 to 0.1/hr at pH 4.3. Steady state and cross-inoculation chemostat runs at a dilution rate of 0.17/hr confirmed the expectation that the mixed culture system is unstable at constant pH with *E.coli* dominating at pH 5 and *Scerevisiae* dominating at pH 4.3. Three pH oscillation experiments were performed at $D=0.17/\text{hr}$ with 1 gm/l glucose feed. The 16 hr/16 hr cycle was stable for six periods with a stable alternating cycle of *E.coli* and *S. cerevisiae* being quickly established. An 18 hr pH5/14 hr pH4.3 cycle was found to be stable with smaller yeast concentrations. A 6hr/6hr cycle was found unstable with yeast washout. Simulation results were compared with these runs and were used to predict the onset of instability. Oscillations of pH can force stable persistence of a competing mixed culture that is otherwise unstable. Thus, varying conditions are experimentally demonstrated to be one explanation for competitive coexistence.

INTRODUCTION

Mixed cultures of organisms are an area of increasing interest in biochemical engineering for several reasons. These systems are more versatile than pure cultures due to the largely increased gene pool. Mixed cultures can offer some important advantages such as higher yields, the ability to grow on simple carbon sources, and the mediation of some multistep chemical transformations. Furthermore, gaining insights into the behavior of mixed culture systems can improve our understanding of many phenomena in natural ecosystems as well as the outcome and control of contamination in pure cultures.

Currently only a few industrial processes involve mixed cultures, most notably waste water processing and manufacture of foods such as cheese. This is understandable as, once a useful organism has been identified, one is reluctant to allow other species to grow in the same production vessel. However, certain multistep transformations catalyzed by mixed cultures may require this attitude to be changed.

Other practical benefits could appear in sustaining unstable systems and in prolonging a desired strain despite competition. A current example is in the growth of recombinant microorganisms. They are mixed cultures of populations differing in the number of plasmid sites they contain. These populations will grow at different rates while competing for the rate-limiting nutrient. In continuous or in batch culture, the recombinant plasmid containing organisms may grow slower and be displaced by the revertant wild type. A better knowledge of mixed culture interactions may help find a strategy to help preserve such a "weaker" strain.

In the light of these possibilities it is useful to try to understand the dynamic behavior of mixed culture systems. At present little experimental work

has been performed, especially when compared to the preponderance of theoretical papers. Theoretical instabilities of continuous mixed cultures are known; but little is understood of how these translate into real systems with their additional operational and genetic instabilities. The interaction of mixed cultures needs more study in a detailed and organized form to test the theories and their limitations, since their behavior is not just the composite of the pure populations but depends on the nature and strength of the interactions.

The most common microbial interaction appears to be competition, alone or in combination with another interaction. Competition has been defined as that situation in which two populations use a resource and the resource has a dynamic effect on at least one of them [1]. Competition is total if every dynamic variable is a resource for every organism; partial, if it is not. When it is the only interaction present, competition is sometimes called "pure" competition to distinguish from competition plus another interaction.

For simplicity, most interest has been on simple competition: two populations compete for one resource which is rate-limiting to both. Gause's [2] demand for analytic study of microbial growth and Monod's [3] pure culture experiments were combined by Powell [4] into a theory of competition. Early work on growth in chemostats led to the competitive exclusion principle [5], which states that, for two populations competing for a nutrient, one population will dominate.

The apparatus used to verify this principle is a chemostat, essentially a well-mixed constant input reactor (CSTR). The dynamic equations for simple competition in a chemostat are well-known and are repeated here.

$$\dot{x} = -Dx + x\mu_1(s)$$

$$\dot{y} = -Dy + y\mu_2(s)$$

$$\dot{s} = D(s_I - s) - x\mu_1(s)/Y_1 - y\mu_2(s)/Y_2$$

Here x , y , and s are the concentrations of population 1, population 2, and the substrate respectively. Y is the yield coefficient and μ the specific growth rate for their respective populations. For simplicity of discussion the specific growth rate is assumed to be of Monod's form. The exact model of the specific growth rate is not important for the analysis. Only the mutual disposition of the two μ versus s curves is needed to determine the stability of the system [6].

For steady state in a chemostat the specific growth rate must equal the dilution rate. In simple competition at a constant dilution rate and constant conditions the population which grows faster at the lower steady state substrate level will eventually dominate the chemostat. When the substrate saturation curves do not cross, no coexistent steady state is possible and the faster growing species dominates (Fig. 1a). When they do cross (Fig. 1b), a coexistent steady state exists at the crosspoint (s_c , D_c). Theoretically if the dilution rate is fixed at D_c the populations should coexist. However, the steady state is metastable with respect to perturbations or even random noise [7], and this supports Hardin's Competitive Exclusion Principle[5] that one species will dominate provided that the reactor operates under conditions of spatial uniformity and time invariant inputs.

The Competitive Exclusion Principle has been used in chemostat studies to select for microorganisms favored at low substrate levels [8]. For cultures with crossing specific growth rate curves, experiments showed that the dilution rate

determined which species would dominate [9,10,11]. Harder and Veldkamp [12] demonstrated the varying effects of temperature and dilution rate on the dominance of obligate and facultative psychrophiles. Meers et al. [13] were able to change the dominating species by drastically altering the dilution rate during the course of a single experiment. Hansen and Hubbel [14] again confirmed the theory by predicting the dominance results from pure culture experiments. Yet when they used an additional inhibitor to make the steady state substrate levels of two *E. coli* mutants equal, the two mutants coexisted for the duration of the experiment.

For multiple populations competing for limited resources, stability analysis shows that coexistence is possible provided that the number of limiting substrates is greater than or equal to the number of species. Hutchinson [15], however, early observed that many apparently stable natural systems can consist of a large number of species competing for a definitely smaller number of nutrients. The common resolution of this paradox was to suggest relaxing the space and time constraints of the Competitive Exclusion Principle and thus allow for temporal and spatial variations in the culture environment. Changing conditions have their obvious example in the seasons. The seasonal fluctuations of natural flora are well-known. Yet these are extremely long on a microbial time scale. Diurnal fluctuations of light, temperature, and other related effects seem more appropriate stabilizing factors. Wall growth as an example of spatial heterogeneity is another such factor.

If interactions other than competition are present, then stable mixed cultures might be possible. This is the case for such common examples as mutualism in yogurt and also in the feeding by a common predator. Most other mixed systems are unstable in a conventional CSTR.

The stability of competing populations in chemostats under conditions of cyclic flow inputs was studied theoretically and was shown to lead to stable periodic trajectories of coexistence [7]. The organisms must have crossing substrate saturation curves. Then coexistence is achieved by cycling the dilution such that one is favored during one part of the cycle, and then the other population is favored. The cycle time and the magnitude of the dilution range are operating parameters necessary to numerically determine the stability.

The creation of stable coexistence by varying conditions for an otherwise unstable mixed culture will increase the possible usable mixed cultures and their applications. Explorations of the interactions and dynamics of mixed cultures will help develop strategies for stable coexistent operations. These operations may have uses and problems for which current pure culture techniques are inapplicable.

The work reported herein looked at nonflow cyclic inputs, specifically the pH. The pH bounds were chosen to favor each organism in turn. Computer simulations and Floquet analysis confirmed that stable cycles are possible within rather broad parameter ranges. The experiments agreed qualitatively with this theoretical analysis. This study showed that stable coexistence of competitors is possible for certain ranges of operating parameters.

MATERIALS AND METHODS

E. coli and *Saccharomyces cerevisiae* were chosen as the mixed culture pair. Both are common, well studied organisms, especially when grown on glucose, our chosen substrate. Their cell volumes are quite separated. *E. coli* is a 2 by 1 μm rod and *S. cerevisiae* is a 5 to 8 μm sphere. This allows particle size analysis to distinguish between the species. The stock cultures were maintained on YPG agar. It was discovered in batch and chemostat runs that care must be taken to ensure that the organisms are sufficiently acclimated to the culture conditions from the refrigerated stock cultures. At least 12 successive generations or three shake flasks were grown in the defined media before initiating the experiments.

The media was a defined glucose media for yeast modified from Oura[16]. The defined yeast media was mixed, the pH adjusted with KOH, and filter sterilized through a 0.2 μm filter. The recipe is for 1 l. water: 12.g $(\text{NH}_4)_2\text{SO}_4$, 0.52g $\text{MgCl}_2 \cdot 6\text{H}_2\text{O}$, 1.g glucose, 0.2g KPhthalate, 0.1g EDTA, 1.6 ml 85% H_3PO_4 , 0.12 KCl, 0.09 $\text{CaCl}_2 \cdot 2\text{H}_2\text{O}$, 0.06g NaCl, 3.8mg $\text{MnSO}_4 \cdot \text{H}_2\text{O}$, 0.5mg $\text{CuSO}_4 \cdot 5\text{H}_2\text{O}$, 7.3 μg H_3BO_4 , 3.3 μg $\text{Na}_2\text{MoO}_4 \cdot 2\text{H}_2\text{O}$, 2.5 μg NiCl, 2.3 μg $\text{ZnSO}_4 \cdot 7\text{H}_2\text{O}$, 2.3 $\text{CoSO}_4 \cdot 7\text{H}_2\text{O}$, 1.7 μg KI, 35.mg $\text{FeSO}_4(\text{NH}_4)_2\text{SO}_4 \cdot 6\text{H}_2\text{O}$, 125. mg m-inositol, 6.25 mg Pyridoxine-HCl, 6.25 mg Ca-D-Pantothenate, 5. mg Thiamine-HCl, 5.mg Nicotinic Acid, and 0.125mg D-Biotin. Essential vitamins for yeast were included. We used 1.0 gm/l of glucose to have moderately low biomass and product concentrations. A low biomass needs less diluting for analysis and avoids clumping and foaming. The temperature was kept at 30 °C for all experiments.

Below pH 5.5 the phosphate buffer in the media is ineffective and most common buffers in this range are organic acids which are readily metabolizable by *E.coli*. Phthalic acid was used as a buffer. It was determined that neither *E.coli*

at pH 7 nor *S. cerevisiae* at pH 6 grow on phthalic acid. There was no apparent effect on growth on glucose from the phthalic acid in any of the experiments. From this point on all media had phthalate buffer.

The primary measure of the biomass was by light absorbance measured at 660 nm by a B&L Spectrophotometer. A correlation was established for the deviation from linearity of the total absorbance and biomass by testing dilution of the samples. Complete batch growth on 1 gm/l glucose gave final absorbances of about 0.400 and 0.450 for *S. cerevisiae* and *E. coli* respectively. The absorbance of *S. cerevisiae* is linear throughout this range, while that of *E. coli* deviates above $A=0.200$ to a maximum of 10%.

The Coulter Counter gives a direct count of particles in a sample. The sample is first diluted in an electrolyte; then a known volume is passed through a small orifice in an electric field. Each particle entering the orifice causes a change in the resistivity, which is measured and counted. This resistivity jump is proportional to the size of the particle - generally linear with the radius of a sphere. Thus the output is the size distribution of the sample. Different species have different resistivities, and live cells count slightly different than dead. For a particular species in a certain stage of growth the results are consistent and stable. Thus if the size distributions of the two species are sufficiently separated, this will distinguish quantitatively between the populations. Mountney and O'Malley [17] found that the precision of electronic counts were better than plate counts for a particular stage of growth. The Coulter Counter is also much easier and quicker.

The particle must be between 2 and 40% of the orifice diameter. We used a 30 μm orifice for all samples. In this system the two species need completely different settings (Table 1). The total resolution (the aperture current times the

amplification) is 32 times greater for *E.coli* than for *S. cerevisiae*. In each case the other species is either off scale or merged with the background. The electrolyte used for diluting the samples for the Coulter is filtered daily through a 0.2 μm millipore filter. The dilution in electrolyte was judged to give a total count between 10,000 and 100,000. This leaves a background about half the size of the *E.coli*. Typical population size distributions for yeast and *E. coli* are shown in Fig. 2. These samples were taken from a mixed culture. The *E. coli* (Fig. 2a) is a shoulder on the background distribution so that both sample and background counts must be taken. At the higher setting for yeast both the bacteria and the blank do not appear (Fig. 2b). The distributions were stored in the computer for analysis of total cell number after subtracting the background. (See Appendix for details).

Table 1	Coulter Counter Settings	
	1/Aperture Current	1/Amplification
<i>E. coli</i>	2	1
<i>S. cerevisiae</i>	8	8

The metabolites were measured using enzymatic test kits and a UV spectrophotometer. Sigma kits #15-UV for glucose and #331-UV for ethanol were used along with a Boehringer UV kit for acetic acid. 2 mls of sample were filtered within three minutes of removal and frozen to await enzymatic testing. The numerical calibrations for glucose and ethanol were checked and found accurate. The difficulty is that the lowest concentrations detectable by this method are 2.0 mg/l glucose and 0.1 mg/l EtOH.

The batch experiments were performed in 125 ml erlemeyer flasks with cotton plugs in a rotary shaker. All batch runs were performed in parallel with three or four identical flasks and the results averaged. Sufficient aeration is provided by shaking at 150 rpm; below 80 rpm growth is affected. No shear

effects were noted for either species at 150 rpm.

The chemostat used was a modified version of the New Brunswick Bioflow system. The level was maintained by overflow; temperature was controlled with a water bath. The pH probe (Ingold), controller (Chemtrix), and base reservoir maintained the pH to within ± 0.03 . The chemostat was aerated at 1.5 l/min with stirring at about 300 rpm. A solution of 0.2 gm/l silicone antifoam emulsion was added as needed to control foaming.

The reactor was sterilized, filled, and inoculated with an actively growing culture. The reactor was run batch while biomass increased to near the expected steady state value. Then flow was started before the second diauxic phase to maintain the glucose metabolism.

Flow rates were checked by measuring the overflow. Samples were taken, the absorbance measured and a filtrate frozen for glucose and ethanol analysis. A steady state was assumed if both the biomass and glucose concentrations were constant within 5% for three samples. Samples were also diluted with electrolyte and run through the Coulter Counter at the appropriate settings (Table 1) for each. Streak plates were made daily to check for contaminants on YPG and EMB agar.

EXPERIMENTAL RESULTS

Batch and Continuous Experiments

The initial batch experiments for both species at pH 4.0, 4.5, 5.0, and 5.5 showed that there was rapid acid production during growth for both and that *E.coli* stopped all growth below pH 4.0. These preliminary experiments indicated that the desired lower pH, for which the maximum growth rate of *S. cerevisiae* is greater than that of *E.coli*, lay between pH 4 and 5.

The effect of pH on the maximum specific growth rate for the two organisms is shown in Fig. 3. *S. cerevisiae* is insensitive to pH between 4 and 5 with a μ_{\max} of 0.41hr^{-1} . *E.coli* is very sensitive. These values were estimated from batch and chemostat washout experiments. It is important to note that while pH 4.0 stops the growth of *E.coli*, the bacteria remain viable. In both batch and chemostat experiments growth stopped at pH 4.0 but would resume when the pH was restored to a higher value.

S. cerevisiae will not grow on acetic acid and *E.coli* will not grow on ethanol as the sole substrates in the defined media. This eliminates commensalism, where one species lives off of the other's products as a possible stabilizing interaction.

Next, the possible inhibition effects of these products on the other organism were examined. The maximum yield of these products is theoretically one mole for every mole of glucose. A maximum of 0.32 gm ethanol/l was achieved by yeast during batch growth on 1 gm/l glucose. Since 1 gm glucose/l is used, we chose 0.5 gm/l of ethanol or acetic acid to be in excess of this maximum for our inhibition studies. Figure 4 shows the results of these inhibition studies. Acetic acid in any concentration up to the maximum had no effect on the

growth of *S. cerevisiae* on glucose. Yeast growth on glucose is then independent of acetic acid.

As expected, ethanol does inhibit *E. coli*, but not at low concentrations. There is no appreciable effect below 0.05 gm/l ethanol and only a slight effect up to 0.2 gm/l. During respiratory growth of yeast, negligible alcohol will be formed. During fermentative (high sugar) growth, alcohol is formed and some inhibition may occur. The experimental yields of about 3 mg ethanol/ gm glucose during continuous culture ($D < 0.2\text{hr}^{-1}$) indicate that the inhibition of *E. coli* will be minor, if at all.

The substrate affinity of *E. coli* for glucose is much higher than that of *S. cerevisiae* at all pH; equivalently the steady state sugar values are lower. This corresponds to the K_s estimates of 4-8 mg/l for *E. coli* and 50 mg/l for *S. cerevisiae* made from continuous culture experiments at a variety of dilution rates. Based on these results and assuming that the effect of pH is predominantly on μ_{\max} (i.e., ignoring any K_s variations with the pH) [18], the specific growth rate curves of Fig. 5 were derived for the two species as functions of glucose concentration and pH. Figure 5 suggests that a pH cycle between pH 5.0 and 4.3 would alternate the competitive advantage.

A dilution rate of 0.17hr^{-1} was chosen for the continuous flow experiments with varying pH. Under these conditions the assumptions of pure competition are satisfied. At low dilution rates ($D < 0.1\text{hr}^{-1}$), the constant yield assumption of the chemostat equations becomes increasingly invalid for continuous cultures. Maintenance energy was found to be important at these flowrates. This change would not affect the nature of the theoretical or experimental results.

pH Oscillation Studies

The first pH oscillation experiment is shown in Fig. 6. The cycle used was 16 hrs. pH4.3/16 hrs pH5. for a total period of 4/3 days with $D=0.17 \text{ hr}^{-1}$.

The course of the experiment was to establish *E.coli* at pH5, observe *E.coli* alone for two cycles, and, after the *E.coli* had been reestablished at steady state at pH 5., to inoculate with *Scerevisiae* at the start of a low pH cycle($t=5.33$ days). The *E.coli* cycled alone produced dramatic shifts in concentration as expected, changing from near its full growth to about a tenth and back again. Similar shifts in the glucose concentration were observed (Fig. 6b). After inoculating with yeast, an alternating cycle of *E.coli* and *S. cerevisiae* was established. The measurement errors are estimated at ± 0.005 Absorbance, ± 0.02 pH, ± 2 mg/l glucose, and $\pm 5\%$ cell number from sensor limits and successive readings. Cumulative errors and sampling problems may produce larger errors. The standard deviation of the cell number counts over six periods is about 20%. But the species persist in comparable numbers that are significantly larger than the errors for six periods.

In the second experiment (Fig.7), the 16/16 period was repeated. A similar response was observed within error. After this a 18 hr pH5./14 hr pH4.3 cycle was begun. The concentrations quickly changed to a new range with a much smaller yeast concentration. The yeast persisted at this very low but detectable level for the three periods. If washout were to occur they would not have lasted this long, as was demonstrated by a washout cycle to be discussed shortly. The magnitude of concentration shifts and the speed at which the system responds to changes in the cycle support the stability of the experimental system. When the cycle was changed again to 14 hr pH5.0/18 hr pH4.3, the yeast quickly increased to a significant level when the run aborted due to contamination. Thus a 2 hour change in the cycle ratio gives another stable yet different cycle.

The third experiment (Fig. 8) again began with a 16/16 cycle. After 2 periods when it was clearly moving to a stable cycle a cycle of 6 hr pH5.0/ 6 hr pH4.3 was begun. After an initial increase the *Scerevisiae* began to steadily wash out. After two periods the sugar levels remained low enough throughout that the yeast could never increase. The yeast count then quickly dropped to negligible levels. This is an unstable cycle achieved by shortening the period.

DISCUSSION

The studies reported in the previous section tested for forced coexistence caused by cycling of the pH. The chemostat was inoculated with one organism and run with a step change between two pH limits. Each organism was favored at one of the pH.

The existence of both stable and unstable cycles can be seen by considering the effect of the total period. In the extreme of a very long switching time, a complete changeover between steady state populations is expected each half cycle. As long as one cell remains of the washout population this species can reestablish itself. This is a stable though impractical cycle. As the switching time decreases the magnitude of these cycles would decrease, and the coexistence may be lost. In the limit when the changes are very rapid, the pH is essentially constant at its average, and coexistence will be impossible by the Competitive Exclusion Principle.

A brief qualitative argument for the stability of these cycles can be made by considering the sugar level and the average growth rates during each part of the cycle. *E.coli* will alternatively dominate (yielding low sugar) or washout (higher sugar). If the sugar levels get large enough during the *E.coli* washout so that *Scerevisiae* increases then there may be a stable cycle. Yeast will be increasing in the spaces between the *E.coli* dominance. Arguments for the restoring force to make this cycle stable are possible but are not simple or clear to present. Therefore computer simulations were used to demonstrate the stability of the mixed system during these cycles.

This analysis follows Stephanopoulos et al.[7], which was developed for cycles of dilution rate. The equations are as before with parameters estimated from the batch and continuous experiments. The effect of changing the pH is to

change these growth parameters. The biomass values are calculated as gram equivalents of sugar. For example, b_1 equals x_1/Y_1 ; where Y_1 is 0.38 gm biomass/gm glucose for *S.cerevisiae*. The equations are integrated using Gear's method with a desired cycle ratio. The μ_{max} of *E.coli* has an instantaneous step change in value when the pH is switched in the cycle. The other parameters were unchanged in the simulation and are reported below.

Table 2 **Monod Growth Constants**
Estimates for Simulation

	μ_{max}	K_s
	hr ⁻¹	mg/l glucose
<i>S. cerevisiae</i>	0.4	50
<i>E.coli</i> pH4.3	0.1	5
<i>E.coli</i> pH5.0	0.6	5

The simplest method to check for a stable cycle is to "inoculate" the simulation with small amount of one species into a dense "established" culture of the other during the cycle as described above. If both increase from small inocula then there must be a stable cycle somewhere in the x-y phase plane. The exact stable cycle can be found by integrating longer.

Using even ratios of time spent at each pH, the simulation found stable cycles for total periods greater than 3 hours. Changing the ratio of time spent at each pH with a fixed total period gave a broad region of stable cycles between 25hrs pH4.3/5hrs pH5 and 5/25. In unstable simulations one population was negligible after about three periods.

In the simulation shown (Fig. 9) the period was set as in the first experiment. A small inoculum quickly increased to near the stable cycle but convergence after that was slow. The simulation (Fig. 9) compares reasonably well with the experiment (Fig. 6). One gm glucose equivalent of cells is 20×10^8 /ml for *E. coli* and 26×10^8 /ml for *S. cerevisiae*. Observe that *E. coli* rises to near complete conversion and falls tenfold in the simulation and fivefold in the experiment. Conversely, *S. cerevisiae* rises to near half conversion in the experiment and two thirds in the simulation from a tenth conversion in both. The glucose follows closely the simulation values at the end of each period. Intermediate glucose values were not measured so that the glucose peaks seen in the simulation are not confirmed.

In comparing the shift between a 16/16 cycle and the 18/14 cycle the experimental change was qualitatively the same as the simulation but the yeast counts were even lower. The simulation predicts instability at a total period of 2 hours not 12 hours as in the third run. But the prediction of instability is met as the period is shortened with confirmation of the key qualitative feature of low sugar values that never allowed *S. cerevisiae* a competitive advantage.

The simulation converged to the exact stable cycle after many periods, and at that point Floquet analysis was done on this cycle. Floquet analysis of periodic systems requires the exact location of the cycle and is the complicated equivalent of eigenvalue stability analysis for a steady state system. The method and equations have been summarized elsewhere [7,19,21, and the Appendix]. Using the calculated 16 hr/16 hr cycle, after one period the moduli of the eigenvalues had shrunk from (1,1,1) to $(10^{-8}, 10^{-4}, 0.998)$. Moduli less than one is a necessary and sufficient condition for stability. Similar results were found for the 18/14 cycle. The 6 hr/6hr cycle had moduli of $(10^{-2}, 10^{-1}, 0.9999)$ indicating the approach to the instability threshold.

There are two complications to the quantitative study of the experiments. *E.coli* changes size during the pH shifts, becoming at most 50% larger at pH 4.3. Size changes due to pH and glucose shifts during unbalanced growth are known. The size of *S. cerevisiae* was not affected. This would change the cell number equivalents for 1 gm glucose but not the qualitative trends or the stability.

Secondly when intermediate samples were taken, lags were noted for *E.coli* at the beginning of each pH shift. Growth would continue at the previous rate for about an hour. These lags can help explain the deviations of the experiment from the simulation. In the first experiment a lag for *E.coli* would keep the sugar low for an additional hour, thus allowing the yeast less time at high sugar to increase. This explains the slightly lower experimental yeast concentrations. In shorter periods this trend caused by the lag would eventually prevent the yeast from increasing at all within a cycle that this simulation predicts as stable. This was seen in the third run.

These lags do not affect the conclusions or general utility of this work. They indicate that a simple instantaneous response Monod simulation is not sufficient to quantitatively predict reality. But even with this crude simulation qualitative features and agreement were achieved.

In conclusion, oscillations of pH can force stable persistence of a competing mixed culture that is otherwise unstable. By varying the period, ratio, and limits of the pH, a good control variable, the two species can be maintained at many different levels. Ramifications extend beyond just the experimental justification of the theory. Ecologically these temporal and spatial variations can create additional environmental niches and help explain the persistence of the great diversity in natural systems. In addition the creation of stable coexistence by varying conditions for an otherwise unstable mixed culture will

increase the possible usable mixed cultures and their applications.

Acknowledgement

The support of ARCO's Young Faculty Investigator Award and the National Science Foundation is gratefully recognized.

NOTATION

D	dilution rate (hr^{-1})
$k_{s,j}$	substrate saturation constant for species j (g/l)
s	substrate (g/l)
s_f	substrate concentration of chemostat feed (g/l)
t	time (hr)
x_j	biomass concentration of species j (g/l); [$j=1, E. coli$; $j=2, S. cerevisiae$]
Y_j	yield coefficient of species j per substrate consumed (g/g)
μ_j	specific growth rate of species j (hr^{-1})
$\mu_{\max,j}$	maximum specific growth rate of species j (hr^{-1})

REFERENCES

1. A.G.Fredrickson, and G.N.Stephanopoulos (1981). Microbial Competition," *Science*, **213**, 972(1981).
2. G.F.Gause, **The Struggle for Existence**. Williams and Williams , Baltimore (1934).
3. J.Monod, **Recherches sur la Croissance des Cultures Bacteriennes**. Paris, Hermann(1942).
4. E.O. Powell, "Criteria for the Growth of Contaminants and Mutants in Continuous Culture," *J. General Microbiology*, **18**, 259(1958).
5. G.Hardin, *Science*, **131**, 1292(1960).
6. R. Aris and A.E. Humphrey, *Biotech. and Bioeng.*, **19**, 1375 (1977).
7. G. Stephanoloulos, A. Fredrickson, and R. Aris, "Growth of Competing Microbial Populations in CSTR with Periodic Varying Inputs," *AICHE J.* **25**, 863 (1979).
8. W.Harder, J.G. Kuenen, A. Matin, "A Review: Microbial Selection in Continuous Culture", *J. Applied Bacteriol.*, **43**, 1(1977).
9. A. Matin and H. Veldkamp, "Physiological Basis of the Selective Advantage of a *Spirillum* sp. in a Carbon-limited Environment," *J. of General Microbiology*, **105**, 187(1978).
10. H.W. Jannasch, "Enrichments of Aquatic Bacteria in Continuous Culture," *Archiv fur Mikrobiologie*, **59**, 165(1967).
11. J.L. Meers and D.W. Tempest, "The Influence of Extracellular Products on the Behavior of Mixed Microbial Populations in Magnesium-limited Chemostat Cultures," *J. of General Microbiology*, **52**, 309(1968).
12. W. Harder and H. Veldkamp, "Competition of Marine Psychrophilic Bacteria at Low Temperatures," *Antonie van Leeuwenhoek*, **37**,R51(1971).
13. J.L. Meers, "Effect of Dilution Rate on the Outcome of Chemostat Mixed

Culture Experiments," *J. of General Microbiology*, **67**, 359(1971).

14. S. Hansen and S. Hubble, "Single Nutrient Microbial Competition: Qualitative Agreement Between Experimental and Theoretical Forecast Outcomes, *Science*, **207**, 1491(1980).
15. G.E. Hutchinson, *Am. Nat.*, **95**, 137(1961).
16. E. Oura, *Biotech. Bioeng.*, **16**, 1197(1974).
17. G.J. Mountney and J. O'Malley, "Statistical Evaluation of Electronic and Plate Counts for Estimating Bacterial Populations," *J. Applied Microbiology*, **14**, 845(1966).
18. J. Bailey and D. Ollis, **Biochemical Engineering Fundamentals**, McGraw Hill, New York (1977).
19. D. Sincic and J.E. Bailey, *Chem. Engr. Sci.*, **32**, 281(1977). 20. L. Cesari, **Asymptotic Behavior and Stability Problems in Ordinary Differential Equations**, pp55-59, Springer-Verlag, Heidelberg(1963). ;

List of Figure Captions

Figure 1. Operating Diagrams for a Chemostat in which Two Populations Compete for a Rate-Limiting Substrate.

Figure 2a. Particle Size Distribution for *E. coli*

Figure 2b. Particle Size Distribution for *S. cerevisiae*

Figure 3. Maximum Specific Growth Rate vs. pH for *E. coli* and *S. cerevisiae* on 1 g/l glucose.

Figure 4. Effect of Products on the Maximum Specific Growth Rate on glucose - Inhibition of *E. coli* by EtOH and of *S. cerevisiae* by Acetate.

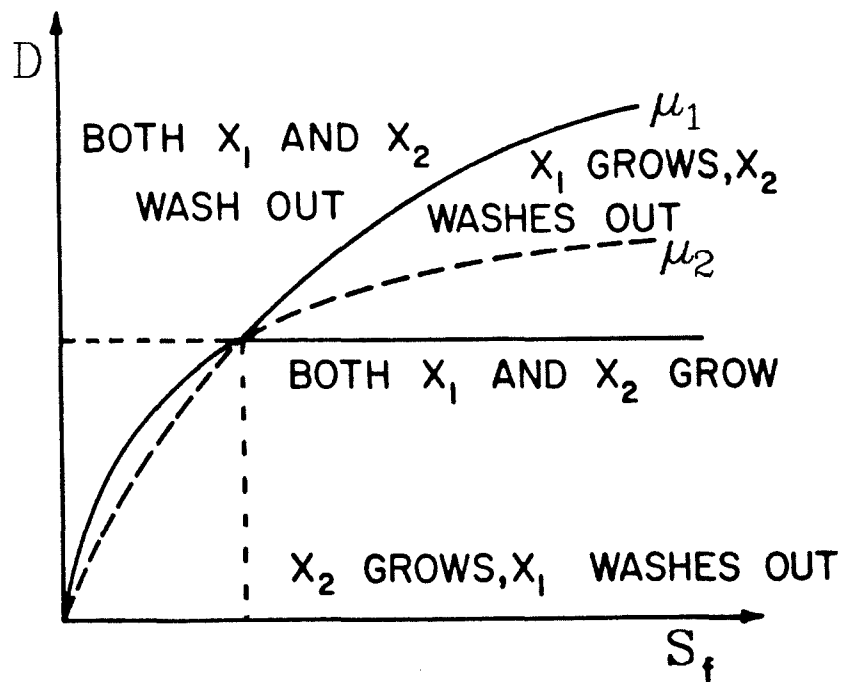
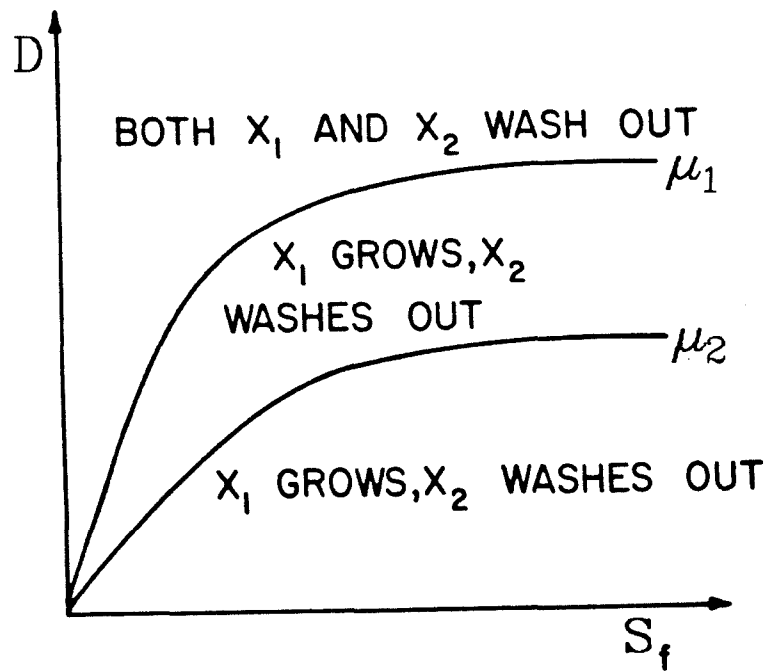
Figure 5. Specific growth rate as a function of glucose for *E. coli* at pH 4.3, 4.5, and 5.0 and for *S. cerevisiae*.

Figure 6. pH Oscillation Experiment - 16 hr. pH5/ 16 hr. pH4.3 - Demonstration of Stability 6a. Cell Number of *E. coli* and *S. cerevisiae* 6b. Glucose concentration

Figure 7. pH Oscillation Experiment - 18 hr. pH5/ 14 hr. pH4.3 - Demonstration of Stability at Different Cycle Ratio 7a. Cell Number of *E. coli* and *S. cerevisiae* 7b. Glucose concentration

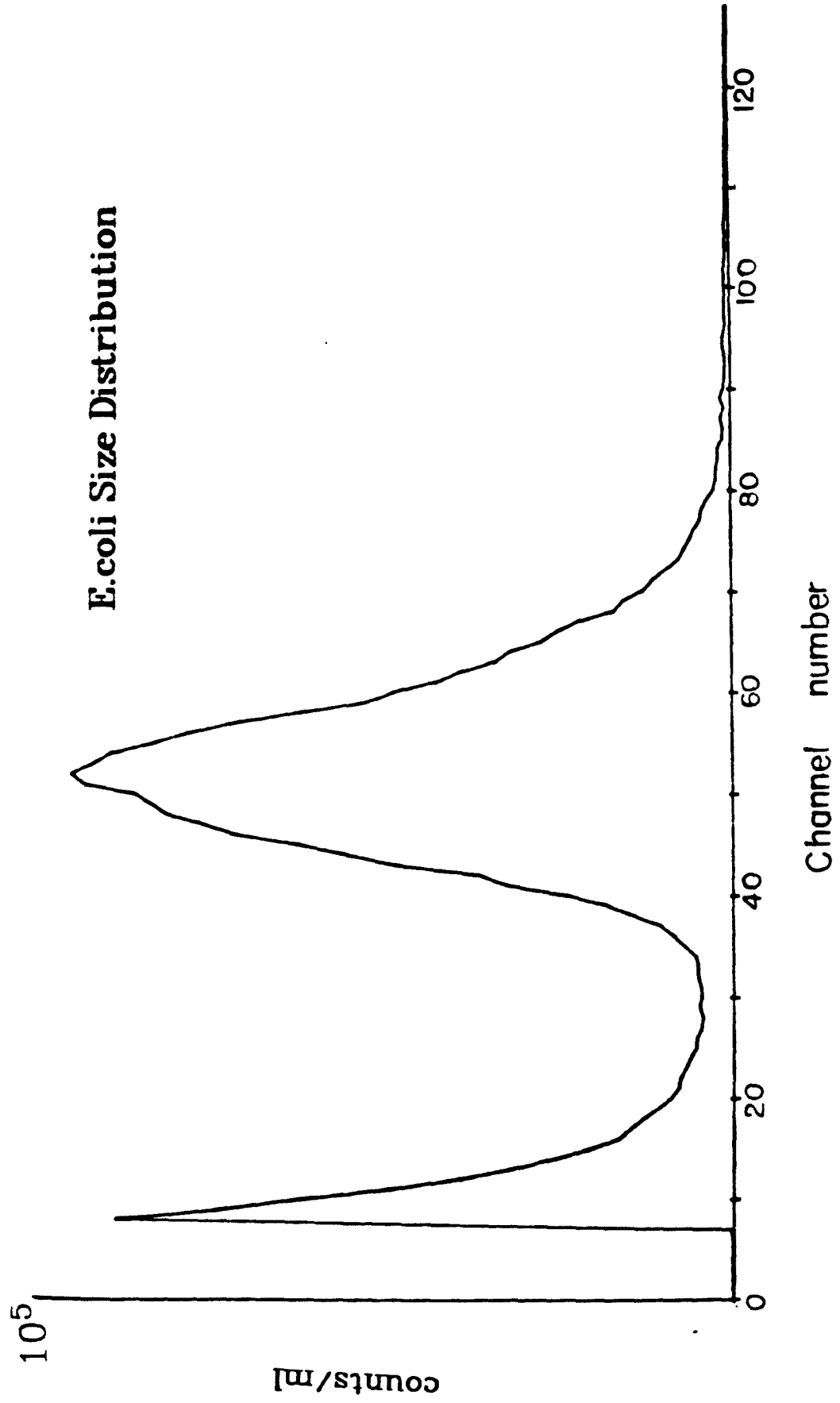
Figure 8. pH Oscillation Experiment - 16 hr. pH5/ 16 hr. pH4.3 changed to 6 hr pH5/ 6 hr. pH4.3 - Shortened Cycle Period is Unstable 8a. Cell Number of *E. coli* and *S. cerevisiae* 8b. Glucose concentration

Figure 9. pH Oscillation Computer Simulation - 16 hr. pH5/ 16 hr. pH4.3 -
9a. *S. cerevisiae* 9b. *E. coli* 9c. Glucose concentration



Operating diagrams for a chemostat in which competition of two populations for a rate-limiting substrate occurs.

FIGURE 1



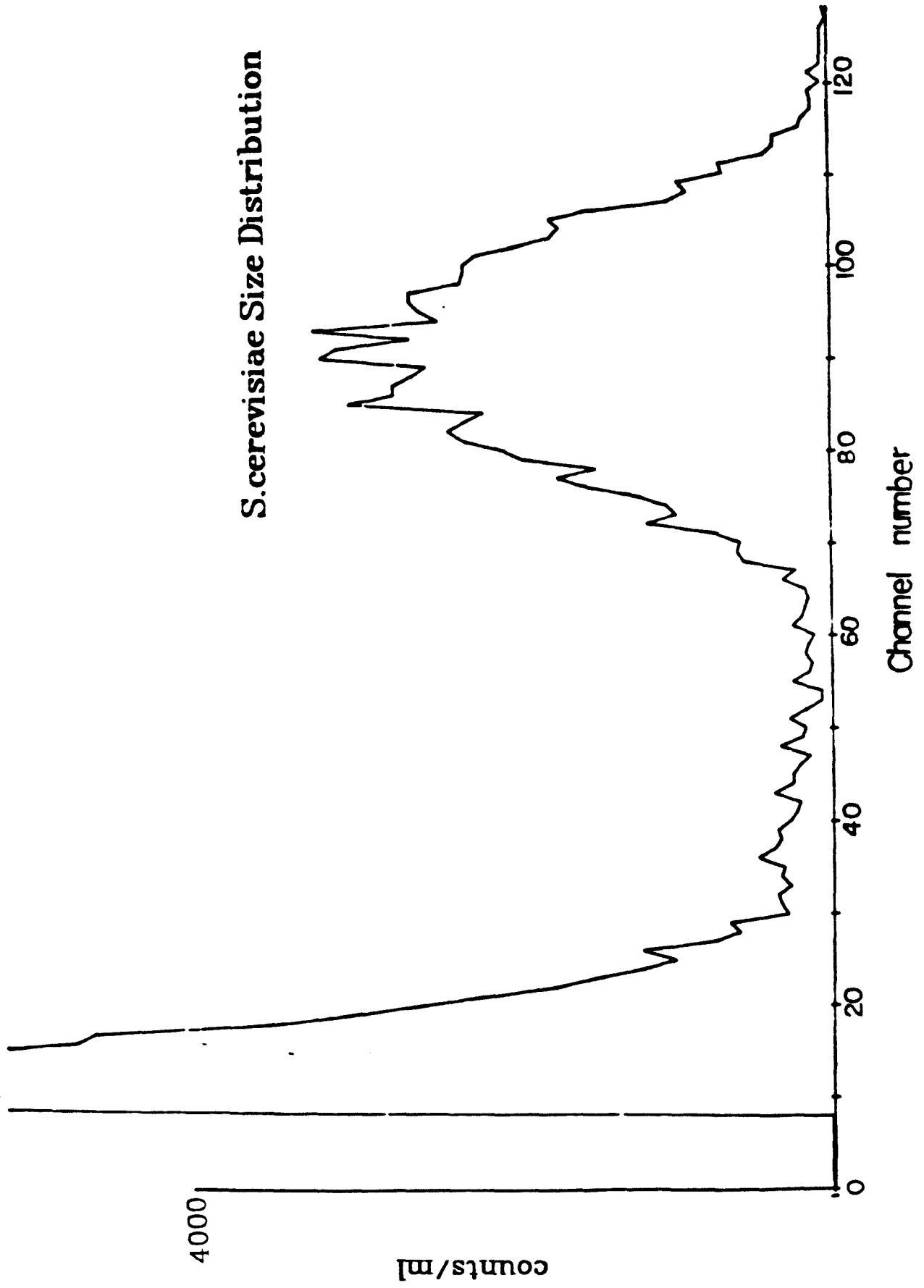
***S.cerevisiae* Size Distribution**

FIGURE 2B

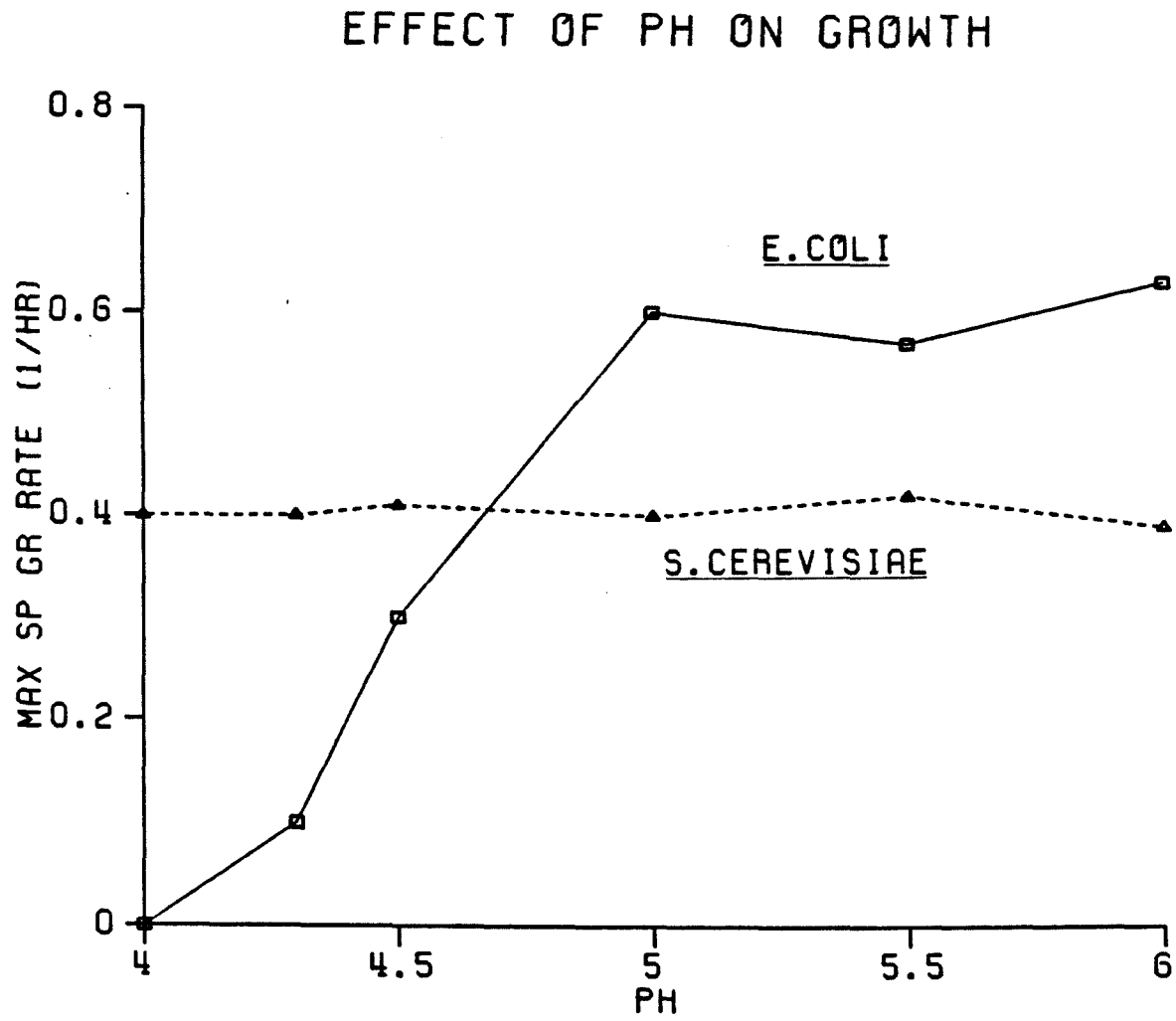


Figure 3. Maximum Specific Growth Rate vs. pH for *E. coli* and *S. cerevisiae* on 1 g/l glucose.

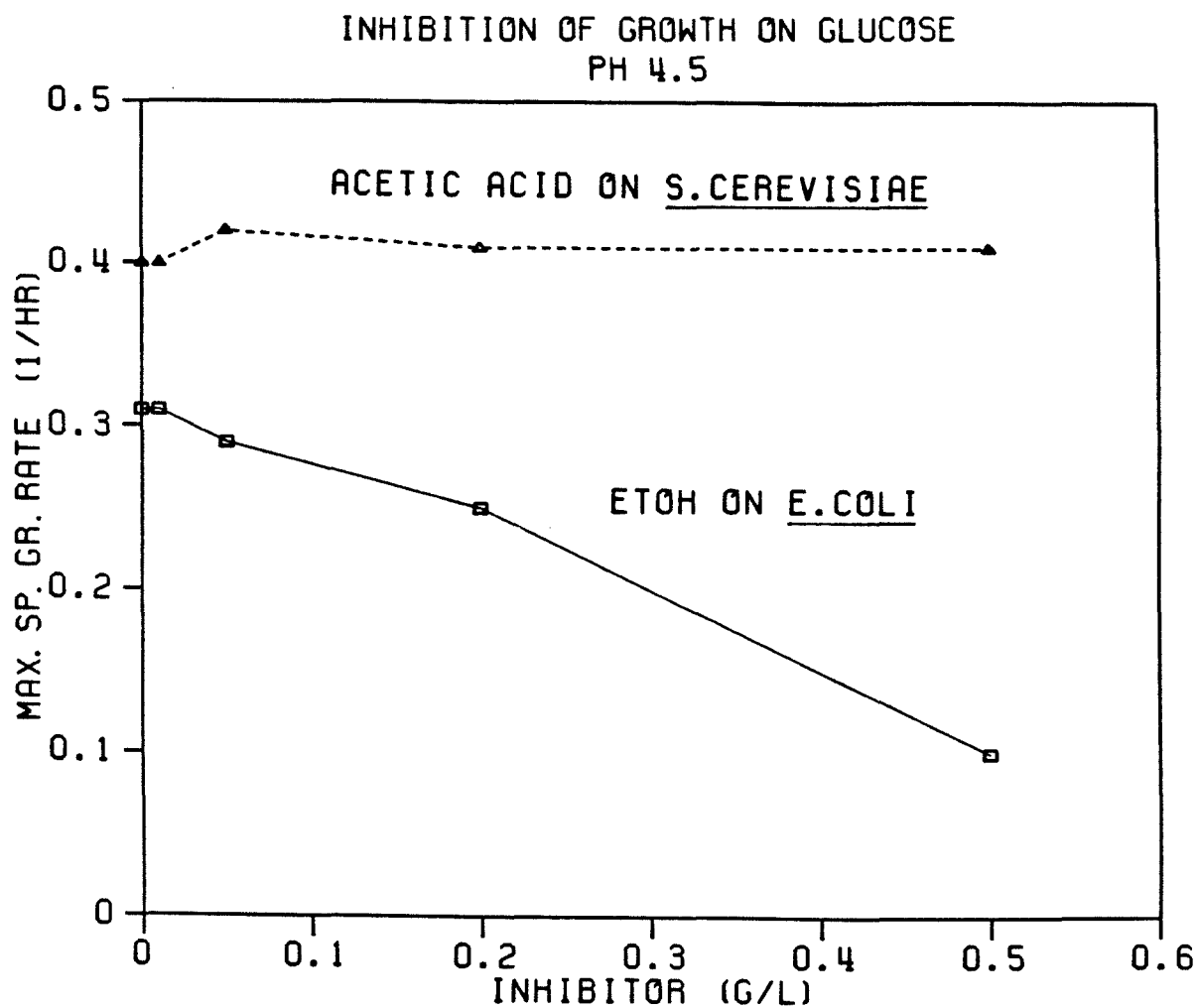


Figure 4. Effect of Products on the Maximum Specific Growth Rate on glucose -
Inhibition of *E. coli* by EtOH and of *S. cerevisiae* by Acetate.

GROWTH RATE vs. SUBSTRATE

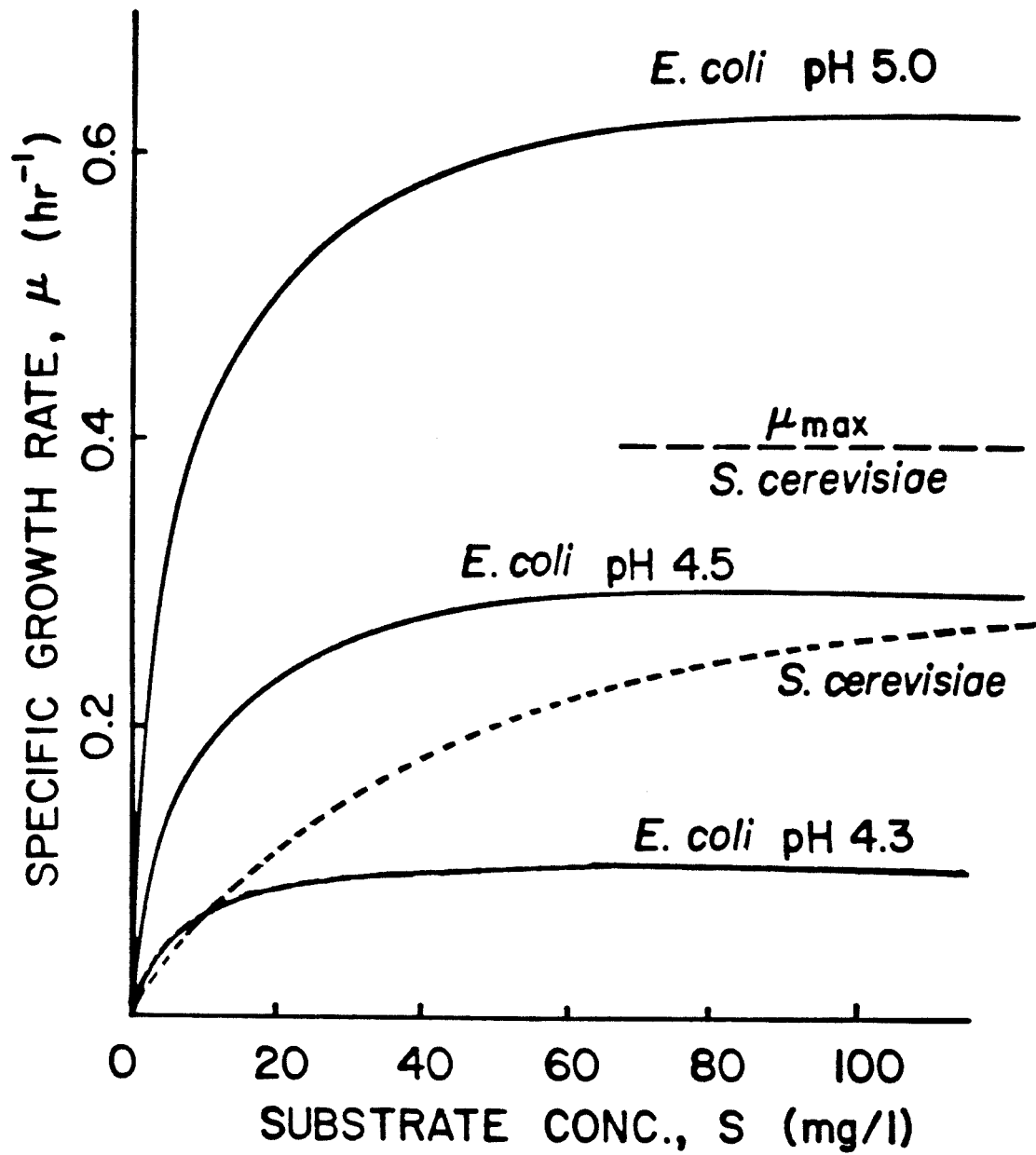


FIGURE 5

pH Oscillations: Stability

16 hr pH5./16 hr pH4.3

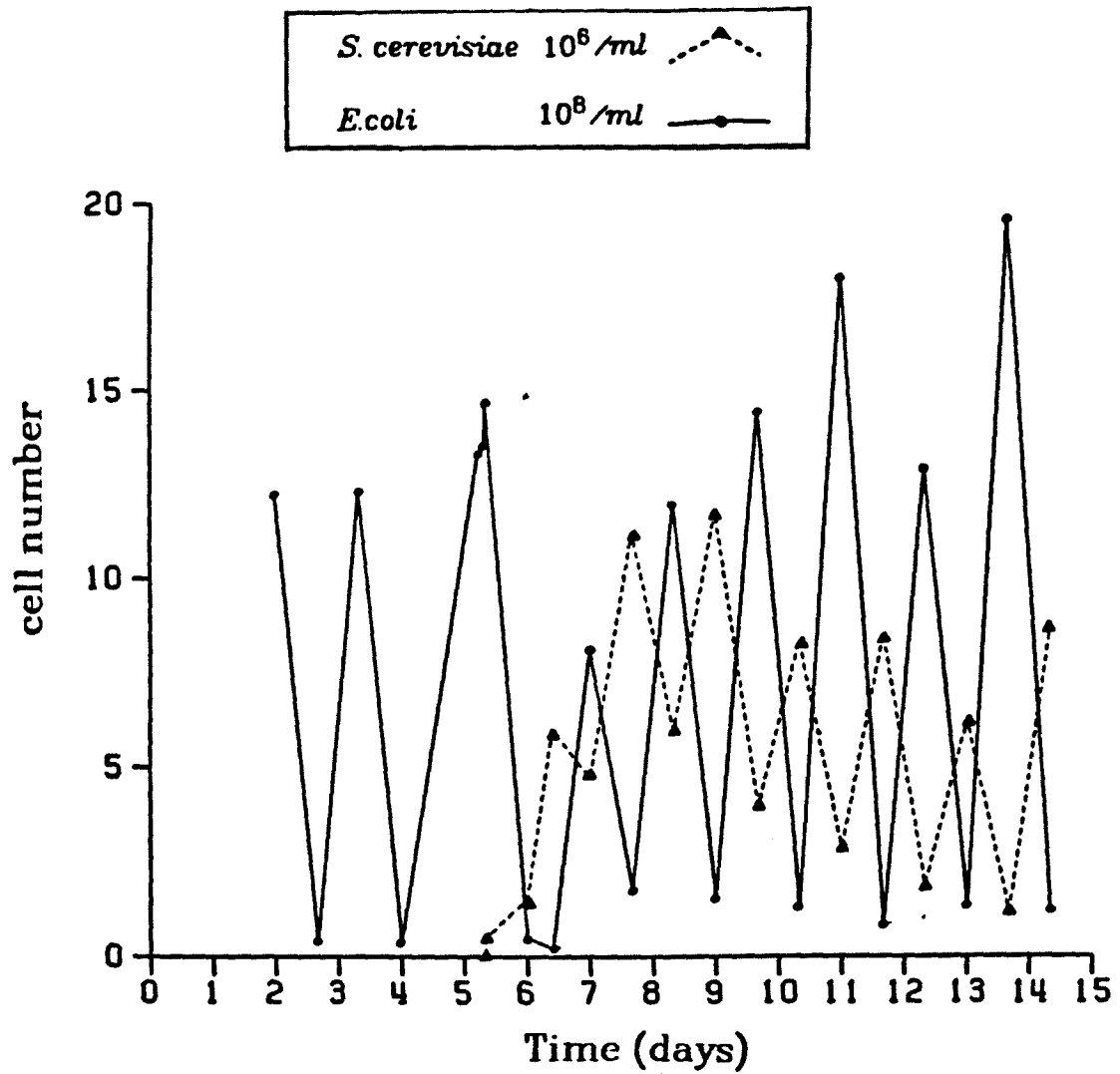
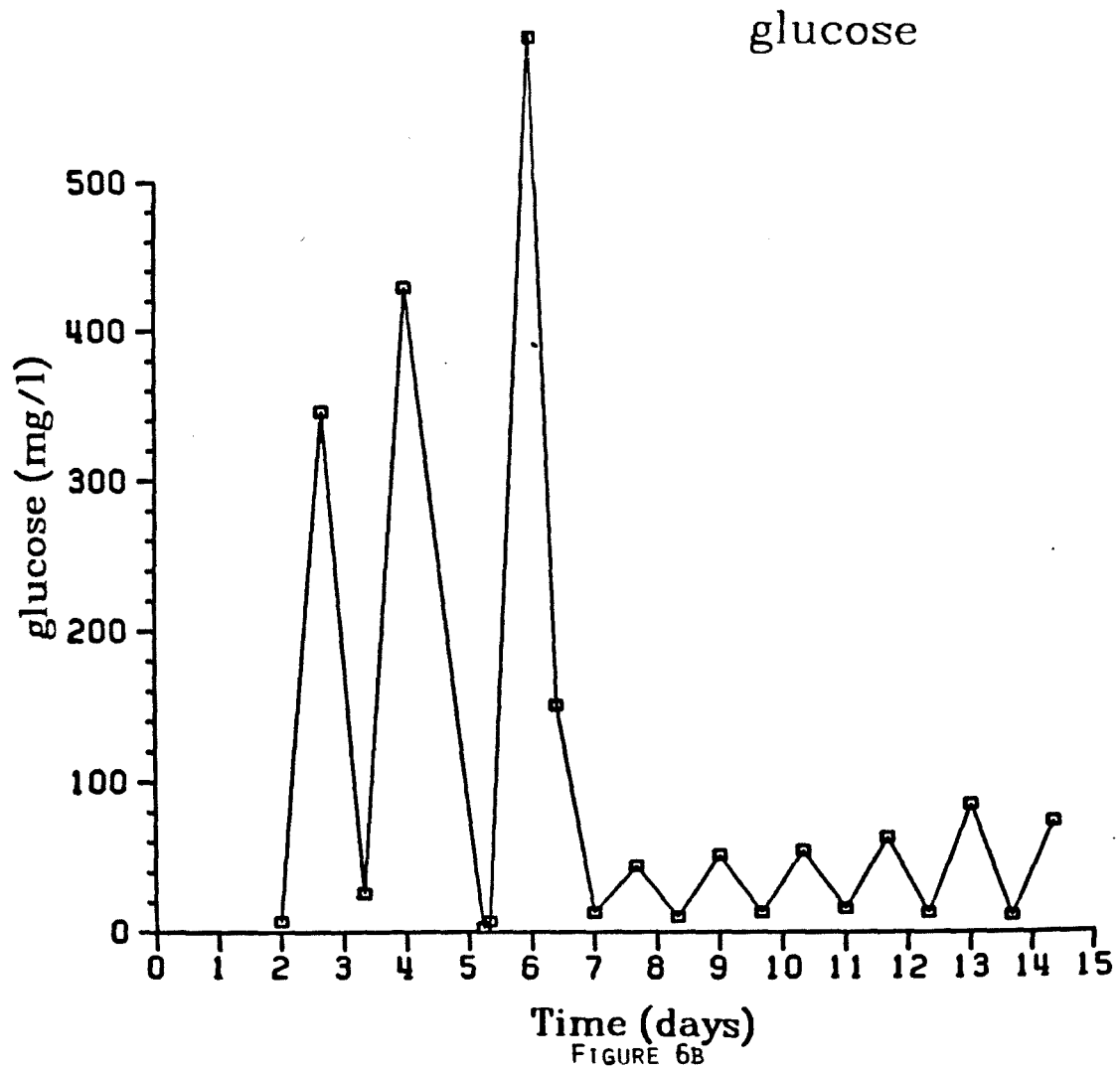


FIGURE 6A

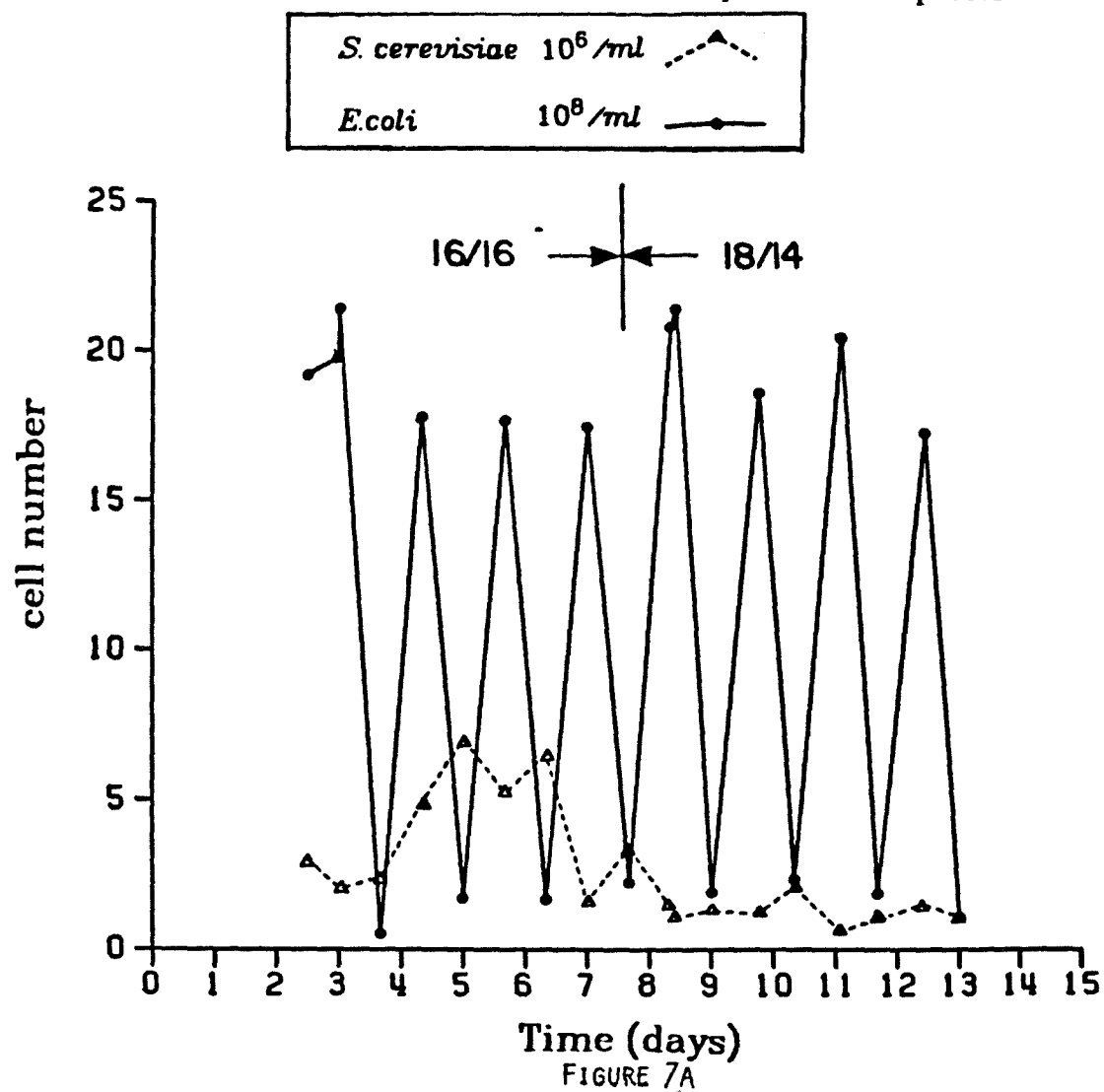
pH Oscillations: Stability

16 hr pH5./16 hr pH4.3



pH Oscillations: Effect of Cycle Ratio

16 hr pH5./16 hr pH4.3 18 hr pH5./14 hr pH4.3



pH Oscillations: Effect of Cycle Ratio

16 hr pH5./16 hr pH4.3 18 hr pH5./14 hr pH4.3

glucose

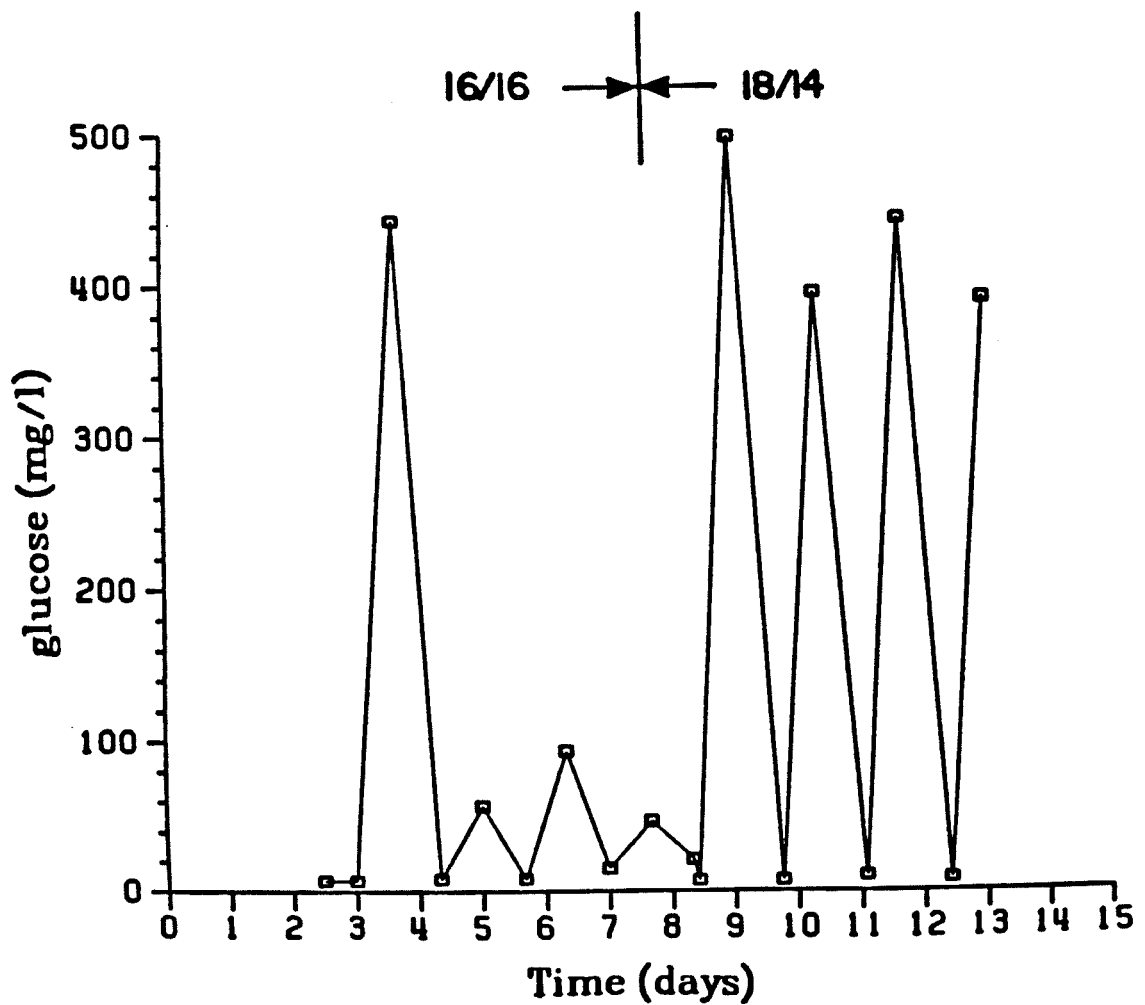


FIGURE 7B

pH Oscillations: Effect of Cycle Period

16 hr pH5./16 hr pH4.3 6 hr pH5./ 6 hr pH4.3

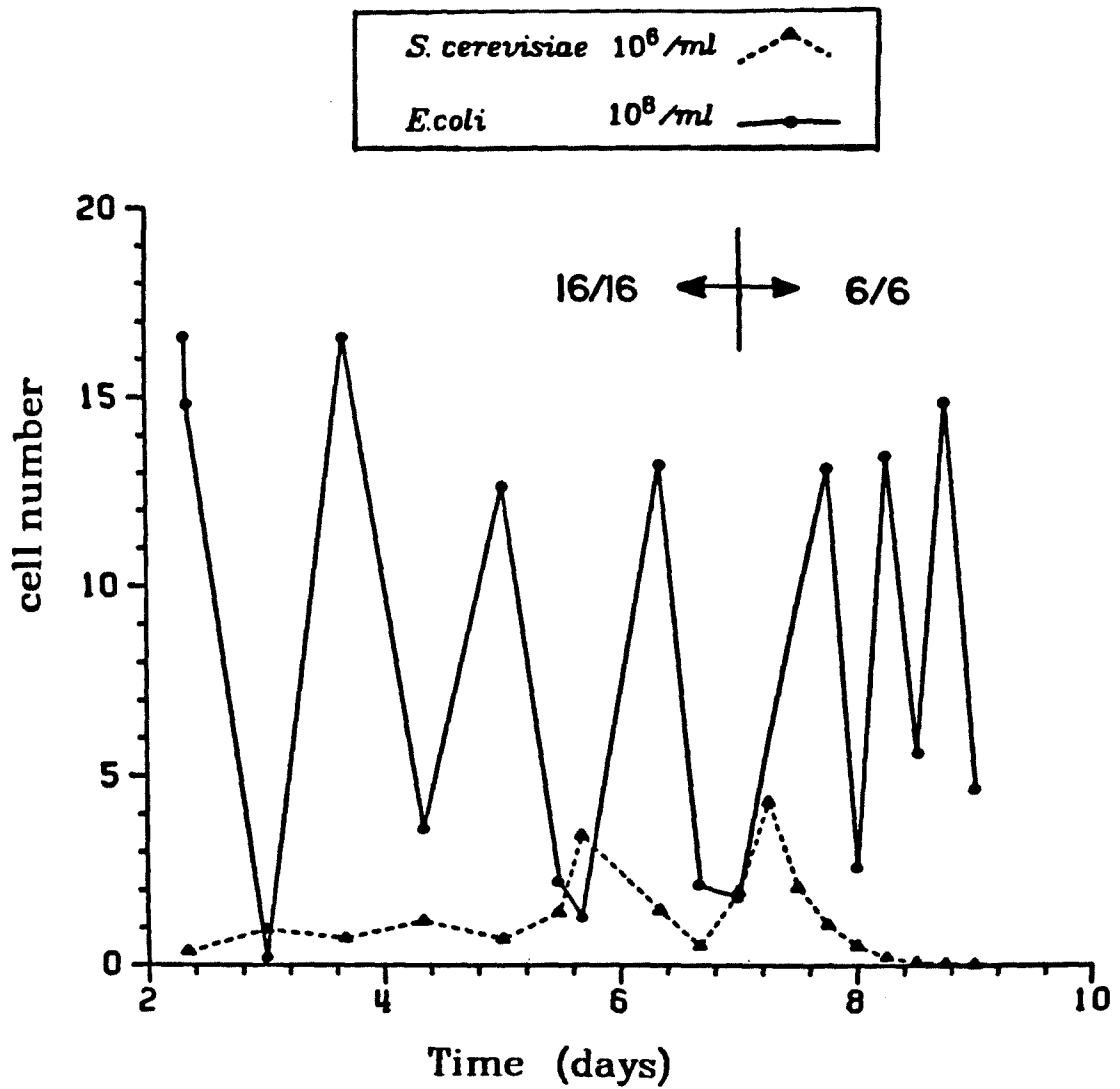


FIGURE 8A

pH Oscillations: Effect of Cycle Period

16 hr pH5./16 hr pH4.3 6 hr pH5./ 6 hr pH4.3

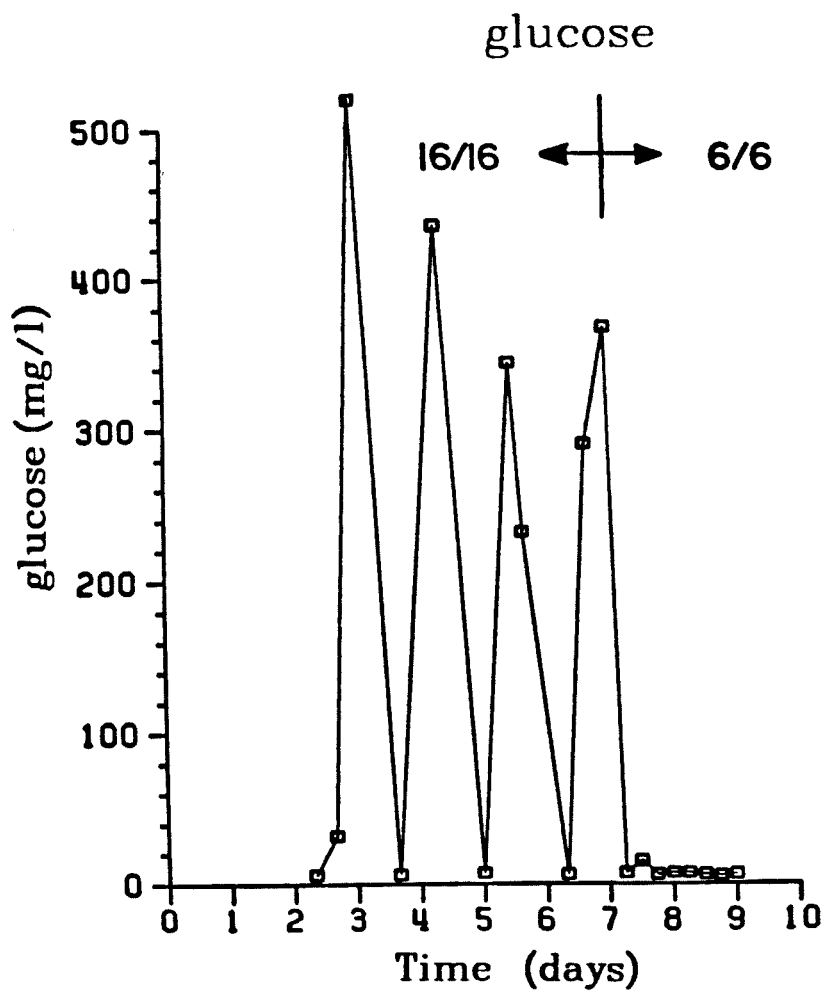


FIGURE 8B

42.
pH Oscillations Computer Simulation
16 hr pH5/16 hr pH4.3

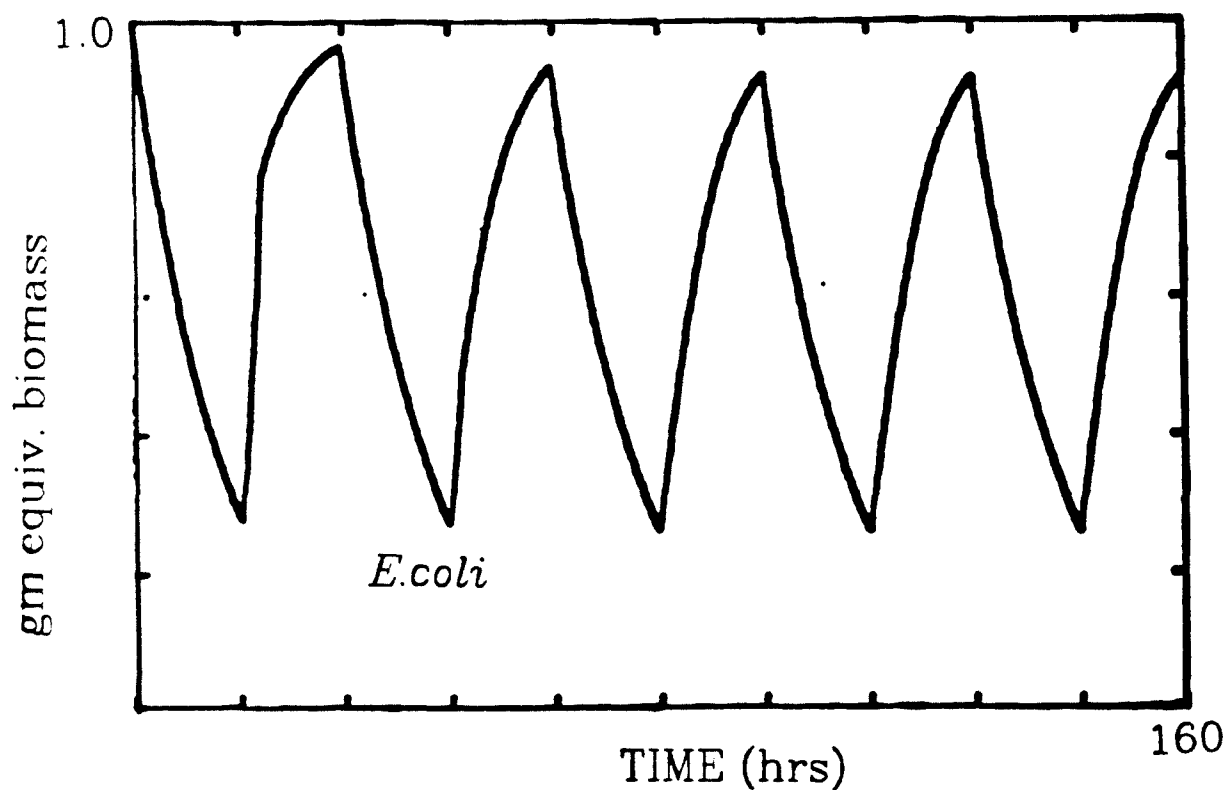
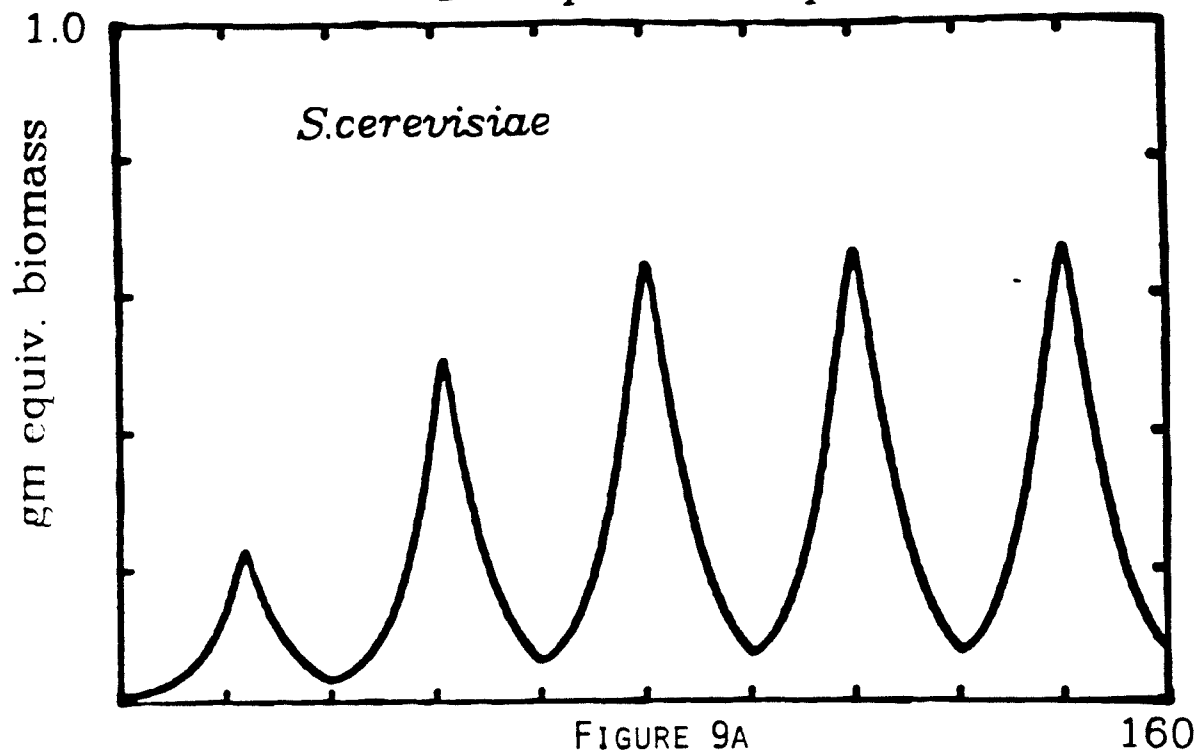


FIGURE 9B

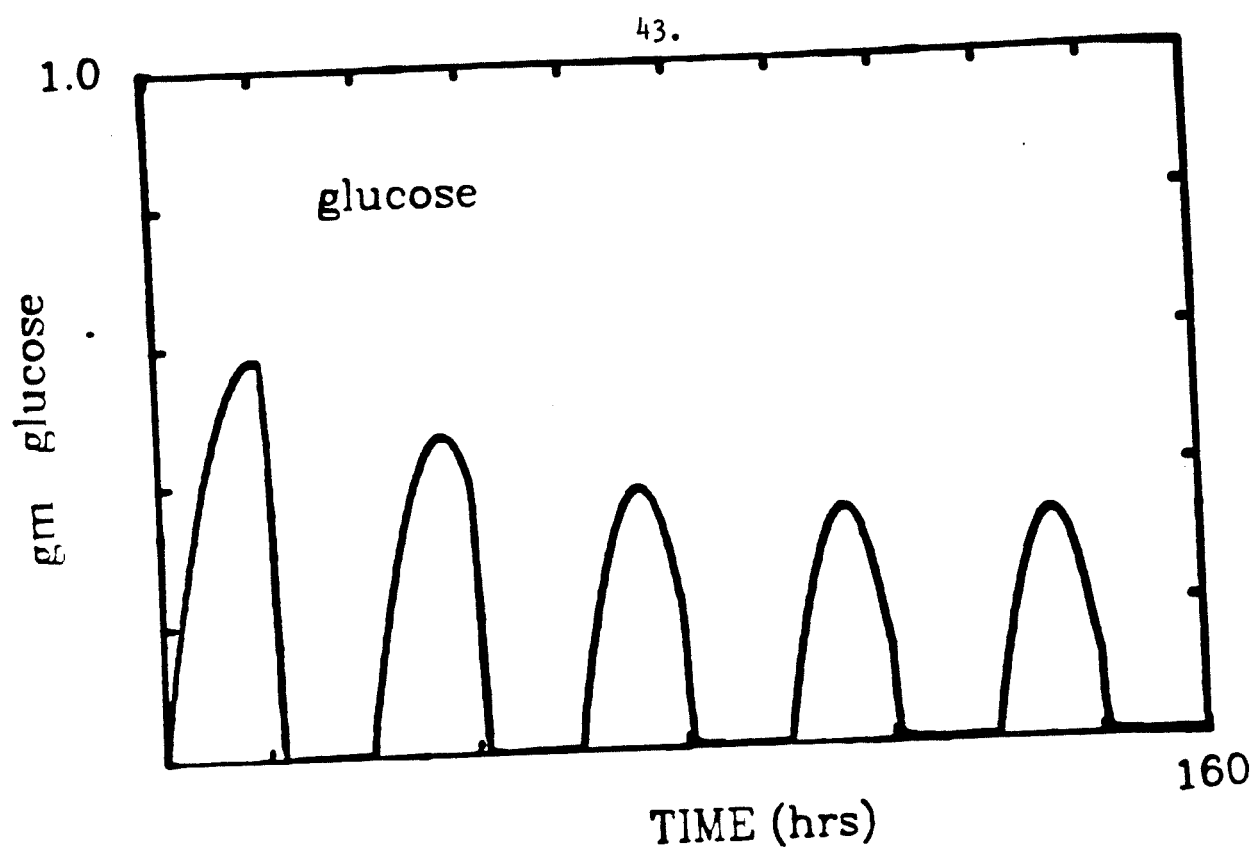


FIGURE 9C

(See **Appendix C** for additional simulations)

18 hr. pH5/ 14 hr. pH4.3

Chapter 3.

**Coexistence of *S. cerevisiae* and *E. coli* in a Chemostat
under Substrate Competition and Product Inhibition**

SUMMARY

A mixed culture of *Saccharomyces cerevisiae* and *Escherichia coli* was established in a stable coexistence steady state in a chemostat under constant operating conditions. The species competed for glucose, the growth limiting resource, and produced acetate and ethanol. The acetic acid was shown to be very inhibitory to *E. coli* in pure culture at pH 5 while ethanol inhibition was only marginal. No significant inhibition of *S. cerevisiae* growth was observed by either acetate or ethanol. Pure culture parameters were measured and used in the analysis. Linearized stability analysis for the case when both organisms produce the inhibitor showed that a transition through three stable outcomes was possible as the feed concentration is lowered. Experimental studies verified these predictions and successive transitions from a yeast growth steady state, to a coexistence steady state, and to a *E. coli* growth steady state were obtained by lowering the glucose concentration in the feed from 10 to 5 to 2.5 g/l. This dynamic behavior is distinctly different from other competition-inhibition combinations and demonstrates for the first time that coexistence is possible due to substrate competition and product inhibition.

INTRODUCTION

Mixed microbial cultures have been studied by microbial ecologists for some time and lately have become the subject of analysis by biochemical engineers. This is due to the increased gene pool that allows a mixed culture system to respond to many situations with potentially higher yields and possible synergistic products. The key to practical use of a mixed culture is understanding and predicting its stability in continuous culture. Mixed culture stability and dominance is also important in comprehending environmental systems.

Pure competition for a single rate-limiting nutrient in a chemostat results in the dominance of the single species which can sustain the lowest steady state substrate concentration. This has been derived theoretically and verified experimentally [Hansen and Hubble, 1980; Jannasch, 1967,1968]. The possibility that the combination of other interactions with competition could allow coexistence was first substantiated by theoretical constructs for many interactions such as growth on mixed substrates, commensalism and predation. Temporal variations can also allow persistence of both species but this is not a coexistence steady state [Chapter 2].

Experimental studies examined some of these interactions and often found additional complicating factors. Commensalism resulted in a stable mixed culture where *Proteus vulgaris* required a growth factor produced by *S. cerevisiae* [Shindala et al., 1965]. Predation can also allow coexistence [Tsuchiya et al., 1972; Canale et al., 1973; Jost et al., 1973]. Coexistence due to multiple substrates is easily understood as each surviving organism grows best on a particular substrate. This has been seen in complex nutrients for two organisms by Lewis [1967], for six species by Lester et al. [1979], and for a pair where each microorganism produces the substrate for the other by Lee et al. [1976].

Many products (and substrates) of microorganisms can be inhibitory, especially at sufficiently high concentrations. Inhibition by products of growth has been considered as a possible stabilizing interaction. An organism producing an inhibitor was thought to gain an edge in persisting in the environment. This evolutionary pressure is thought to be behind antibiotic production and high ethanol levels. Defreitas et al. [1978] analyzed theoretically some combinations of inhibition and competition and found some ranges of parameters, operating conditions, and interactions that could allow coexistence. Till now no experimental studies of inhibition and competition in a defined system have been performed to substantiate this.

The defined system of microorganisms in this study consisted of *Escherichia coli* and *Saccharomyces cerevisiae* on glucose. To grow them together, pH 5 was selected where the yeast grows optimally but where *E. coli* grows but suboptimally. Each species has products from growth on glucose. *E. coli* produces acetate while *S. cerevisiae* produces ethanol and other products including a small amount of acetate [Oura, 1977]. The specific rate of growth and the amount of product formed are related to the nutrient feed concentration. Without product inhibition the product concentration increases linearly with the feed concentration in both batch and continuous culture. At low glucose feed concentrations these by-products concentrations are relatively low and can be ignored. Conversely these product concentrations increase by increasing the glucose in the feed and eventually making product inhibition significant.

In this paper it is experimentally demonstrated that dominance and coexistence can be predicted and explained from pure culture data on the basis of a stability theory for a system of one substrate, two species, and two possibly inhibitory products. Pure culture data are presented first from which the kinetic

growth parameters and the formation rate and inhibitory effect of the products are estimated. The specific growth rate equation assumed is based on Aiba and Shoda's [1969] modification of Monod's model.

$$\mu_j = \frac{\mu_{\max_j} S}{(k_{Sj} + S)(1 + I/K_j^I)} \quad (1)$$

Here μ_{\max} and k_s are Monod's constants for the maximum specific growth rate and substrate saturation respectively. K^I is the inhibition constant, which is equivalent to the concentration of the inhibitor at which the specific growth rate is halved from its value with no inhibitor present. Next a stability analysis of the chemostat equations is developed and the possible outcomes discussed. Stability conditions and operating diagrams are constructed from the independently determined growth parameters. Finally chemostat runs at various operating conditions are presented confirming the theoretical findings and demonstrating the predicted changes in the stability and dominance of the mixed culture as the effect of the level of inhibition is increased by increasing the feed concentration.

Materials and Methods

E. coli and *Saccharomyces cerevisiae* were chosen as the mixed culture pair. Both are common, well-studied organisms, especially when grown on glucose, our chosen substrate. The culture conditions for this pair were described in detail earlier [Chapter 2]. Important features and differences are summarized here.

The cell volumes of the two species are quite separated. *E. coli* is a 2-by-1 μm rod and *S. cerevisiae* is a 5-to-8 μm sphere. This allows particle size analysis by the Coulter Counter to distinguish between the species. [Chapter 2].

The media was a defined glucose media for yeast modified from Oura [1974]. The defined yeast media was mixed, the pH adjusted with KOH, and filter sterilized through a 0.2 μm filter. The recipe is for 1.1 water: 12g $(\text{NH}_4)_2\text{SO}_4$, 0.52g $\text{MgCl}_2 \cdot 6\text{H}_2\text{O}$, 1g glucose, 1.0g KPhthalate, 0.1g EDTA, 1.6 ml 85% H_3PO_4 , 0.12 KCl, 0.09 $\text{CaCl}_2 \cdot 2\text{H}_2\text{O}$, 0.06g NaCl, 3.8 mg $\text{MnSO}_4 \cdot \text{H}_2\text{O}$, 0.5 mg $\text{CuSO}_4 \cdot 5\text{H}_2\text{O}$, 7.3 μg H_3BO_3 , 3.3 μg $\text{Na}_2\text{MoO}_4 \cdot 2\text{H}_2\text{O}$, 2.5 μg NiCl, 2.3 μg $\text{ZnSO}_4 \cdot 7\text{H}_2\text{O}$, 2.3 $\text{CoSO}_4 \cdot 7\text{H}_2\text{O}$, 1.7 μg KI, 35 mg $\text{FeSO}_4(\text{NH}_4)_2\text{SO}_4 \cdot 6\text{H}_2\text{O}$, 125 mg m-inositol, 6.25 mg Pyridoxine-HCl, 6.25 mg Ca-D-Pantothenate, 5 mg Thiamine-HCl, 5 mg Nicotine Acid, and 0.125 mg D-Biotin. Essential vitamins for yeast were included for most batch studies. Glucose feed concentrations were 10, 5 and 2.5 g/l as reported below. The temperature was kept at 30°C for all experiments. Phthalic acid was used as a buffer at pH 5.

The total amount of biomass was estimated by light absorbance measured at 660 nm by a B&L Spectrophotometer.

2 ml of sample were filtered within 3 min. and frozen to await testing for metabolites. The glucose was measured using enzymatic test kit (Sigma # 15-UV) and a UV spectrophotometer. The numerical calibrations for glucose and ethanol were checked and found accurate. Glucose could be detected to 2 mg/l. The ethanol and acetic acid concentrations were above that measurable by enzymatic kits and so ethanol and acetic acid were measured by gas chromatography on Chromosorb 101 in 6' glass column at 150°C with He carrier. The samples must be acidified below pH 3 to ensure accurate AcH detection. Calibration was linear and integration of peak performed automatically with a on-line Shimadzu integrator. The GC results were reproducible to $\pm 5\%$.

The batch experiments were performed in 125 ml erlemeyer flasks with cotton plugs in a rotary shaker. All batch runs were performed in parallel with two or three identical flasks and the results averaged.

Of special note is the experimental procedure followed in order to determine the stability of the various steady states. Instead of running a single chemostat and measuring the biomass composition after a long period of operation when a steady state is presumably reached, two identical chemostats were run in parallel under the conditions of interest. By crossinoculating these chemostats a small perturbation is introduced in the form of a small quantity of inoculum from the other chemostat, then the response of each chemostat to this small perturbation could be studied, and, hence, the stability of the corresponding steady state determined.

The two parallel chemostats allowed each organisms to be acclimated and actively growing in continuous culture before cross inoculation. Since each culture was under identical reactor conditions (the concentration differences being due to the different pure culture steady states of the two organisms), culture shock upon transfer was minimized and lags eliminated. This also allowed effect of starting at two very different initial conditions of biomass to be observed simultaneously under identical reactor conditions and potentially removing some experimental artifacts.

The chemostats used were modified versions of the New Brunswick Bioflow system. The level was maintained by an overflow pump; temperature was controlled by a thermistor and heater. The pH probe (Ingold), controller (Chemtrix), and base reservoir maintained the pH to within ± 0.03 . The chemostat was aerated at 1.5 l/min with stirring at about 300 rpm. A solution of 0.5 gm/l silicone antifoam emulsion was added as needed to control foaming.

Each reactor was sterilized, filled and inoculated with an actively growing culture. The reactor was run batch while biomass increased. Then flow was started before the second diauxic phase to maintain the glucose metabolism.

Flow rates were checked by measuring the overflow. Samples were taken, the absorbance measured and a filtrate frozen for glucose, acetic acid and ethanol analysis. A steady state was assumed if both the biomass and glucose concentrations were constant within 5% over a few residence times. Samples were also diluted with electrolyte and run through the Coulter Counter at the appropriate settings for each. Streak plates were made daily to check for viability and contaminants on YPG and EMB agar.

Pure Culture Parameter Estimation

Multiple batch runs of each pure culture in shaker flasks were performed to determine the maximum specific growth rates and the effects of the two possible inhibitors, ethanol and acetic acid, on the growth rate with glucose as the limiting substrate. All runs were on 1 g/l glucose at pH 5 with phthalate buffer and inoculated with an actively growing culture.

Autoinhibition of ethanol on yeast growth does not occur below 4 g ethanol/l for self-produced ethanol and 100 g/l for added ethanol [Novak, 1981]. Ethanol autoinhibition effects were not observed either in this study. The change of the specific growth rate of *S. cerevisiae* on glucose with increasing acetic acid concentration is shown in Fig. 1. There is no effect at 1 g/l acetic acid and only a small decrease at 4 g/l. Throughout these experiments, even at 10 g/l glucose in the feed, the ethanol and acetic acid concentrations remained below 3 g/l and 0.5 g/l, respectively. The yeast did grow slowly on the acetate after lag phase but only after preferentially consuming all the glucose and ethanol. The *S. cerevisiae* in these experiments is not inhibited or benefited by the major products, ethanol and acetate, of glucose metabolism, and the growth rate of yeast can be written as a function of just glucose, the substrate.

The effect of added ethanol on *E. coli* growth rates is reported in Fig. 2. At pH 5 there is no effect below 2 g/l and only a 20% decrease in μ_{\max} with 12 g/l added ethanol. A K^I for *E. coli* yielding half of the maximum specific growth rate by ethanol inhibition could be extrapolated at 20 g/l EtOH. This is in marked contrast to the inhibition effects observed at pH 4.5. Here the maximum specific growth rate has already been halved due to the acidic condition alone, and K^I is about 0.4 g/l. This is mentioned to point out that while k_s values appear relatively independent of pH, K^I values seem to be strongly pH dependent. Yet since ethanol levels never exceeded 3 g/l in our experiments, the ethanol inhibition of *E. coli* would be negligible at pH 5. Quantitatively there would never be enough ethanol produced by yeast on 10 g/l glucose to lower the growth rate of *E. coli* below the maximum specific growth rate of yeast so that no change in dominance could result from ethanol levels alone.

Experimental results on the inhibition by acetic acid of *E. coli* growing on 1 g/l of glucose at pH 5 are summarized in Fig 3. At 1, 2 and 4 g/l added acetic acid no growth occurs. The batch run at 0.5 g/l acetic acid grew very slowly after a 12-hour lag. Below this acetic acid concentration the batch runs are ineffective as *E. coli* produces about 0.1 g/l acetic acid from growth on 1 g/l glucose. Under these conditions the changing acetate concentration in a batch run would prevent accurate determination of a specific growth. In support of this when *E. coli* was grown batch on 10 g/l glucose all growth ceased after slightly over 500 mg/l acetic acid was produced, despite excess glucose remaining. The rest of the data points in Fig. 3 were garnered from various pure culture chemostat runs where the sugar was in excess (residual sugar greater than 1 g/l). Since K^I is the inhibitor concentration at which the specific growth rate is halved, this indicates a K^I value of about 0.23 g/l HAc. Both the added acetic acid in batch runs and the self-produced acetic acid in continuous runs fell on

the same line and so inhibition effects of internally produced acetate and externally added acetate is assumed to be the same.

Inhibition by acetic acid has not been reported at moderate glucose concentrations under optimal conditions of *E. coli* growth at 37°C and pH 7 [Meyer et al., 1984; Ishikawa et al., 1981]. This appears to be another demonstration of the fact that there is a pronounced increase of inhibition effects under nonoptimal conditions, as was observed earlier with ethanol inhibition. A qualitative observation was that a pH increase from 5 to 5.5 decreased the acetate inhibition effects on *E. coli* growing at steady state in a chemostat. Further work is planned to elucidate this.

Other parameters of concern are the product formation rates. Growth associated production indicates a linear relation as seen in Eq. 2b where the specific formation rate is $\alpha\mu$. Due to the Crabtree effect, ethanol production in yeast is not purely growth associated and we presume that neither that of is acetate. The Crabtree effect explains that yeast respiration is predominant at low growth rates ($D < 0.2 \text{ hr}^{-1}$) and little ethanol is produced, while at higher growth rates fermentation is significant and ethanol is produced. Acetate production in *E. coli* has been reported to be growth and nongrowth associated [Meyer et al., 1984, Doell et al. 1982]. But the specific product formation rates are largely dependent on the growth rate of the culture, which is constant for a particular fixed dilution rate at steady state. Thus for a particular fixed D , the specific formation rate can be treated as a constant. The inclusion of nongrowth associated product formation will not affect the qualitative features [DeFreitas et al., 1978].

The steady state relation ($\alpha_{ij}Y_j = I_i/(s_f - s)$) was used to calculate the yield of product per substrate consumed from the pure culture chemostat runs. The

values are reported in Table 1. αY for acetate is constant when excess sugar is present.

Finally the μ_{\max} and k_s values were estimated from many batch and chemostat runs under different conditions and are also reported in Table 1. As reported earlier [Chapters 2 and 5] the μ_{\max} of *E. coli* is very pH dependent while the μ_{\max} of *Scerevisiae* as well as both k_s values appear virtually pH independent.

Theory

This is a system of two microorganisms, x_1 and x_2 , competing for a single rate-limiting substrate, s , and producing two potentially inhibitory products, I_1 and I_2 . In the most general form, this system may be represented schematically by Fig. 4. The dynamics of this mixed culture growing in a chemostat is described by the following equations:

$$\dot{x}_i = x_i(\mu_i - D) \quad i = 1, 2 \quad (2a)$$

$$\dot{I}_i = \sum_{j=1}^2 \alpha_{ij} \mu_j x_j - DI_i \quad i = 1, 2 \quad (2b)$$

$$\dot{s} = -\sum_{j=1}^2 x_j \mu_j Y_j + D(s_f - s) \quad (2c)$$

where μ_j , the specific growth rate of x_j , may be a function of s , I_1 and I_2 , Y_j is the biomass yield of population j per substrate s consumed, and α_{ij} is the formation yield of I_i per new biomass j . As discussed before, α_{ij} is assumed constant. The specific growth rates are assumed to be given by

$$\mu_i = \frac{\mu_{\max i} s}{(k_{s i} + s)(1 + I_1/K_j^{I_1})(1 + I_2/K_j^{I_2})} \quad (3a)$$

This is derived from Aiba and Shoda's modification of Monod's model where $K_j^{I_i}$ is the inhibitor concentration at which μ_j is reduced by to half the value with no inhibitor. $k_{s i}$ and $\mu_{\max i}$ are the typical Monod parameters.

A linear equation for the effect of an inhibitor would agree better than does the hyperbolic form used here, with the observation that there is a maximum inhibitor concentration above which no growth occurs. But the linear form such as

$$\mu_j = \frac{\mu_{max_j} s}{(K_{sj} + s)} \left[1 - \frac{I_i}{2K_j^I} \right] \quad (3b)$$

would complicate analysis while only making an appreciable difference when the inhibitor concentration was greater than $2K_j^I$. Throughout the continuous runs the inhibitor concentration was always below $2K_j^I$, and so the use of the simpler hyperbolic form is valid.

These system equations were analyzed for stability with respect to small perturbations of the various coexistence (C.S.S.) and partial washout steady states (P.W.S.S.) following DeFreitas [1978]. This system of five variables can be reduced to two by making use of the following time invariants:

$$s = s_f - \frac{x_1}{Y_1} - \frac{x_2}{Y_2} \quad (4a)$$

$$I_1 = \alpha_{11}x_1 + \alpha_{12}x_2 \quad (4b)$$

$$I_2 = \alpha_{21}x_1 + \alpha_{22}x_2 \quad (4c)$$

It should be noted that for constant Y_1 and Y_2 one can obtain from Eqns. 2:

$$\left(s_f - s(t) - \frac{x_1(t)}{Y_1} - \frac{x_2(t)}{Y_2} \right) = \left[\left(s_f - s(0) - \frac{x_1(0)}{Y_1} - \frac{x_2(0)}{Y_2} \right) \right] e^{-t} \quad (5)$$

Eqn. 5 indicates that if the initial state of the chemostat lies on the hyperplane defined by Eqn. 4a then it remains on this hyperplane indefinitely. If the state is not on the hyperplane initially, then the state will approach it exponentially in time. In either case the stability characteristics of the steady state of interest,

which lies on the hyperplane, are not affected for small perturbations, and so, for this purpose, Eqn. 4a can be assumed to be valid at all times. Similar arguments can be employed to justify the substitution of the dynamic equations (2b) by the algebraic equations (4b and 4c) in order to greatly facilitate the stability analysis of the system. With this substitution the system dynamics are described by the biomass differential equations (2a) and the algebraic equations (4) for the abiotic medium. Effectively the system has been reduced from a fifth order system to a second order system with x_1 and x_2 as the independent variables.

There are three types of possible steady states: the washout of both populations (W.S.S.), the washout of only one population while the other grows - also called a partial washout steady state (P.W.S.S.), and the coexistence of both populations (C.S.S.). Two additional equations are required to solve for the steady state in the reduced system. The W.S.S. is defined by $x_1=0=x_2$. The P.W.S.S. with x_1 remaining is defined by $x_1>0$, $x_2=0$ and $\mu_1=D$. The C.S.S. requires that both x_1 and x_2 are positive and that $\mu_1=\mu_2=D$. For these equations, if the C.S.S. exists it will be real, of a nodal type, and so no oscillatory behavior is expected.

The stability of each steady state found from the equations above was determined by linearized stability analysis. Here the differential equations are rewritten using perturbation variables, δx , around the steady state \mathbf{x}^* . All nonlinear terms are linearized around the steady state values and the invariants are used to eliminate I_1 , I_2 , and s . The eigenmatrix of the linearized system of equations is constructed. The eigenvalues are the roots of the quadratic characteristic equation. The steady state is stable if and only if both eigenvalues are negative for the set of kinetic parameters used. The Routh test was used to determine the conditions under which both eigenvalues are negative and real for the

steady state under scrutiny. Results can be easily summarized and presented in the form of stability diagram [Jost,1978] which defines the regions of stability of the various steady states in the operating plane (D, s_f). Similar results and diagrams can also be found in DeFreitas and Fredrickson, [1978] who studied the effect of various parameter values for two subsets of Fig. 4: specific autoinhibition (Fig. 5a) and specific cross inhibition (Fig. 5b). They found that some cases of autoinhibition could allow coexistence while no cases of specific cross inhibition could produce this result.

On the basis of the pure culture experiments reported in the previous section and the pure culture parameters summarized in Table 1, some of the possible interactions of the all-inclusive structure of Fig. 4 can be eliminated and the overall situation significantly simplified. Fig. 6 illustrates the interactions that were examined where x_1 is *E. coli*, I_1 is acetic acid, x_2 is *S. cerevisiae* and I_2 is ethanol. No inhibition of yeast is considered. Operating diagrams for three further simplifications of Fig. 6 were constructed and presented in Fig. 7a, 7b and 7c to observe separately the effects of various interactions. Here the growth rate of *S. cerevisiae* is a function of just substrate and independent of the inhibitors.

The curves that form the boundaries between different regions of stability are found by setting $D=\mu_1(s,I_1,I_2)=\mu_2(s)$ and using the invariants (Eqns. 4) for various extremes of biomass (e.g. by setting x_1 , or x_2 , or both equal to 0). For example the W.S.S. has $x_1=x_2=0$, therefore $I_1=I_2=0$ and $s=s_f$ from the invariants. Thus the boundary occurs at $D = \max [\mu_1(s_f),\mu_2(s_f)]$. The stable steady states on each side of the boundary must still be found. This is because the boundary curves are found from existence criteria of the different possible S.S., not from stability arguments. The existence of a S.S. does not imply it is stable. The stability tests are necessary for the possible S.S. within each region and the stable outcomes

are indicated on the diagrams.

If there was no production of inhibitors ($\alpha_{ij} = 0 : i,j=1,2$), the stability diagram reduces to that of pure competition consisting of just the two curves $\mu_1(s_f)=D$ for each species. Then there are only two possible stable outcomes: a P.W.S.S. for $D < \mu_1(s_f)$ with *E. coli* dominance and yeast washout since the *E. coli* will always grow faster (i.e. $\mu_1(s_f) > \mu_2(s_f)$), or a total washout if $D > \mu_1(s_f)$. Both of these curves, $\mu_1(s_f)$ and $\mu_2(s_f)$, are included on the following stability diagrams for clarity.

In Fig. 7a all acetate production and inhibition was neglected (i.e. $\alpha_{1j}=0, K_j^{I1} \rightarrow \infty, j=1,2$). Here μ_1 for *E. coli* is just a function of substrate and ethanol or $\mu_1(s, I_2)$. Considering only ethanol inhibition, the outcomes are a W.S.S. if $D > \mu_1(s_f, 0)$, a P.W.S.S. with *E. coli* growing, and a third region where a C.S.S. exists but is an unstable saddlepoint and both P.W.S.S. are stable. The boundary between the W.S.S. and the *E. coli* dominant P.W.S.S. is, of course, the curve $D = \mu_1(s_f, 0)$. Between the two different P.W.S.S. regions, the boundary is found by finding where a P.W.S.S. with *Scerevisiae* can exist, or more explicitly by setting $x_1=0, D = \mu_1(s, I_2) = \mu_2(s)$, and using the invariants (Eqns. 4a and 4c). The curve is $D = \mu_1(s, I_2)$ where s and I_2 are evaluated as $s = \frac{Dk_{s2}}{\mu_{max2} - D}$ and $I_2 = \alpha_{22}(s_f - s)Y_2$.

In the third region both P.W.S.S are stable and either P.W.S.S. may result depending on the initial conditions. This region occurs for glucose feed concentrations larger than 40 g/l which are far above the range of conditions used in our experiments.

Ethanol and acetate production by yeast is ignored in Fig. 7b and only *E. coli* autoinhibition by acetate is considered (i.e. $\alpha_{12}=0=\alpha_{22}$). Thus μ_1 can now be

written as $\mu_1(s, I_1)$, a function of just glucose and acetate. Again washout occurs when $D > \mu_1(s_f, 0)$. The other two outcomes are an *E. coli* dominant P.W.S.S. and a broad region of coexistence. For the C.S.S. to be real it is necessary but not sufficient that $D < \mu_2(s_f)$. Similar to the previous case the boundary was found by setting $D = \mu_1(s, I_1) = \mu_2(s)$ and using the invariants, Eqns. 4a and 4b, with $x_1 = 0$. The curve is $D = \mu_1(s, I_1)$ where s and I_1 are evaluated as $s = \frac{Dk_{s2}}{\mu_{max2} - D}$ and $I_1 = \alpha_{12}(s_f - s)Y_2$. The region within this curve was found to be one of stable coexistence. Here coexistence is achieved by *E. coli* producing sufficient acetate to slow its own growth rate to match that of *S. cerevisiae*.

Finally Fig. 7c neglects only ethanol inhibition but includes inhibition by the acetate produced by both *E. coli* and *S. cerevisiae*. Surprisingly four outcomes are predicted: a W.S.S. as before, a P.W.S.S. with *E. coli*, a C.S.S., and a P.W.S.S. with *S. cerevisiae*. For the yeast P.W.S.S. or the C.S.S. to be real it is necessary but not sufficient that $D < \mu_2(s_f)$. The boundary curve between the P.W.S.S. with *E. coli* growth and the C.S.S. is $D = \mu_1(s, I_1)$ where $s = \frac{Dk_{s2}}{\mu_{max2} - D}$ and $I_1 = \alpha_{12}(s_f - s)Y_2$. This is identical to the boundary in Fig. 7b. The boundary between the C.S.S. and the P.W.S.S. with *S. cerevisiae* growth is found in the same way except x_2 is set equal to 0 instead of x_1 . Therefore the curve is $D = \mu_1(s, I_1)$ where $s = \frac{Dk_{s2}}{\mu_{max2} - D}$ and $I_1 = \alpha_{11}(s_f - s)Y_1$. Remember that *E. coli*'s specific acetate formation rate, α_{11} , is more than twice that of *S. cerevisiae*, α_{12} . The P.W.S.S. of *S. cerevisiae* washout and *E. coli* dominance occurs at low feed concentrations and low growth rates where inhibition is not important and the faster growing species (*E. coli*) wins, and also occurs when at high D when the μ_{max} of *S. cerevisiae* is exceeded. As earlier explained the C.S.S. occurs primarily from *E. coli* autoinhibition from acetate. Finally at high feed concentrations the yeast alone

can produce sufficient acetate to severely inhibit *E. coli* and cause *E. coli* to washout.

The magnitude of $K^1/\alpha Y$, a ratio of inhibition effect to production rate, shows that ethanol inhibition is an order of magnitude smaller than acetate inhibition in *E. coli* and can be ignored. Comparing the full effects of ethanol (Fig. 7a) and acetate (Fig. 7c) the addition of ethanol will have a negligible effect on the acetate case when $s_f \leq 10g/l$. Thus the outcomes of Fig. 7c are the ones to be tested for experimentally.

A useful tool for interpreting and expediting experimental tests for stability is a phase plane diagram. Since the use of invariants reduces the systems to two independent variables, the state trajectories are restricted to the (x_1, x_2) plane are bounded by the line $s_f + x_1/Y_1 + x_2/Y_2 = 0$. The conceptual utility is to check the stability of the two P.W.S.S. If a pure continuous culture of one species is inoculated at steady state with a small amount of the second species and the second species washes out, the P.W.S.S. with species 1 growing is stable. On the other hand, if the second species increases, the outcome must be either a C.S.S. or the P.W.S.S. with species 2 present. This also can be tested by inoculating a pure culture of species 2 with species 1 and comparing the results in a similar manner. If both the P.W.S.S. are unstable at the same conditions, then the C.S.S. must exist and be stable. These three possible phase planes are schematically represented in Fig. 8. They show the initial trajectories and possible outcomes of cross inoculation experiments by testing the two P.W.S.S.. For the schematic trajectories shown the conclusions are that species 1 is stable in the schematic of Fig. 8a, species 2 is stable in Fig. 8b, and the C.S.S. is stable in Fig. 8c. Thus the stability of C.S.S. and P.W.S.S. can be tested by the initial trajectories of two cross-inoculation experiments at a particular set of operating conditions without necessarily waiting for the system converge to any

particular steady state. The use of chemostats in parallel allowed these stability tests to be performed simultaneously.

Experimental Results of Continuous Mixed Culture

The experiments were run at high dilution rates ($0.2/\text{hr} < D < 0.37/\text{hr}$) and at three feed concentrations (10, 5 and 2.5 g/l glucose). Earlier experiments [Chapter 2] with 1 g/l feed showed no or minimal inhibition effects and *E. coli* dominance at pH 5.0 at all D . Two identical chemostats were run simultaneously, each chemostat containing one species established at steady state. The chemostats were cross inoculated with small but detectable amounts of actively growing acclimated cultures from the other chemostat as necessary. The results are reported in Fig. 9-18 as the change of cell number of *E. coli* and *S. cerevisiae* with time after cross inoculation. Glucose, ethanol and acetic acid are also reported in the adjoining figures (Fig. 9-18b). The run number designates the chemostat (A or B) and the order of experiments. The two chemostats were kept at identical flow rate and feed concentration. Table 2 summarizes the important points of certain critical runs and their experimental plots are described below in detail.

At $D = 0.31/\text{hr}$ and a feed of 10 g/l glucose, a small inoculum of *E. coli* washes out of a yeast culture (Figs. 9 and 10). In light of the inhibition studies above the approximately 150 mg/l acetic acid present in the yeast culture is important. In the other chemostat, Run B1, Fig. 11, a small inoculum of yeast increases steadily on the excess glucose present in the *E. coli* steady state while the *E. coli* washes out. These runs of *E. coli* vs. *S. cerevisiae* are comparable to the phase plane of Fig. 8b and clearly demonstrate the stability of only the pure yeast steady state under these conditions.

Next with $D = 0.34/\text{hr}$ and $s_f = 5 \text{ g/l}$ (Fig. 13), Run A4 shows that *S. cerevisiae* will increase against an established pure *E. coli* culture, while in Run B3 (Fig. 15), *E. coli* increases against a *S. cerevisiae* culture. These results and an examination of the phase plane in Fig. 8c require that each pure culture partial washout steady state is unstable, therefore the coexistence steady state of the mixed culture must be stable. It appears that the coexistence steady state was actually achieved by the end of Run B3 but this is not essential for the above argument to be valid. The final important observation is from Run B6 (Fig. 17). A yeast pure culture at $D = 0.2/\text{hr}$ and $s_f = 2.5 \text{ g/l}$ lost to a small inoculum of *E. coli* which quickly established a near steady state culture with a residual glucose level of 10 mg/l far below the yeast steady state value. This indicates the stability of the *E. coli* pure culture and the instability of the yeast culture under these conditions with a trajectory like that of Fig. 8a.

Discussion

It is useful at this point to be reminded of the continuous pure culture data. When *E. coli* grew on a feed of 10 g/l the residual sugar was in excess for all the dilution rates used to construct Fig. 3. This was due to the significant autoinhibition of *E. coli* due to acetate production. In contrast, *S. cerevisiae* at the same operating conditions had minimal sugar and significant acetate and ethanol concentrations. These observations are further substantiate that at high s_f values the P.W.S.S. with *E. coli* growing is unstable and the P.W.S.S. with yeast growing may be stable. At 2.5 g/l and below both cultures have minimal residual sugar and low product concentrations. Here competition should be the major interaction and *E. coli* should dominate. A summary of the mixed culture results is in Table 2.

All parameters used are summarized in Table 1. With respect to the complete

model of interactions depicted in Fig. 4, certain parameters of the model equations (2) were assumed to be zero or infinite as needed. Of the three simplifications described earlier and presented in Figs. 7 only the case 3 (Fig. 7c) can account for the full dynamic behavior observed, namely the transition from *E. coli* dominance to coexistence to pure *S. cerevisiae* with increasing s_f . These experiments thus demonstrate that inhibition can cause a coexistence steady state. This is the first experimentally stable coexistent mixed culture not involving multiple substrates, a commensal culture isolated from nature, or reinoculation from the walls. Also the existence of the C.S.S. or P.W.S.S. can be predicted from pure culture data with unstructured models and linearized stability analysis. These experiments show that defined mixed cultures and conditions can be used to test and possibly confirm the many theories of stability for mixed culture abounding at present.

A caution is that the use of an "a priori" defined mixed culture such as this necessarily may involve nonoptimal conditions for one or both organisms in some compromise chosen by the operator. This nonoptimality can expand the possible interaction with a mixed culture pair but the pure cultures must be reevaluated under these nonoptimal conditions and care exercised in use of published optimal growth data.

Finally this work demonstrates dramatically the hazards in increasing feed concentration for higher productivity. Inhibition which was negligible at low s_f became very important at moderate s_f and gave rise to unexpected dynamic phenomena. For this reason successful mixed culture must be based on a careful analysis and evaluation of possible population interactions as obtained from pure culture growth experiments.

Acknowledgement:

This work was supported by the National Science Foundation through Grant # xxxxxx and through a Presidential Young Investigator Award to one of the authors (G.N.S.)

NOTATION

D	dilution rate (hr^{-1})
I_i	inhibitor concentration (g/l); [$i=1$, acetic acid; $i=2$, ethanol]
$K_j^{I_i}$	inhibition constant of species j to inhibitor i (g/l)
k_{s_j}	substrate saturation constant for species j (g/l)
s	substrate (g/l)
s_f	substrate concentration of chemostat feed (g/l)
t	time (hr)
x_j	biomass concentration of species j (g/l); [$j=1$, <i>E. coli</i> ; $j=2$, <i>S. cerevisiae</i>]
Y_j	yield coefficient of species j per substrate consumed (g/g)
α_{ij}	formation yield of I_i per new biomass j (g/g)
μ_j	specific growth rate of species j (hr^{-1})
$\mu_{\max j}$	maximum specific growth rate of species j (hr^{-1})

REFERENCES

- Aiba, S., and M. Shoda (1969). 'Reassessment of the Product Inhibition in Alcohol Fermentation," *J. Fermentation Technol.*, **47**, 790.
- Canale, R.P., T.D. Lustig, P.M. Kehrberger, and J.E. Salo (1973). 'Experimental And Mathematical Modeling Studies of Protozoan Predation on Bacteria," *Biotech. Bioengr.*, **15**, 707.
- DeFreitas, Max J., Fredrickson, A.G. (1978). 'Inhibition as a Factor in the Maintenance of the Diversity of Microbial Ecosystems," *J. General Microbiology*, **106**, 307.
- Doelle, H.W., K.E. Ewings, and N.W. Hollywood (1982). 'Regulation of Glucose Metabolism in Bacterial Systems," *Adv. in Biochemical Engr.*, **23**, 1.
- Hansen, S., Hubble, S. (1980). 'Single Nutrient Microbial Competition: Qualitative Agreement Between Experimental and Theoretical Forecast Outcomes, *Science*, **207**, 1491.
- Ishikawa, Y., Y. Nonoyama, and M. Shoda (1981). 'Microcalorimetric Study of Aerobic Growth of *E. coli* in Batch Culture," *Biotech. & Bioengr.*, **23**, 2825.
- Jannasch, Holger W. (1967). 'Enrichments of Aquatic Bacteria in Continuous Culture," *Archiv fur Mikrobiologie*, **59**, 165.
- Jannasch, Holger W. (1968). 'Competitive Elimination of Enterobacteriaceae from Seawater," *J. Applied Microbiology*, **16**, 1616.
- Jost, J.L., Drake, J.F., Tsuchiya, H.M., Fredrickson, A.G. (1973). *J. Theoretical Biol.*, **41**, 461.
- Lee, I.H., Fredrickson, A.G., Tsuchiya, H.M. (1976). *Biotech. Bioeng.*, **18**, 513.
- Lester, J.N., R. Perry, and A.H.Dadd (1979). 'Cultivation of a Mixed Bacterial Population of Sewage Origin in the Chemostat," *Water Res.*, **13**, 545.
- Lewis, P.M. (1967). 'A Note on the Continuous Culture of Mixed Populations of Lactobacilli and Streptococci," *J. Appl. Bact.*, **30**, 406.

- Meyer, H-P., C. Leist, and A. Fiechter (1984). "Acetate Formation in Continuous Culture of E.coli K12 D1 on Defined and Complex Media," *J. Biotech.*, **1355**.
- Novak, M., P. Strehaiano, M. Moreno, G. Goma (1981). "Alcoholic Fermentation: On the Inhibitory Effect of Ethanol," *Biotech. and Bioengr.*, **23**, 201.
- Oura, E. (1974). "Effect of Aeration Intensity on the Biochemical Composition of Baker's Yeast. I. Factors Affecting the Type of Metabolism," *Biotech. and Bioengr.*, **16**, 1197.
- Oura, E. (1977). "Reaction Products of Yeast Fermentations," *Process Biochemistry*, April, 19.
- Shindala, A., H.R. Bungay, N.R. Krieg, and K. Culbert (1965). "Mixed Culture Interactions: I. Commensalism of *Proteus vulgaris* with *Saccharomyces cerevisiae* in Continuous Culture," *J. Bacteriol.*, **89**, 693.
- Tsuchiya, H.M., J.F. Drake, J.L. Jost, and A.G. Fredrickson (1972). "Predator-Prey Interactions of *Dictyostelium discoideum* and *Escherichia coli* in Continuous Culture," *J. Bacteriol.*, **6**, 1147.

Table 1. Kinetic Growth Parameters pH5

	<i>S. cerevisiae</i>	<i>E. coli</i>
μ_{\max} (hr ⁻¹)	0.4	0.6
k_s (mg/l glucose)	50	5
K^I_1 (g/l AcH)	8	0.23
K^I_2 (g/l EtOH)	100	20
αY (g AcH/g glucose)	0.025	0.052
αY (g EtOH/g glucose)	0.3	0.

Table 2. Stability Results

Runs	s_f	D	
A1,A2,B1	10	0.31	<i>S. cerevisiae</i> dominates
A3,B2	5	0.37	<i>E. coli</i> appears dominate, not confirmed by inoc pure <i>E. coli</i>
A4,B3	5	0.34	Coexistent S.S.*
B5,B4	2.5	0.34	<i>E. coli</i> dominant
B6		0.20	<i>E. coli</i> dominant

* Abs₁₀ = 0.075, s = 0.104, ETOH = 1.50 g/l, HAc = 0.182 g/l, #Ec/ml = 6.06E8,
#Sc/ml = 15.1 E6.

List of Figure Captions

Figure 1. Inhibition by Acetic acid of μ_{\max} of *S. cerevisiae* on 1 g/l glucose at pH 5.

Figure 2. Inhibition by ethanol of μ_{\max} of *E. coli* on 1 g/l glucose at pH 5 and at pH 4.5.

Figure 3. Specific growth rate of *E. coli* in the presence of excess glucose at pH 5 as a function of acetic acid concentration.

Figure 4. System of all possible interactions of two species, one substrate, and two inhibitory products.

Figure 5. Subcases of Fig. 4, theoretically examined by DeFreitas et al. [1978], 5a. Specific Autoinhibition, 5b. Specific Cross Inhibition.

Figure 6. Possible important interactions for *E. coli*, x_1 , and *S. cerevisiae*, x_2

Figure 7. Stability diagrams showing the stable outcomes for different regions of the operating conditions (D, s_f) . All figures include the curves $\mu_1(s_f, 0, 0)$ — and $\mu_2(s_f)$ ----.

Figure 7a. Stability diagram - only ethanol inhibition is considered, acetate production is neglected.

Figure 7b. Stability diagram - only acetate production by *E. coli* is considered, ethanol and acetate production by *S. cerevisiae* is neglected.

Figure 7c. Stability diagram - acetate production by both *E. coli* and *S. cerevisiae* is considered, ethanol production by *S. cerevisiae* is neglected.

Figure 8. Schematics of phase plane diagrams of x_1 vs. x_2 showing three possible outcomes for dual initial trajectory tests and the steady state stability required for each. • denotes a stable P.W.S.S., O denotes an unstable P.W.S.S..

Figure 9. Run A1: pure culture S.S. of *S. cerevisiae* perturbed with *E. coli* at $D=0.31/\text{hr}$ and $s_f = 10 \text{ g/l}$.

Figure 10. Run A2: pure culture S.S. of *S. cerevisiae* perturbed with *E. coli* at $D=0.31/\text{hr}$ and $s_f = 10 \text{ g/l}$.

Figure 11. Run B1: pure culture S.S. of *E. coli* perturbed with *S. cerevisiae* at $D=0.31/\text{hr}$ and $s_f = 10 \text{ g/l}$.

Figure 12. Run A3: pure culture S.S. of *E. coli* perturbed with *S. cerevisiae* at $D=0.37/\text{hr}$ and $s_f = 5 \text{ g/l}$.

Figure 13. Run B2: pure culture S.S. of *S. cerevisiae* perturbed with *E. coli* at $D=0.37/\text{hr}$ and $s_f = 5 \text{ g/l}$.

Figure 14. Run A4: pure culture S.S. of *E. coli* perturbed with *S. cerevisiae* at $D=0.34/\text{hr}$ and $s_f = 5 \text{ g/l}$.

Figure 15. Run B3: pure culture S.S. of *S. cerevisiae* perturbed with *E. coli* at $D=0.34/\text{hr}$ and $s_f = 5 \text{ g/l}$.

Figure 16. Run B4: pure culture S.S. of *S. cerevisiae* perturbed with *E. coli* at $D=0.34/\text{hr}$ and $s_f = 2.5 \text{ g/l}$.

Figure 17. Run B5: pure culture S.S. of *S. cerevisiae* perturbed with *E. coli* at $D=0.34/\text{hr}$ and $s_f = 2.5 \text{ g/l}$.

Figure 18. Run B6: pure culture S.S. of *S. cerevisiae* perturbed with *E. coli* at

$D=0.20/\text{hr}$ and $s_f = 2.5 \text{ g/l}$.

Figure 19. Phase Plane of Runs A1, A2, and B1. (arrows denote temporal sequence of readings)

Figure 20. Phase Plane of Runs A4 and B3. (arrows denote temporal sequence of readings)

Figure 21. Phase Plane of Run B6. (arrows denote temporal sequence of readings)

FIGURE 1.
ACETIC ACID INHIBITION OF S.CEREVISIAE
1 G/L GLUCOSE, PH5

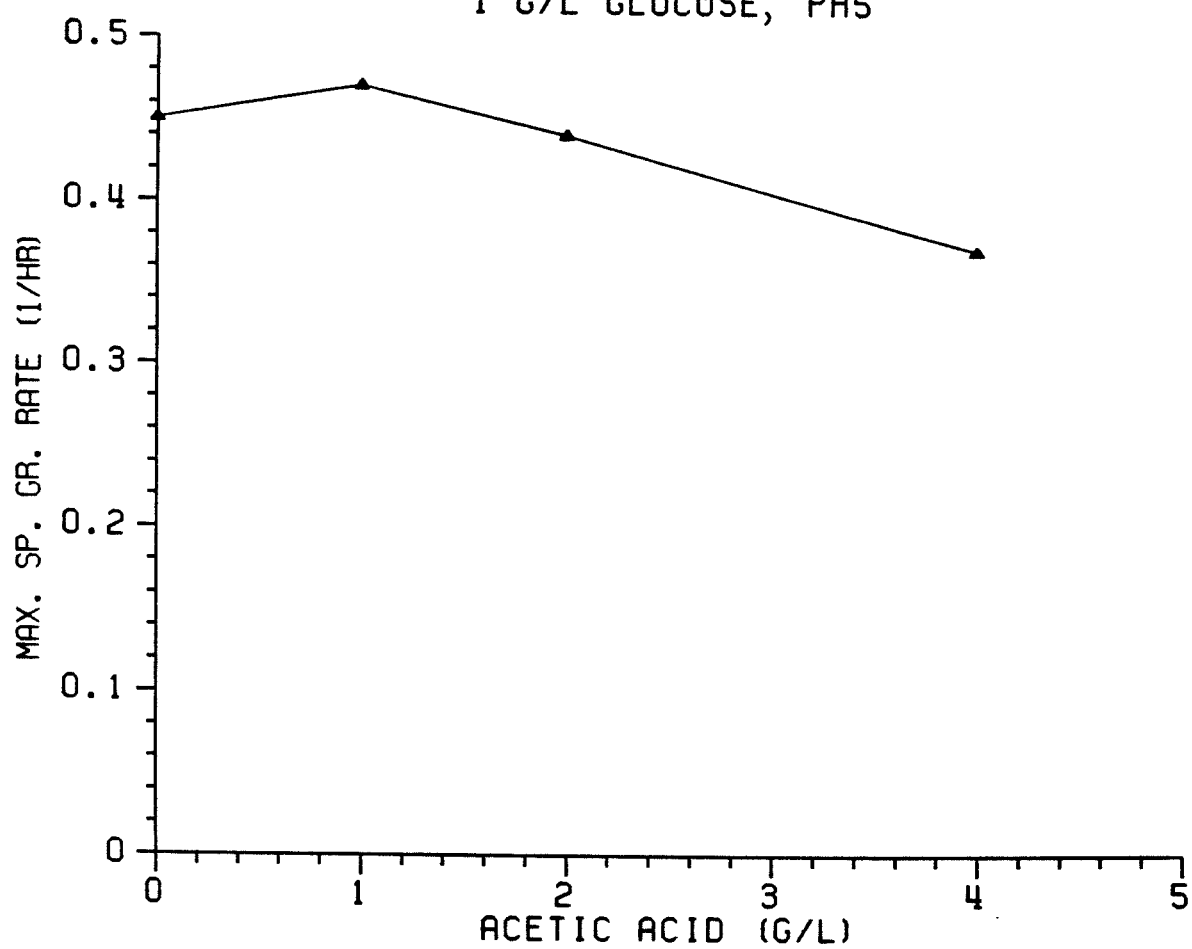


FIGURE 2.
ETOH INHIBITION OF E.COLI
SF=1 G/L GLUCOSE

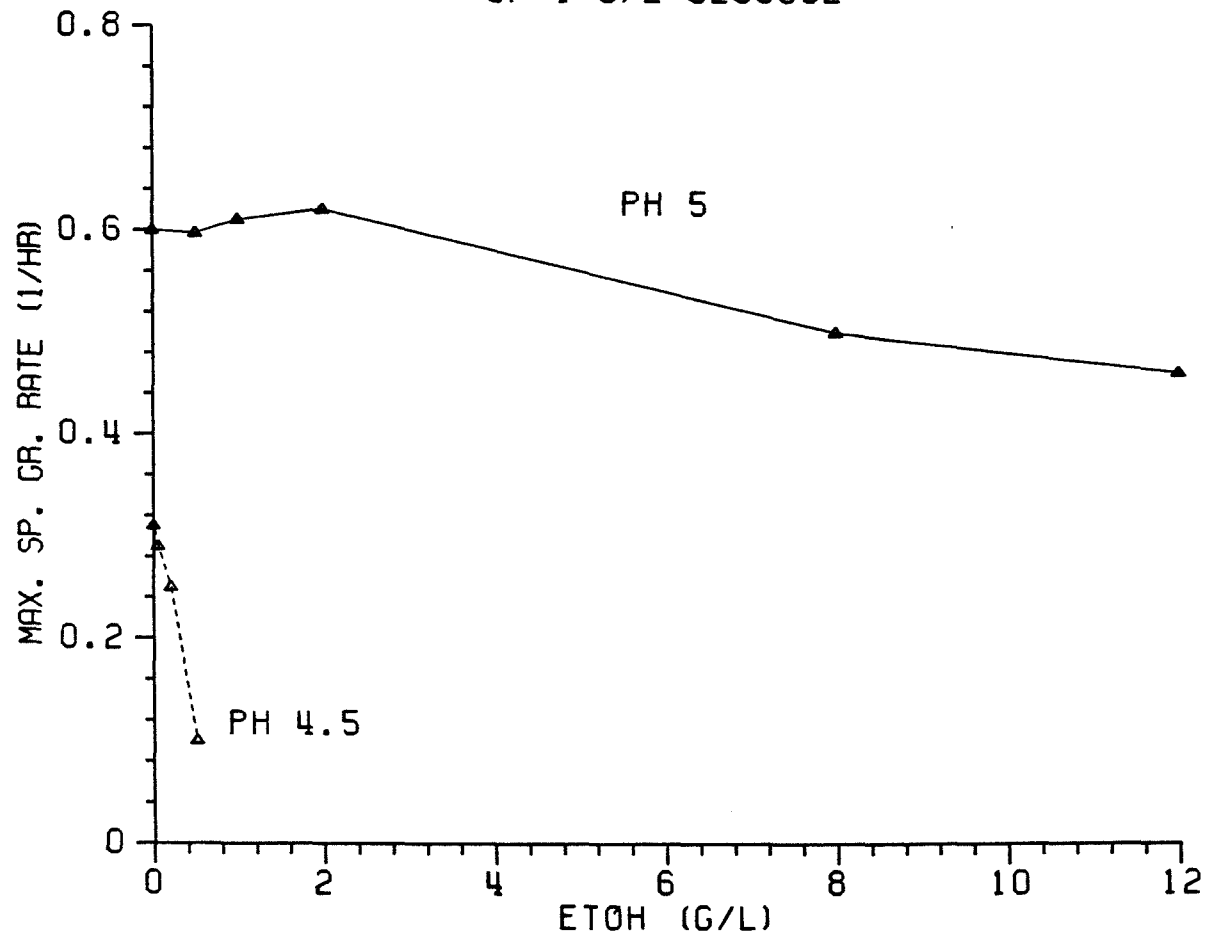
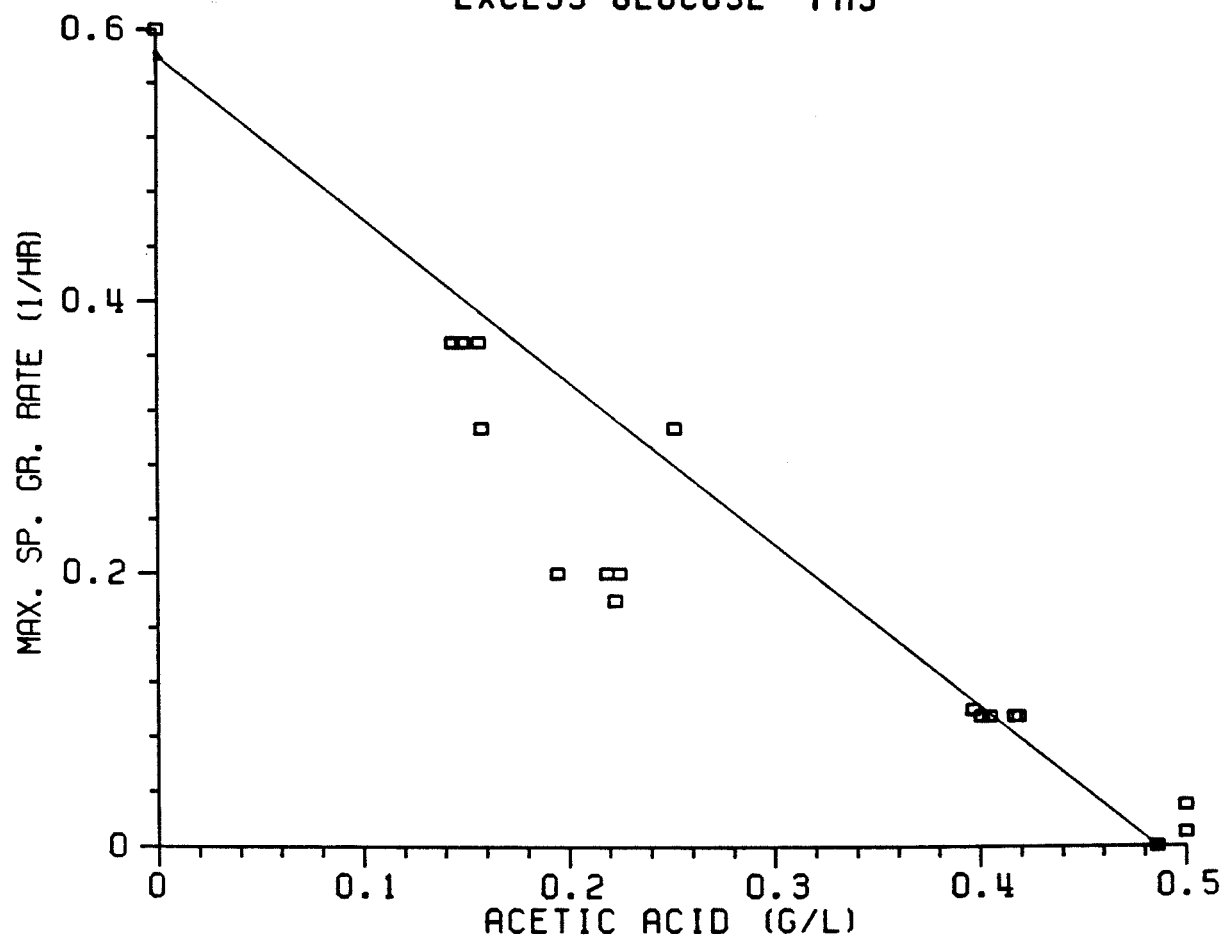


FIGURE 3.
ACETIC ACID INHIBITION OF E.COLI
EXCESS GLUCOSE PH5



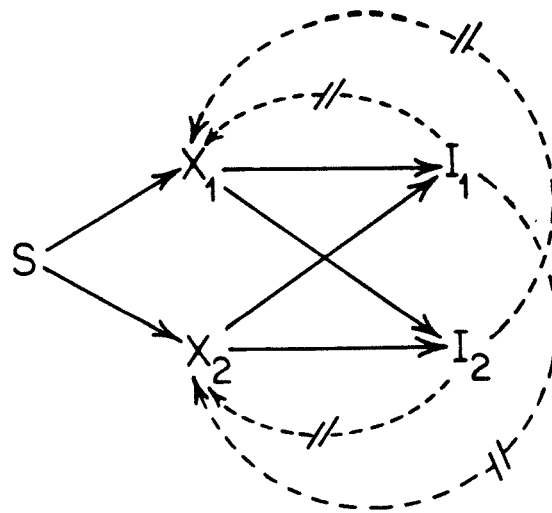
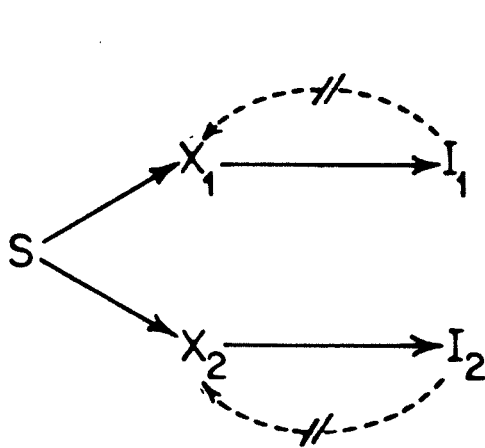
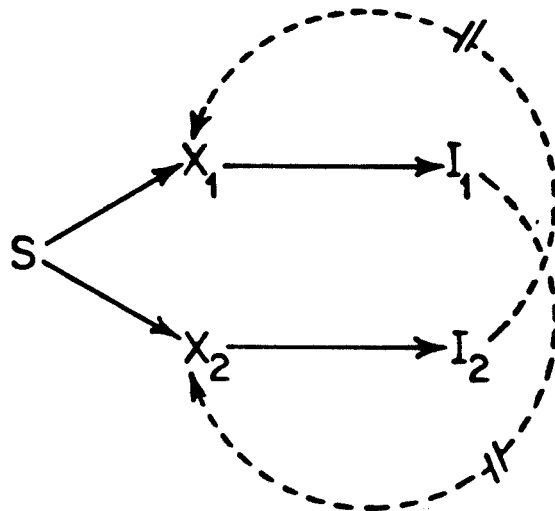


Figure 4. System of all possible interactions of two species, one substrate, and two inhibitors.

Figure 5. Subcases of Figure 4, examined by De Freitas et al. (1978).



Specific autoinhibition.
Figure 5a.



Specific cross inhibition.
Figure 5b.

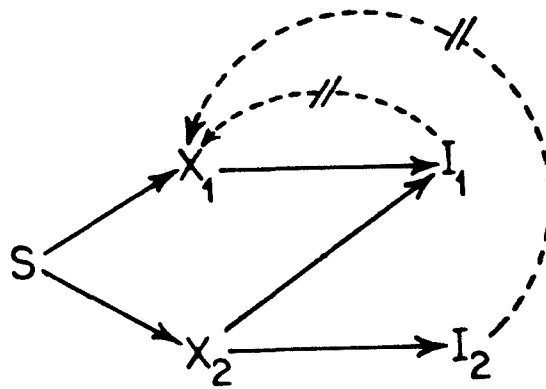


Figure 6. Possible interactions for *S. cerevisiae* and *E. coli*.

Figure 7. Stability diagrams showing the stable outcomes for different regions of the operating conditions (D, s_f) . All figures include the curves $\mu_1(s_f, 0, 0)$ — and $\mu_2(s_f)$ ----

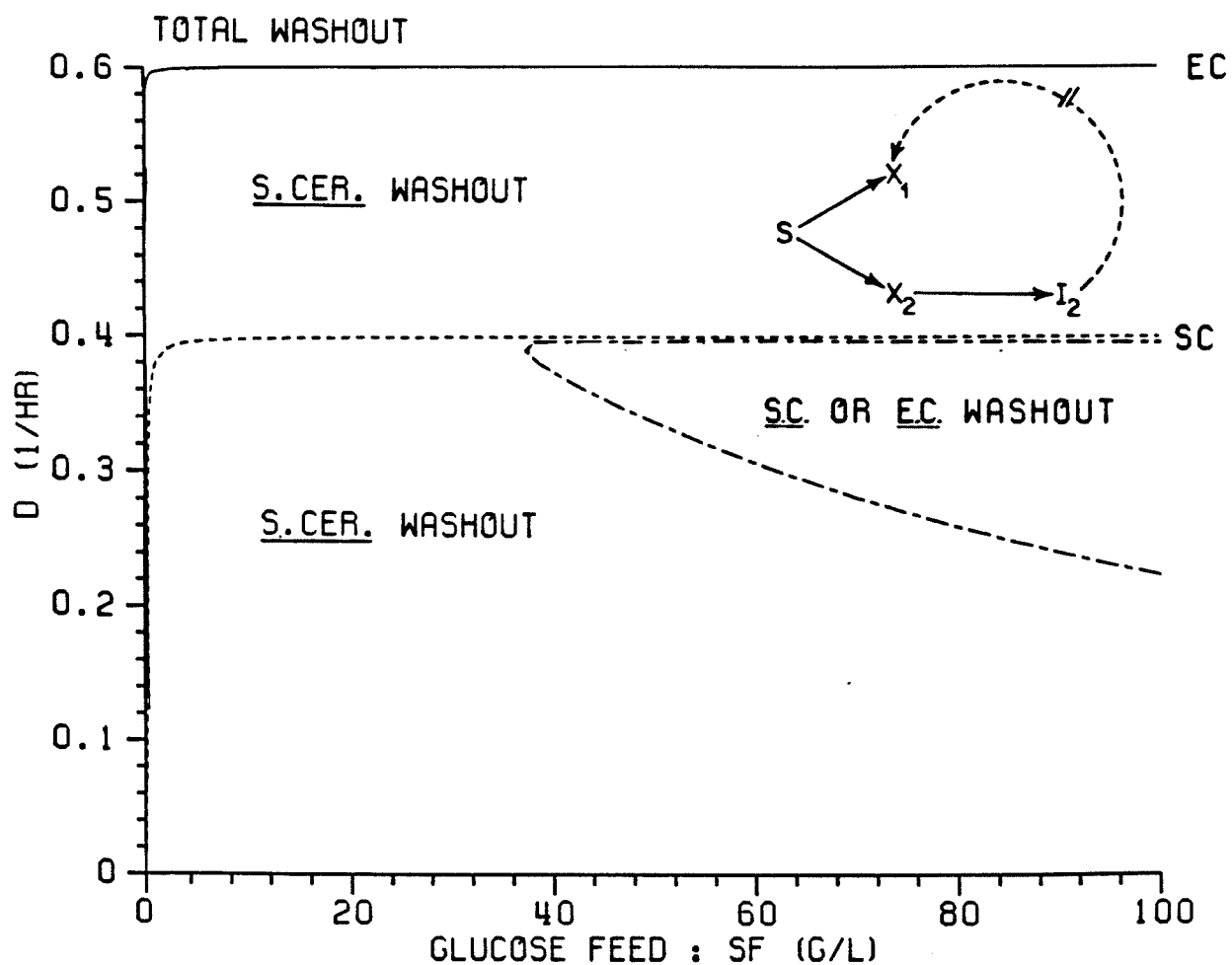


Figure 7a. Stability diagram - only ethanol inhibition is considered, acetate production is neglected.

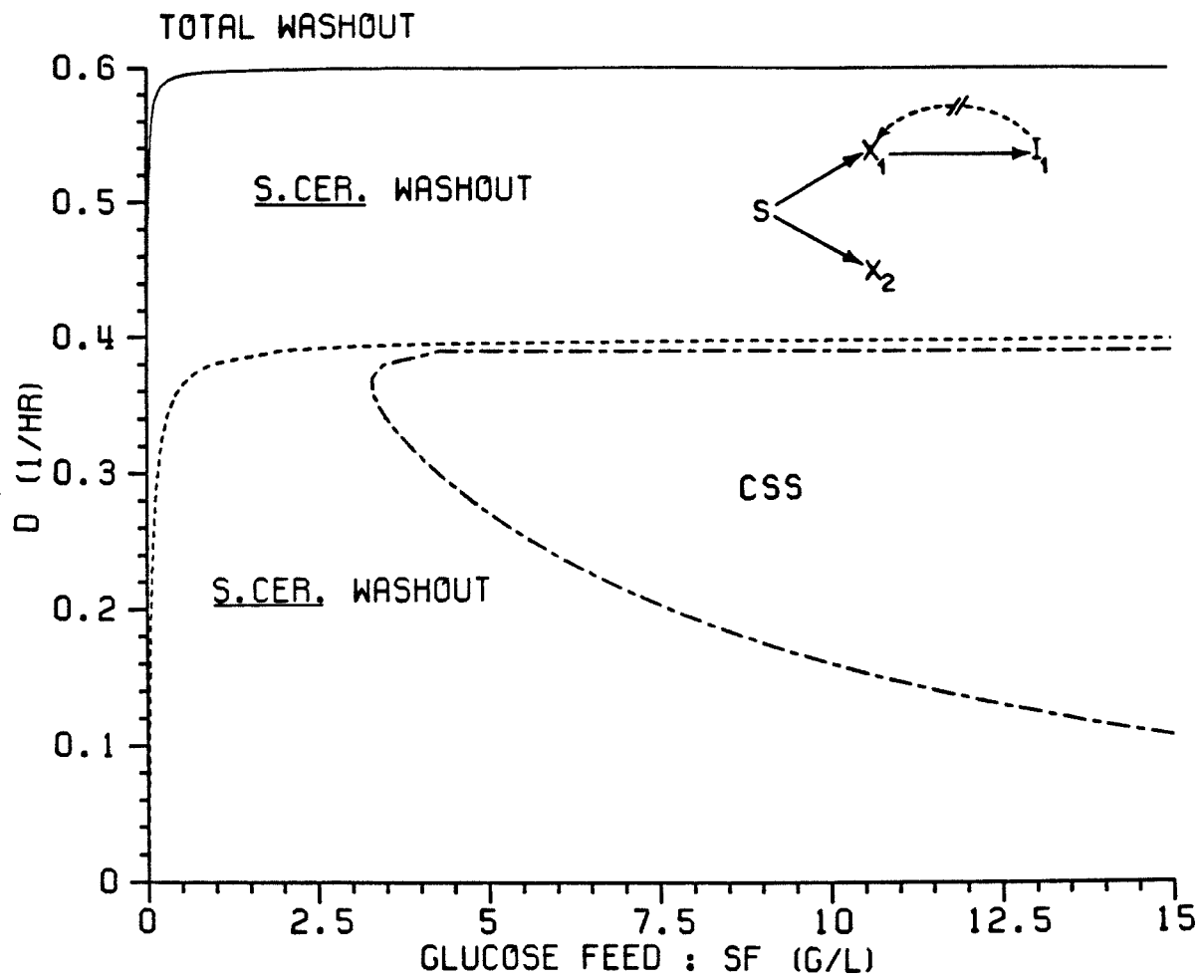


Figure 7b. Stability diagram - only acetate production by *E. coli* is considered, ethanol and acetate production by *S. cerevisiae* is neglected.

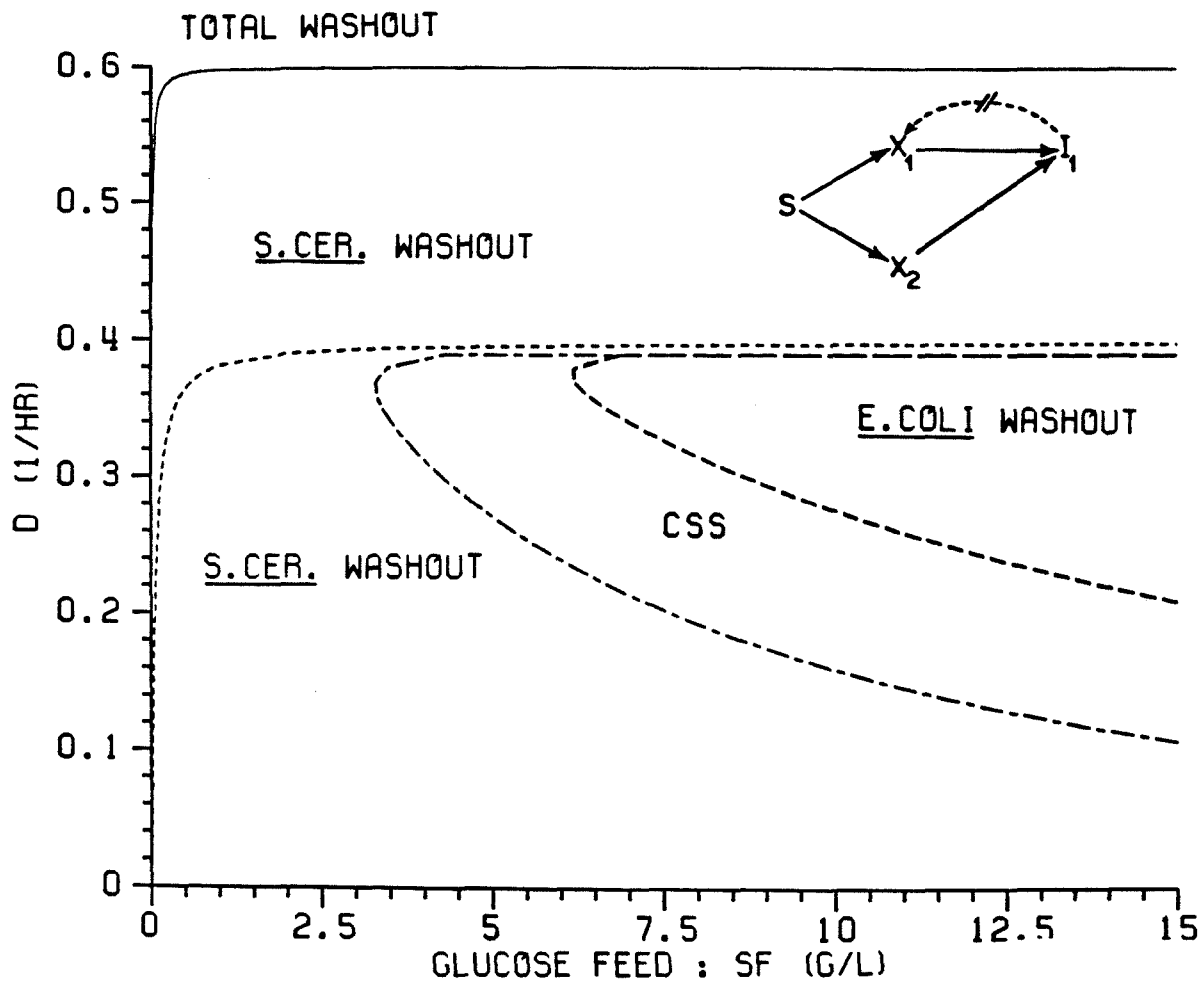
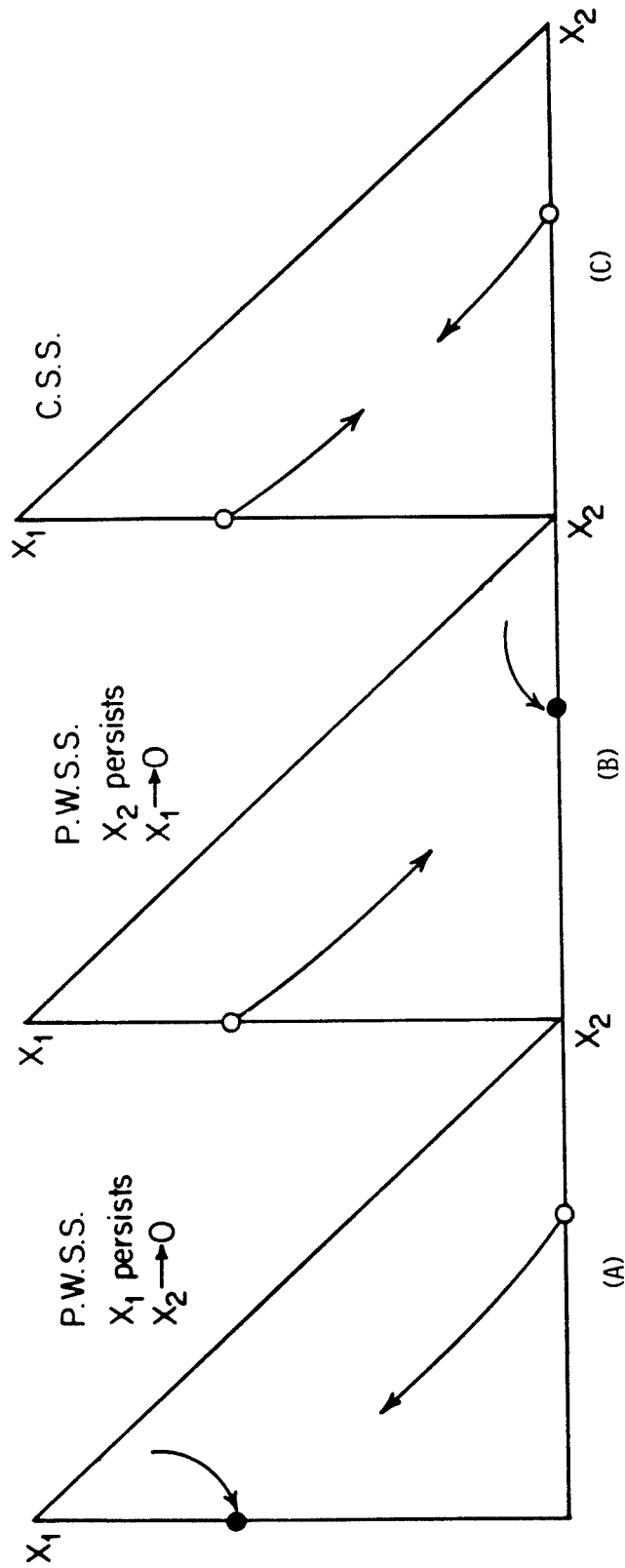


Figure 7c. Stability diagram - acetate production by both *E. coli* and *S. cerevisiae* is considered, ethanol production by *S. cerevisiae* is neglected.



INITIAL TRAJECTORY TESTS FOR STEADY STATE STABILITY

FIGURE 8

- Denotes stable P.W.S.S.
- Denotes unstable P.W.S.S.

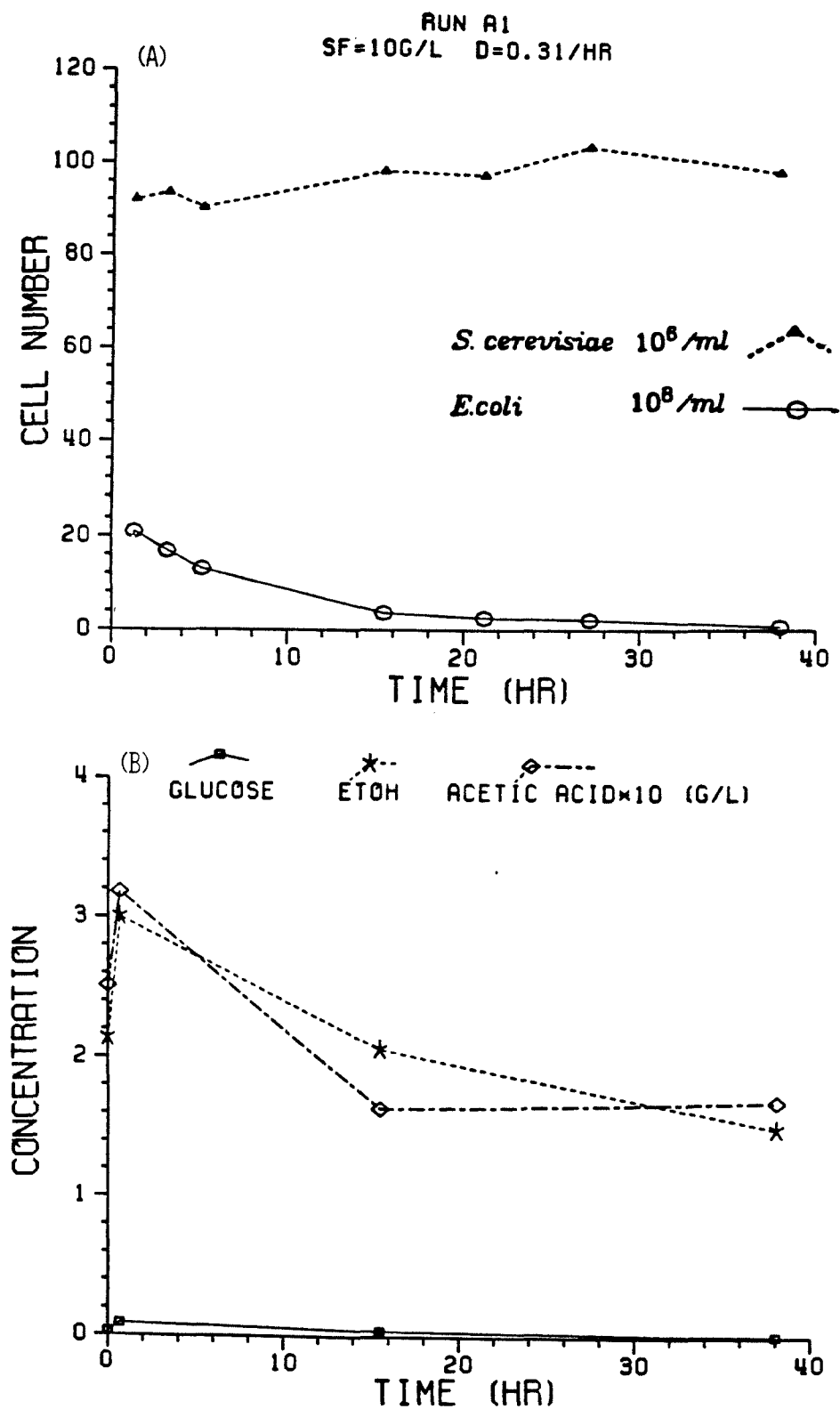


Figure 9.

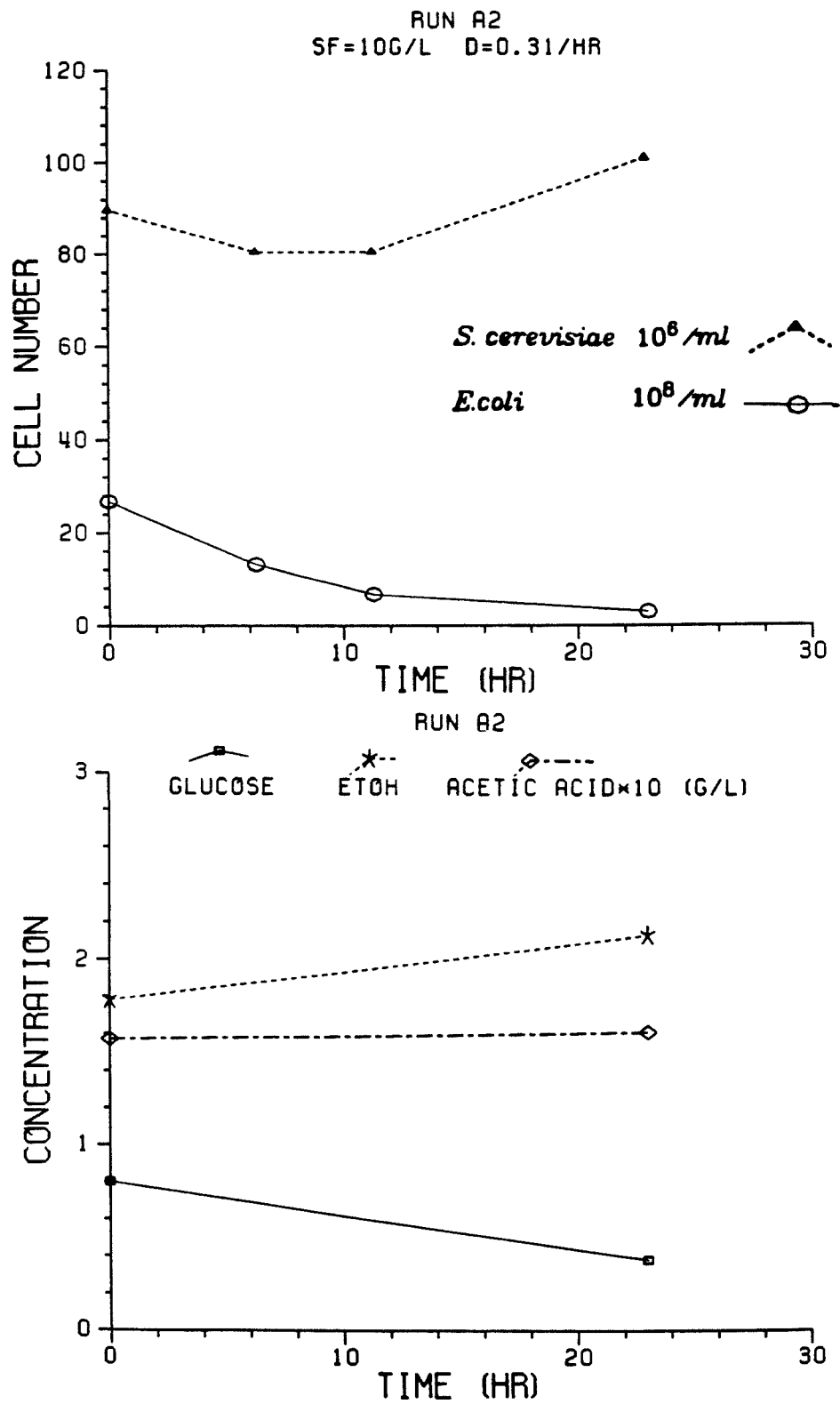


Figure 10.

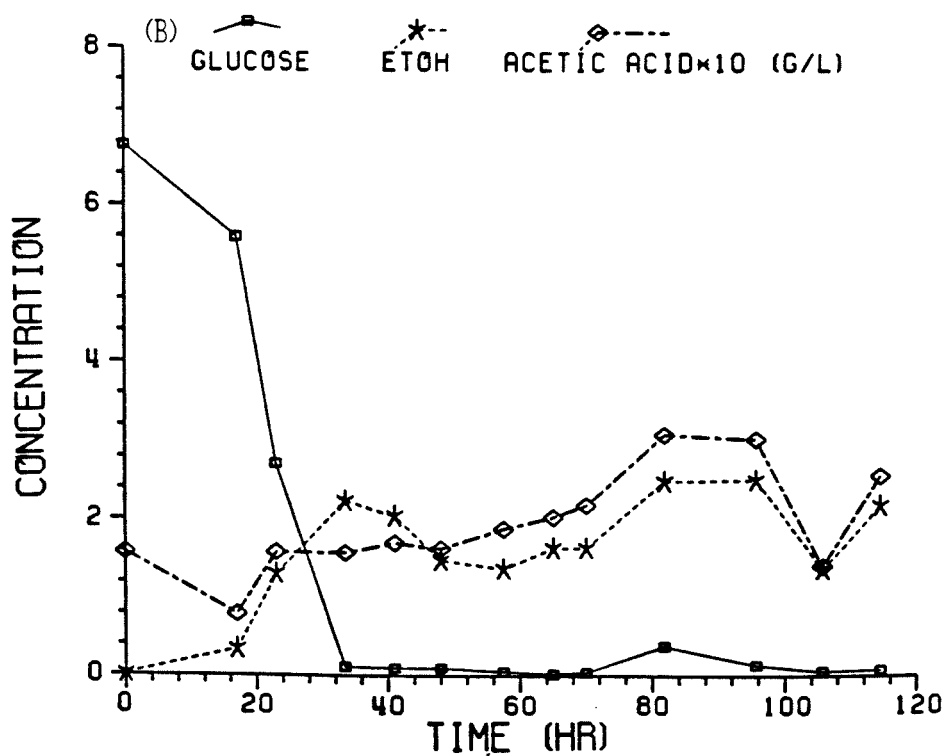
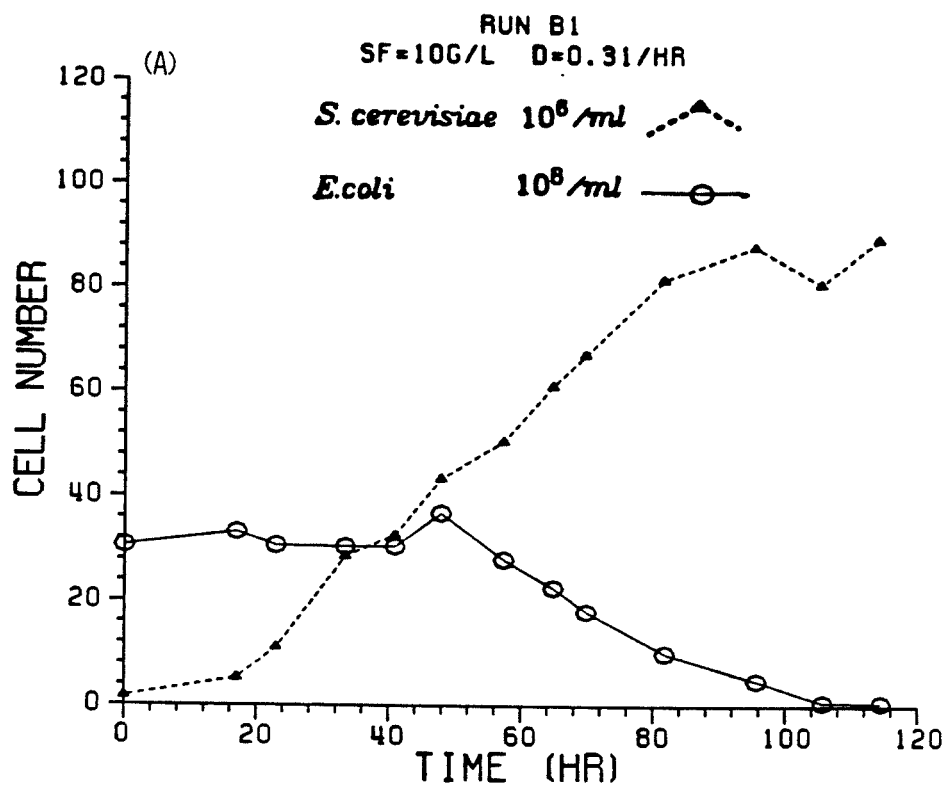


Figure 11.

84.

RUN A3
SF=5G/L D=0.37/HR

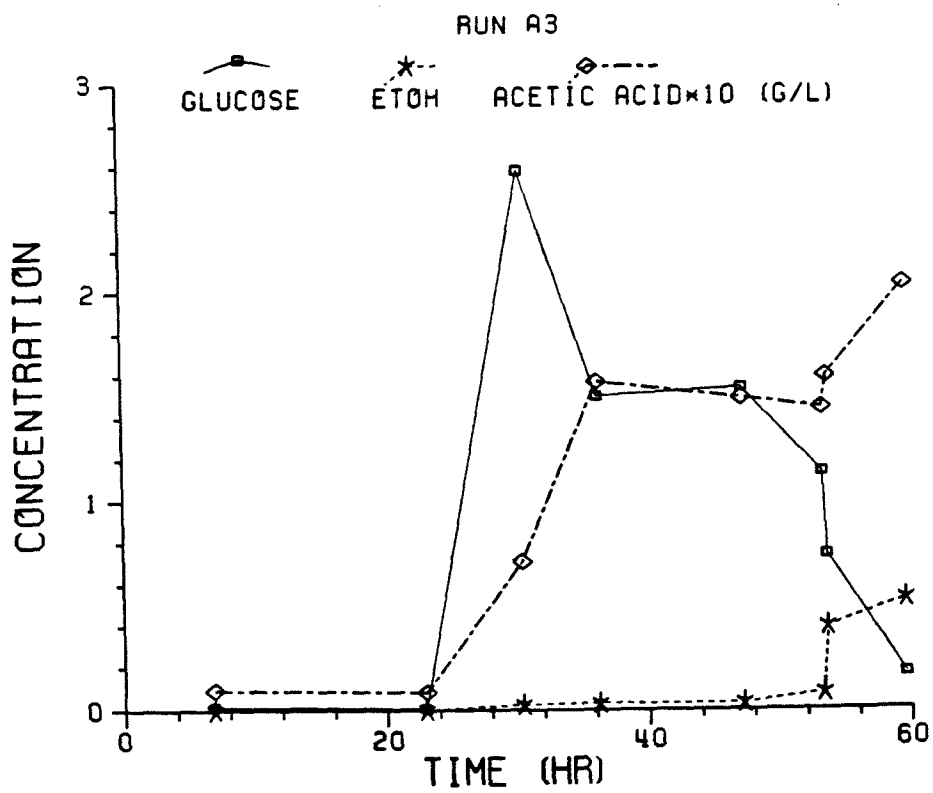
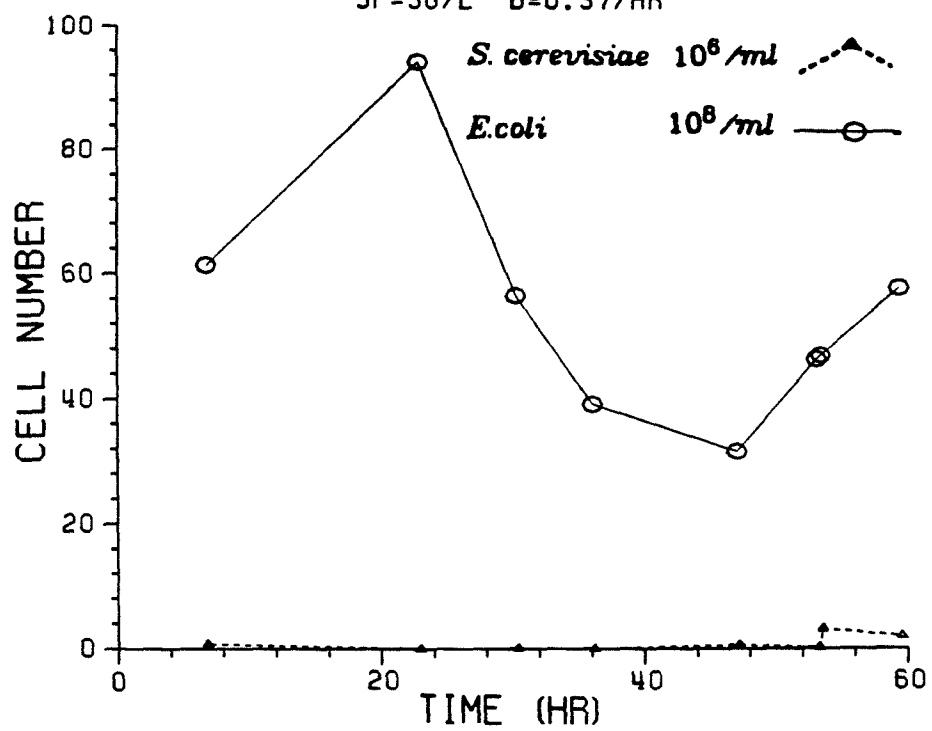


Figure 12.

85.

RUN B2
SF=5G/L D=0.37/HR

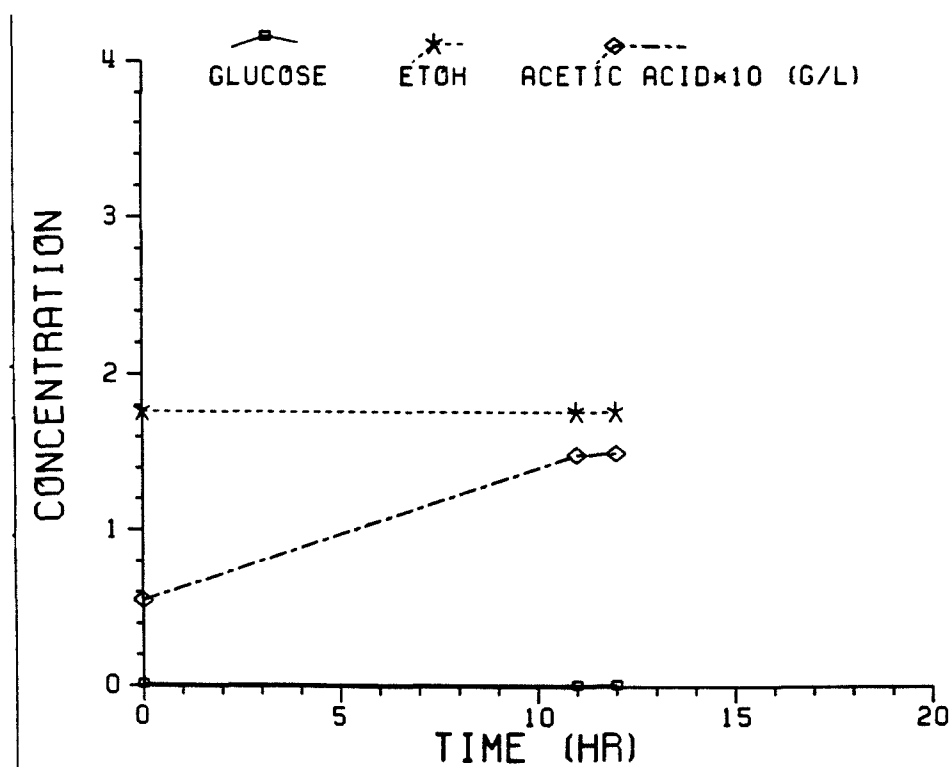
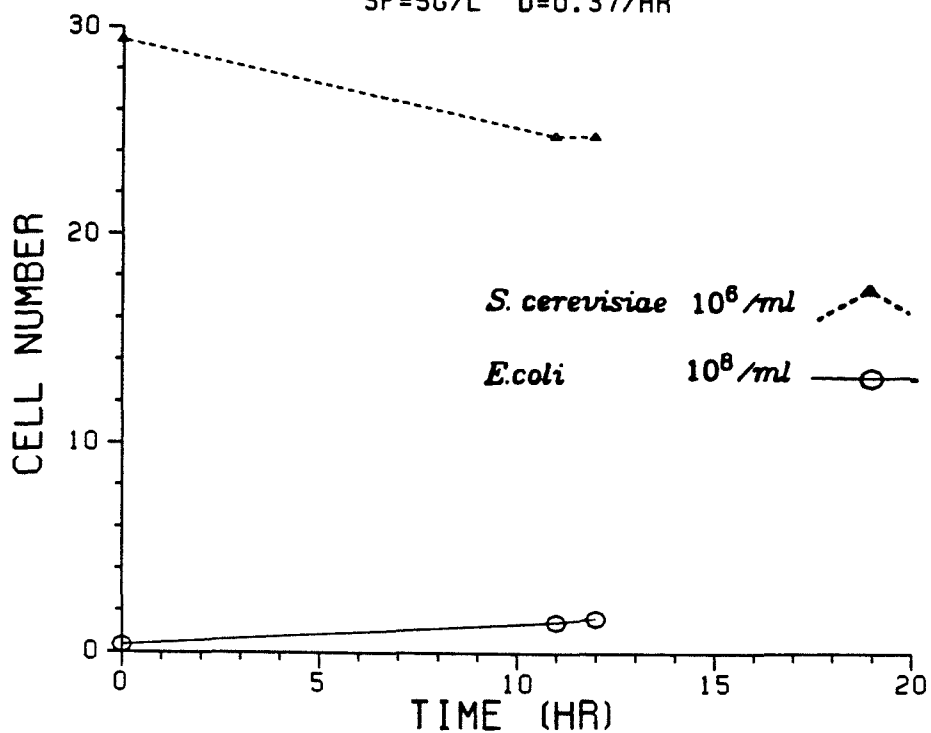


Figure 13.

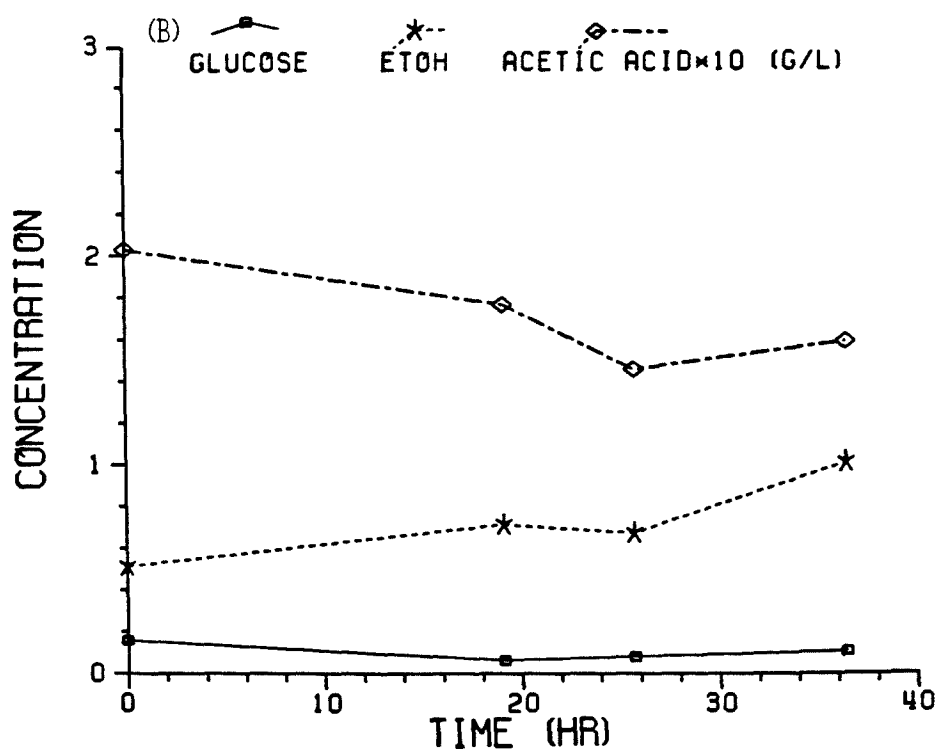
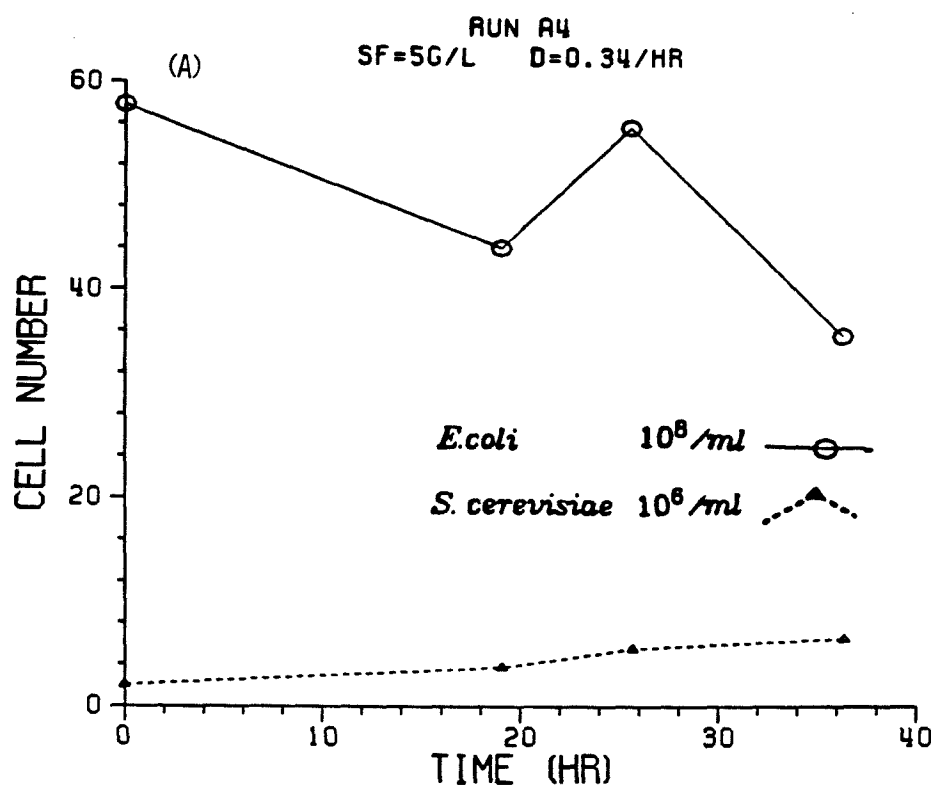


Figure 14.

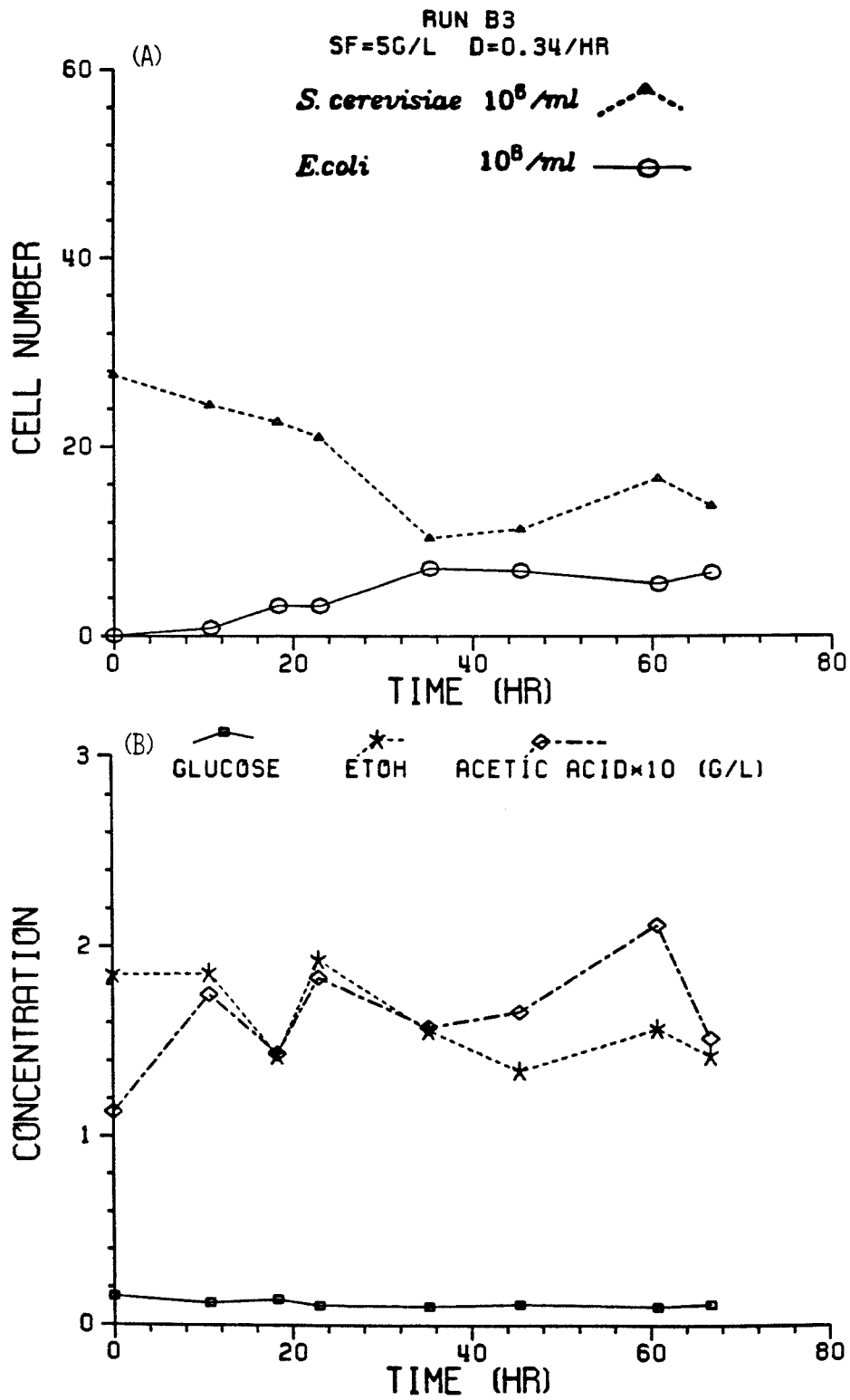


Figure 15.

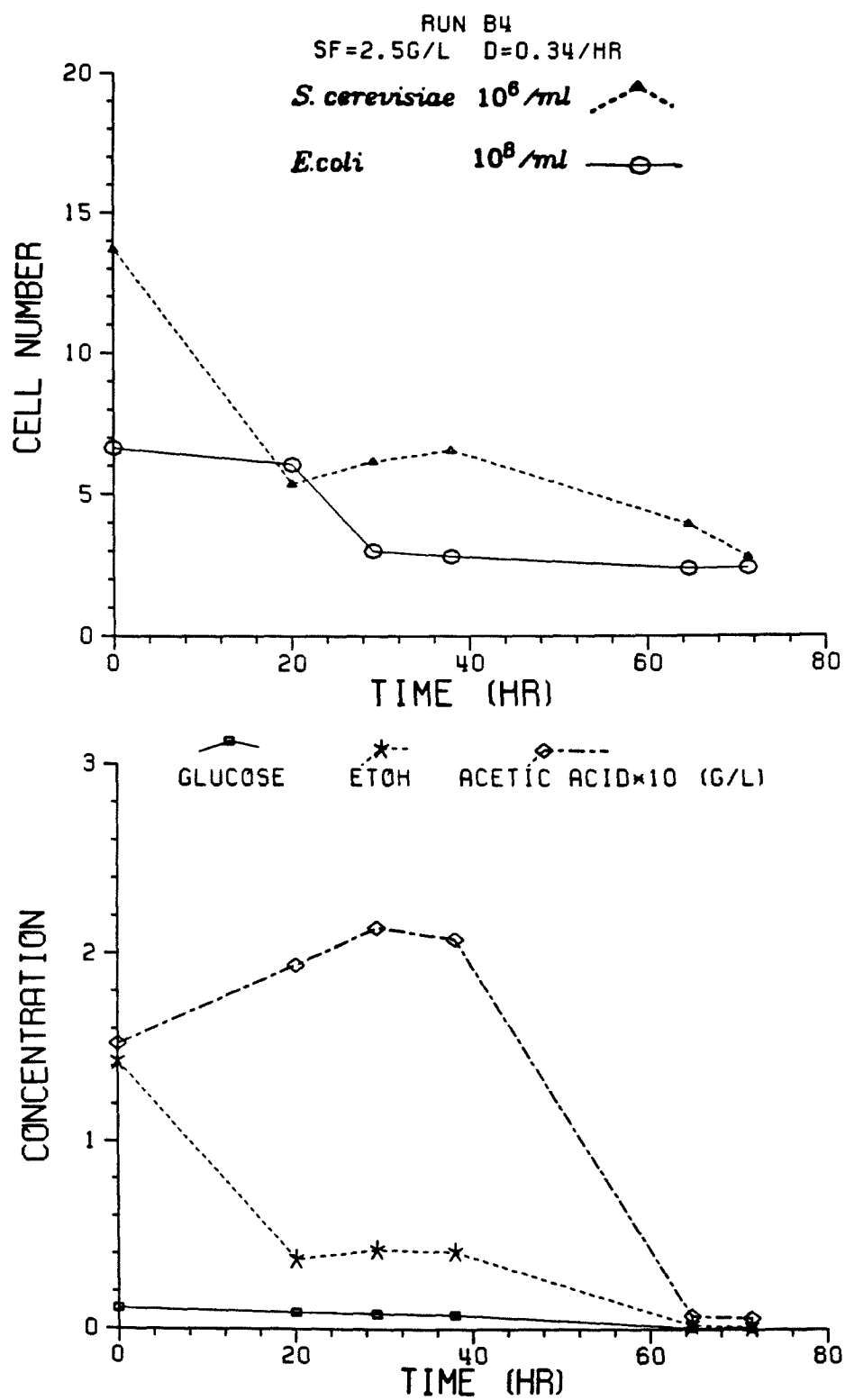


Figure 16.

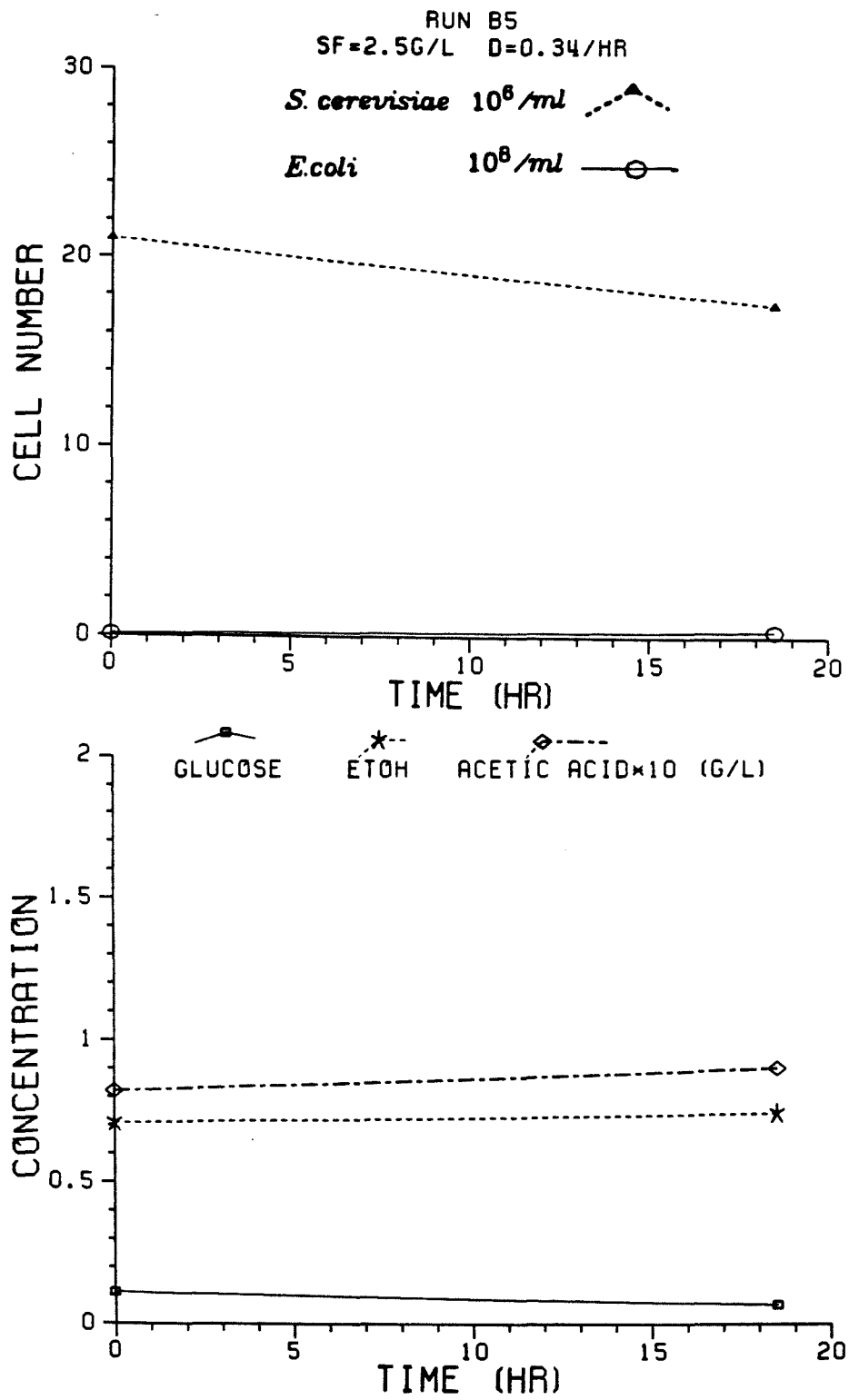


Figure 17.

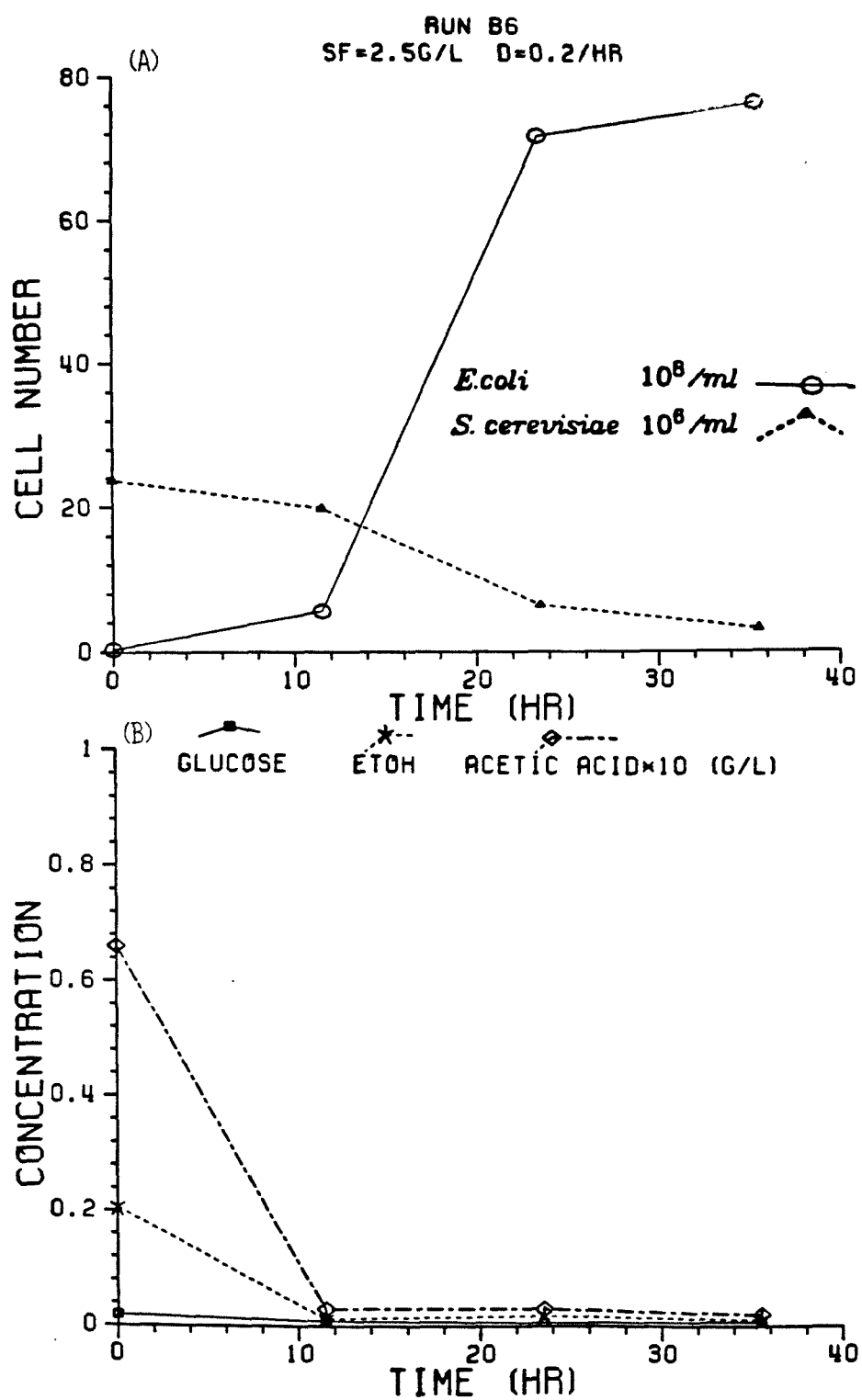


Figure 18.

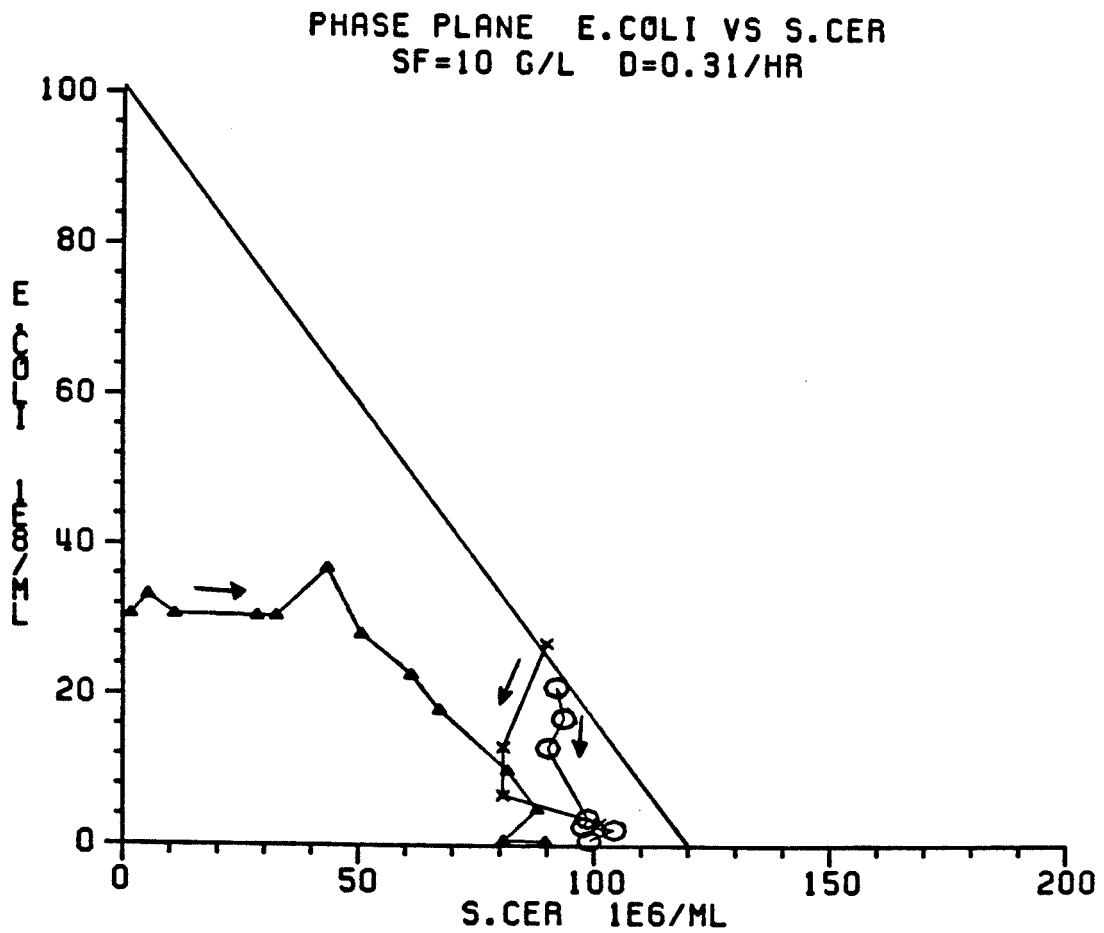


Figure 19 . Phase plane of Run A1, A2, and B1.
(arrow denotes temporal sequence of readings)

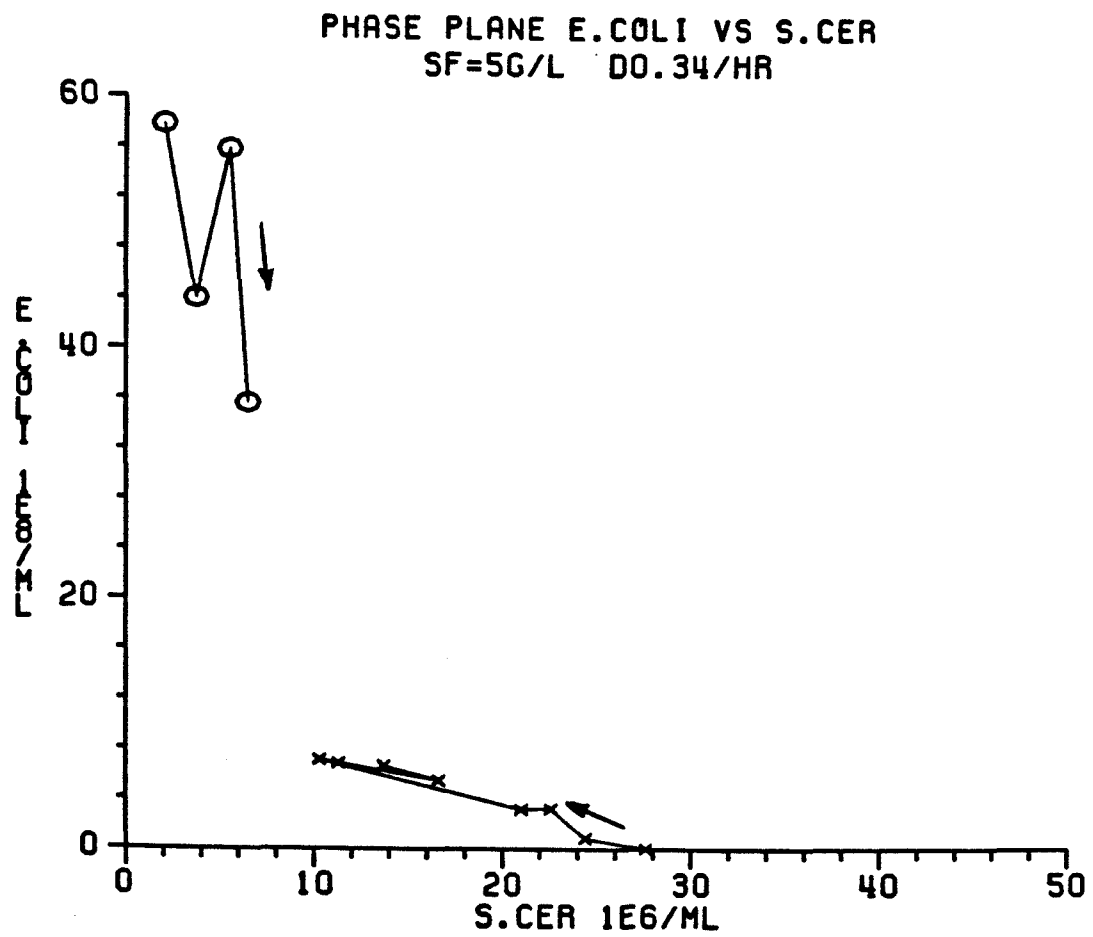


Figure 20. Phase plane of Run A4 and B3.
(arrow denotes temporal sequence of readings)

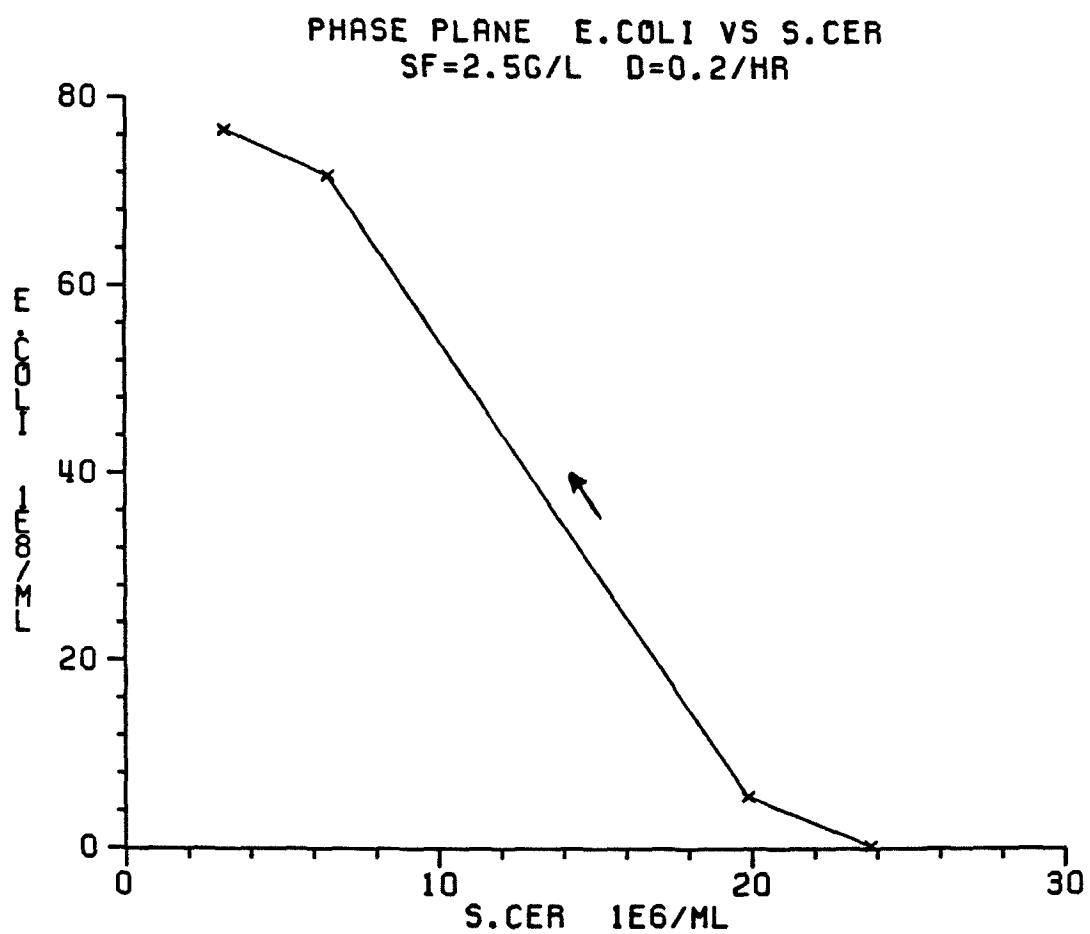


Figure 21. Phase plane of Run B6.
(arrow denotes temporal sequence of readings)

Chapter 4.

**A Novel Bioreactor-Cell Precipitator Combination for
High-Cell Density, High-Flow Fermentations**

originally prepared as *A Novel Bioreactor-Cell Precipitator Combination
for High-Cell Density, High-Flow Fermentations*

by G.N. Stephanopoulos, K.-Y. San, and B.H. Davison

SUMMARY

A novel bioreactor design has been investigated for carrying out in a single unit a fermentation and cell recycle process simultaneously. The reactor consists of a typical fermentor and a side-arm attached at a certain fixed angle to the fermentor. Due to the enhanced sedimentation in the inclined side-arm, the cells precipitate quickly and flow back into the fermentor. This allows an essentially cell-free fermentation broth to be withdrawn at high rates through the side-arm while maintaining a high cell density culture in the fermentor. Continuous flow fermentation runs of S. cerevisiae demonstrated these features and showed that many fold increases in the steady-state cell density could be achieved using high flowrates which in an ordinary chemostat would lead to washout. Ethanol productivities were high and can further be increased several-fold through a straightforward scale-up of the precipitator side-arm to sustain even larger flow rates. Discussed also are various other reactor features such as the enhanced resistance to contamination, possible reduction of the plasmid instability problems of recombinant microorganisms, potential applications with flocculent strains, steady-state coexistence of competing populations in mixed culture, and the possibility of carrying out fermentations with stationary cultures under continuous flow conditions.

INTRODUCTION

The flow rate and culture cell density are the two primary factors that determine the productivity of a continuous flow fermentation. In a typical operation these two variables cannot be manipulated independently and the usual practice is to set the flow rate at a certain value which subsequently determines the steady state values of the cell density and limiting substrate concentrations. In recent years, several studies have appeared in the literature about high cell density fermentations achieved through the introduction of some cell retention device. The objective of these systems has been to increase the productivity by increasing the rates and/or the yields of a process.

Cells can be retained inside a biological reactor by a variety of methods. The methods can be distinguished between those which involve a recycle stream of concentrated cells and those which physically immobilize the cells by entrapping or linking them on a support. Cell recycle has already found several applications in the recycle fermentor for ethanol production¹ and in waste water treatment processes. These processing schemes usually involve an external cell separation step by filtration, centrifugation or precipitation, and a recycle step of the concentrated cells to the reactor. These steps are not in general trouble free and several complications may arise because of changes in the physiology of the recycled cells, from equipment malfunction (for instance membrane fouling during ultrafiltration), and also because of sensitivity to the introduction of contaminants.

In this work, studies with a new bioreactor design which could reduce or even eliminate several of the above difficulties are presented. The basic feature of the reactor is the integration of the fermentation and

cell precipitation steps in a single unit which allows high cell density fermentations to be carried out under high continuous flow conditions. The high flow conditions can be sustained in this reactor system because of the fast precipitation that takes place in the precipitator part of the reactor. The reactor is based on the enhanced sedimentation phenomenon first observed by Boycott² (1920) and is rigorously analyzed and described in the work of Herbolzheimer and Acrivos³⁻⁴. A note by Walsh and Bungay⁵ on the same subject has demonstrated the above phenomenon on the sedimentation of yeast cell suspensions. This phenomenon has occasionally been applied to waste water treatment plants in the form of lamellar clarifiers.

As an introduction to the new reactor concept, the phenomenon of enhanced sedimentation is described first and the achievable enhancement factors for cell precipitation velocities under realistic fermentation conditions are subsequently presented. Following this introduction, the basic design characteristics of the new reactor are described and experimental studies on the basic precipitation properties of Saccharomyces cerevisiae cells along with results on the reactor performance under a variety of operating conditions are reported. In addition to pure cultures, mixed culture fermentations were also carried out in an attempt to determine the ability of the new reactor to either sustain in coexistence mixed culture systems or to enhance the selection properties of known chemostat systems. Only the results on the selection properties are reported in this publication and discussed in connection with the potential of this reactor design to reduce the risk of contamination by small size contaminants. Analysis of the dynamics of mixed culture fermentations and the possibility of using this system to sustain microbial competitors in

coexistence will be the subject of another publication.

Experimentation with the proposed reactor scheme demonstrated that very high cell densities can be established while maintaining high rates of flow through the overall system at the same time. The subsequent several-fold increases in product formation productivities, and also the possibility of further increasing these productivities by straightforward scale-up, make this reactor design an attractive alternative to typical cell recycle operations. Several other applications including the reduction of plasmid instability problems with recombinant microorganisms, the coexistence of competing cultures in the same continuous flow environment, and the possibility of operating stationary culture fermentations under continuous flow conditions are also discussed.

THE PHENOMENON OF ENHANCED SEDIMENTATION

Perhaps the best way to describe the basic phenomenon that underlies the novel reactor design is by examining the precipitation of a single spherical particle in a dilute suspension contained between two parallel plates as presented in Fig. 1a. If ρ_p is the density of the particle and ρ_f and μ_f are the density and viscosity of the fluid respectively, then for the case of low particle concentrations and low Reynolds number, the settling velocity is given by Stokes law as

$$v_s = \frac{2}{9} \frac{R^2 g (\rho_p - \rho_f)}{\mu_f} \quad (1)$$

where R is the radius of the particle and g the acceleration of gravity. The velocity v_s is usually referred to as Stokes velocity. According to Eq. (1) the time required for precipitating a suspension of particles to form a clear liquid in the region defined by the vertical parallel plates is $\frac{H}{v_s}$ where H is the height of the suspension. Suppose now that the

parallel plates of Figure 1a are tipped at an angle θ (Fig. 1b) from the vertical direction. It was observed that the time required to precipitate the same suspension is decreased by many times. This phenomenon was first observed by Boycott² (1920) with blood cells and is known as the "Boycott Effect." An initial qualitative explanation of such an effect can be obtained by assuming that for the inclined part of the plates, the particles still precipitate vertically until they reach the upward facing surface of the plates. Upon reaching that surface, the particles flow down along the surface to be collected at the bottom of the slit. Then, a particle in the inclined plates has only to travel a distance of $O(b)$ (order of b) to be removed, compared to $O(H)$ for the vertical orientation. Thus one can reach the conclusion that the enhancement in the sedimentation rate is of $O(H/b)$. This is correct for the enhancement factor but the mechanism described above is faulty and fails to explain other observed experimental phenomena.

If the above mechanism by which all the particles in the inclined plates are just settling vertically was correct, a clear fluid would be formed at the top of the vessel as well as directly under the entire downward-facing surface. In this case, the interface between the clear fluid and the suspension both at the top of the suspension and under the downward-facing surface would fall vertically at a velocity equal to the Stokes velocity. However, what has been observed experimentally is quite different. First the thickness of the clear liquid layer formed under the downward-facing surface is small and is almost independent of time as shown in Fig. 1c. Second, the interface between the clear liquid and the suspension at the top is settling vertically at a velocity which is typically several times larger than the Stokes velocity.

A kinematic model was presented by Ponder⁶ and independently by Nakamura and Kuroda⁷ which explained the above experimental observations and also provided a quantitative prediction of the settling rates. The arguments according to that model were as follows. As soon as a thin film of clear liquid is formed just below the downward-facing surface of the plates, a convective current is established because of the density difference between the suspension and the clarified layer just below the downward-facing plates. This convective current pushes the clarified fluid upwards towards the fluid above the horizontal interface. Since the thickness of the fluid layer just below the downward-facing surface is observed to be small and time-independent, all the clarified liquid which is formed at that interface must be added to the one just above the horizontal interface which therefore is falling at a rate larger than that indicated by the Stokes velocity. By continuity, on the bottom side of the plates a denser cell layer is quickly formed and flows down the plates in order to replace the clear liquid that was removed from the top layer. These convective currents keep the cells below the interface in suspension and provide for well-mixed conditions in this central region of the precipitator between the clarified and denser layers. This dense cell sediment on the bottom plate collects rapidly at the lowest point of the entire precipitator. According to this mechanism, the apparent (enhanced) volumetric settling rate, Q_e , at the top of the suspension (equal to the product of the enhanced vertically settling velocity times the interfacial area, $v_e b/\cos\theta$) must be equal to the sum of the volumetric settling rate at the horizontal interface (given by v_s times the interfacial area $b/\cos\theta$) and the volumetric settling rate of the clear fluid layer below the downward-facing surface (given by v_s times the horizontally projected area

below the suspension, $H \tan \theta$). This balance for the case of inclined vertically plates reads as

$$Q_e = v_e \frac{b}{\cos \theta} = v_s \frac{b}{\cos \theta} + v_s H \tan \theta \quad (2)$$

where $Q_e(t)$ is the volumetric settling rate per unit depth in the third dimension. From Eq. (2) one can calculate the enhanced sedimentation velocity v_e as

$$v_e(t) = \frac{dH}{dt} = v_s \left(1 + \frac{H}{b} \sin \theta\right) \quad (3)$$

A rigorous analysis of this phenomenon is beyond the scope of this presentation and can be found in Herbolzheimer and Acrivos³⁻⁴. Two points of this analysis should be mentioned here. First, the above-presented model provides a good prediction of the sedimentation rate when the ratio of the sedimentation Grashof number to Reynolds number Λ is large;

$$\Lambda = \frac{\ell^2 g (\rho_P - \rho_F) C_0}{\mu u_s} \quad (4)$$

where ℓ is a characteristic length of the microscale motion and $u_s = v_s \cdot f(C_0)$ with $f(C_0)$ a monotonically decreasing function of C_0 which accounts for the interactions between particles. C_0 is the concentration of the suspension. Second, for the case of continuous operation and $O(H/b)$ proportional to $O(\Lambda)^{1/3}$, only certain combinations of the position of the suspension input and the clear liquid withdrawal point will allow stable steady-state operation.

Equation 3 indicates that two parameters determine the enhancement factor namely, the aspect ratio H/b and the angle θ . A large aspect ratio implies a large volume for the precipitation unit, and practical considerations for small residence times inside the precipitator put a limit on the maximum aspect ratio that can be used. As far as the angle θ is concerned, the latter must be determined by balancing the enhancement

effect which requires a large θ with the relative ease of cell removal by gravity which is facilitated by a smaller θ . Typically, a 30° angle is regarded as a good compromise between these two factors.

PRECIPITATOR DESIGN

In light of the above described phenomenon, a new design was conceived to facilitate the retention of the cells in a continuous-flow fermentor. The design of the new fermentor is shown schematically in Fig. 2. The system basically consists of two parts, a typical fermentor with the usual controls for dissolved oxygen, pH and temperature, and a precipitator unit consisting of a set of inclined parallel plates attached to the bottom of the fermentor and at an angle θ from the vertical direction. There is a continuous supply of growth media into the fermentor through a tube submerged in the culture and a continuous removal of cell-free liquid from the top of the inclined plates. Due to the large sedimentation velocities of the cells in the plates region, the cells quickly precipitate and flow back into the fermentor; this allows for virtually cell-free fluid to be removed at very high rates from the top of the plates. The cells that precipitate on the plates flow by gravity back to the fermentor where well-mixed conditions prevail. Proper design of the connection between the fermentor and the plates can prevent the entrance of air bubbles into the plates region which could disturb the smooth precipitation mechanism described earlier. Conditions inside the plates are usually anaerobic but this can be relatively unimportant for most fermentations due to the small residence times inside the plates that can be achieved with appropriate flow rates and small angle θ from the vertical. Various designs can be employed in the construction of the side-arm of Fig. 2 with the purpose of maximizing the cell precipitation enhancement and facilitating the smooth

recycle of the cells to the fermentation zone. In the design shown in Fig. 2, the height of the suspension H remains constant yielding a constant sedimentation velocity according to Eq. (3).

A final note of the applicability of this fermentor design to various fermentation systems is in order. As can be seen from Eq. (1) the Stokes velocity depends basically on the size of the particle. For bacterial cultures, cell sizes are usually small, of the order of 1-2 microns. The resulting Stokes velocity is very small and in a region where Brownian motion is dominant. For enhancement factors that can be achieved under realistic experimental conditions, the final precipitation velocity still is too small for any practical application. For yeast cells, the size of which ranges from 3 to 10 microns, Stokes velocities are significantly increased over those of the bacterial cultures and therefore, by enhancing those velocities by a factor of 50-100, a significant sedimentation velocity can be obtained by using the design of Fig. 2. This consideration limits the fermentations that can benefit from the proposed design to those involving cells larger than approximately 3-5 microns in size. The experiments reported in this publication were carried out with cells of S. cerevisiae the size of which was determined experimentally. It is also possible to employ the same design for cultures employing larger cells such as fungi, molds and possibly mammalian cell cultures in suspension or on microcarriers.

EXPERIMENTAL WORK

Several preliminary experiments were carried out in order to test the feasibility of the above scheme. First, the basic precipitation properties of S. cerevisiae cells were studied in a simple precipitator system consisting of two parallel plates. The objective was to determine the

Stokes velocity of these cells, and, based on this information, to proceed with a design of the precipitator part of the scheme of Fig. 2. Following these experiments, the dynamics of the full system and the rates at which liquid could be withdrawn while sustaining very high cell density in the fermentor were studied.

The Stokes velocity of S. cerevisiae cells can be determined theoretically by using Eq. (1). The density and the size of the cells are needed for this calculation. However, both of these parameters are usually unavailable at the accuracy required for a reliable calculation calling for the experimental determination of the Stoke's velocity of the S. cerevisiae cells

To achieve this, a parallel plate configuration settler was constructed with 1/8 in. plexiglass. The settler was initially filled with a well-mixed suspension of cells obtained from the effluent of an NBS Microform fermentor where S. cerevisiae was cultivated in a continuous mode with a glucose-limiting medium. The settler was placed at an angle of 45° and the suspension was allowed to precipitate with no flow through the system. The vertical height of the suspension was continuously monitored as a function of time. For a nonflow situation it can be seen by integrating Eq. (3) that the group $b \ln(1+H \sin\theta/b)/\sin\theta$, varies linearly as a function of time. The negative of the slope of such a straight line yields the Stokes velocity. Experimental results are shown in Fig. 3 yielding a value of 0.23 cm per hour for the Stokes velocity of S. cerevisiae cells. This value corresponds to a smallest cell size present in the culture of approximately 3 microns in diameter. The same experiment was repeated by changing the settler angle and flow rates, and the same values for the Stokes velocity and the size of the smallest cells

in suspension were obtained.

Based on these findings, the settler of Fig. 4 (top view) was designed to be used as the precipitator part of the integrated fermentor. The settler consists of four parallel $1/8$ in. plexiglass plates at a distance of 0.32 cm from one another which form three channels for the removal of fluid and the precipitation of cells. Each plate has an area of 1,225 cm square so that each channel has a volume of 392 mL. The trapezoidal design of Fig. 4 was arrived at in order to satisfy the following two constraints. First, the left hand had to be small enough to be connected to a small volume fermentation vessel. Second, it was desirable to have an increase in cross sectional area in order to accommodate a larger flow rate for the removal of clear liquid.

Due to the variable fluid velocity along the plates, the separation efficiency and maximum flow rate through the settler alone were determined experimentally by dipping the settler of Fig. 4 at a 30° angle into a reservoir of a well mixed-cell suspension and withdrawing liquid constantly with a peristaltic pump (masterflex, Cole Parmer) from the top of the settler. In this way the cells that are precipitated do not accumulate at the bottom of the settler but they are recycled back into the reservoir.

Several experiments were carried out to determine optimal operating parameters by varying the angle and the flow rate of liquid withdrawal from the top of the settler. The optical densities of the suspension were measured with a spectrophotometer (Bausch & Lomb, Spec 21) at both the entrance and the exit points of the settler. Also, since the cells constitute a poly-dispersed suspension, the cell size distributions were measured by using the Coulter counter.

An inclination of 30° was found to be optimal overall. Some representative results are summarized in Fig. 5 where the cell size distributions achieved at steady state in the feed and exit stream for different withdrawal rates are shown. At slow withdrawal rates a negligible amount of cells (less than 1% of the reservoir concentration) was removed in the top exit stream; while at a much higher flowrate the cell removal was about 10%. One also should bear in mind that the cell suspension at the entrance is not generally uniform in size, and, if it is required that clear liquid be withdrawn at the top, then the system should be designed on the basis of the smallest cell size present at the entrance to the settler. If a small cell density is to be tolerated in the exit stream, the exit stream will be enriched in the smaller size cells while most or all of the larger cells will be recycled back into the reservoir. The obtained separation efficiencies were judged to be satisfactory for the intended purpose since they demonstrated that the settler could sustain flow rates larger than 700 ml per hour at a larger than 90% retention efficiency.

Finally the settler was integrated with the fermentor by connecting the former to a typical NBS Bioflow fermentation jar with a 1.5l working volume. The fermentor was equipped with an adjustable overflow pump for level control, a temperature controlling unit, magnetic stirrer, a pH electrode probe (Ingold Co.), and a pH controller (Chemtrix).

Materials and Methods

Saccharomyces cerevisiae ATCC #4126 inocule were prepared by cultivating the yeast in 100 mL flasks of the fermentation medium at 30°C on a rotary shaker. The growing culture was transferred several times before inoculation. After inoculation, the culture was allowed to grow

batch for 12 hours before starting the continuous mode. The fermentation was conducted at pH 5 and a temperature of 30°C. Antifoam (0.2 grams per liter) was added continuously at a rate of about 2 mL per hour. Aeration was provided by a filtered flow of about 3 liters per minute.

The composition of the defined glucose medium is given in Table 1. The medium was filter-sterilized by passing it through a 0.2 μ m filter (Gellman Science, Inc.) into a sterile 13 liter reservoir and was fed to the reactor by a peristaltic pump (Masterflex, Cole-Parmer). The antifoam solution was autoclaved separately.

Samples taken from the reactor and from the exit of the plates were analyzed for cell biomass, cell counts, glucose, and ethanol concentrations. The optical density was determined spectrophotometrically at 660 nm and cell size distributions were also obtained by a Coulter Counter. Part of the sample was filtered immediately through a 0.4 μ m filter after withdrawal from the reactor or from the plates, and the filtrate was subjected to chemical analyses. Glucose and ethanol concentrations were determined enzymatically with glucose and ethanol kits (Sigma Chemical Co.), respectively.

Continuous fermentations were carried out with this system by feeding a constant stream of growth medium into the fermentor. The fermentor contents were withdrawn from two different parts. The largest part of the flow was withdrawn from the top of the settler at a rate F_p by a peristaltic pump, and this fluid was practically cell free. The remainder was pumped directly from the reactor at a rate F_r through the overflow tube extending down into the fermentor. The level of the fermentation liquid was thus controlled by adjusting the position of this tubing. Furthermore, the direct removal of cells from the fermentor

counterbalanced the effect of cell growth and allowed for steady-state operation to be established even at perfect settler operation of 100% cell retention. Results reported in this paper were obtained with a reactor volume of 0.9 liters.

RESULTS

The maximum specific growth rate of the employed culture was determined first. After the system had reached a steady state with a total flow rate of 38 mL per hour, the feed rate was raised to 545 mL per hour to exceed the max sp. gr rate and wash out the actively growing yeast. In this experiment the fermentor acted as a normal chemostat ($F_p = 0$), since no liquid was withdrawn through the plates. This was achieved by bubbling filter-sterilized air back through the plates and into the fermentor to prevent the contents of the fermentor from entering the plates. The concentration of glucose was monitored during the course of this washout transient. After an initial period, it was found to be high and at levels at which the specific growth rate is equal to its maximum. The washout rate and the dilution rate yielded a $\mu_{\max} = 0.5 \text{ hr}^{-1}$ consistent with the results of batch growth experiments.

A series of steady-state experiments with different feed rates and F_p values were performed next. A small concentration of 5g/lt of the limiting nutrient in the feed was chosen for these runs in order to test the cell separation efficiency and to evaluate the overall performance of the integrated fermentor-separator combination. The results of these experiments are summarized in Fig. 6 where cell densities and ethanol concentrations in the reactor have been plotted as a function of $D_r (= F_r/V)$. This D_r is the specific overflow rate which is equivalent to the usual dilution rate when $F_p = 0$. Also, for 100% cell retention in the plates

and at steady state the specific growth rate equals D_r . Cell densities and ethanol concentrations achieved with a typical chemostat operation are also shown in this figure for comparison. It can be seen that the typical pattern of decline of cell densities as dilution rate increases is also followed with this system. However, several-fold increases in cell density can be observed especially for $D_r < 0.2 \text{ hr}^{-1}$. In this dilution rate regime, the majority of the cells are retained in the reactor while the total flow rate is maintained at high levels by a correspondingly large F_p . Ethanol concentrations are consistently higher than those of chemostat operation for reactor dilution rates less than 0.3 hr^{-1} due to a higher cell densities in the new fermentor. For even higher D_r at constant feed rates, both cell densities and ethanol concentrations become comparable to those of an ordinary chemostat since the liquid withdrawal through the precipitator, F_p , becomes relatively smaller in this case and the operation approaches that of a chemostat. It should be also pointed out that within experimental error, the cell density in the stream removed from the precipitator was found to be independent of the reactor cell concentration as well as of the rate of withdrawal (F_p) under the range of conditions investigated. This finding was consistent with the theoretical predictions according to which the separation efficiency should be independent of the rate of withdrawal as long as the liquid velocity inside the settler is smaller than a critical velocity.

The ability of the reactor to sustain very large flow rates while maintaining large cell densities was tested in another experiment in which the growth medium was fed at a total rate of 800 mL per hour. F_p was equal to 446 mL hr. Even at these high flow rates the reactor optical density was high and the system operated at better than 90% retention

efficiency. In a usual chemostat operation the culture would have been washed out at these dilution rates which corresponded to twice the maximum specific growth rate.

Table 2 shows the results of another series of runs that were carried out with a much higher concentration of the growth-limiting substance in the feed, namely 50 grams per liter. The reactor was operated under both aerated and nonaerated conditions. No attempt was made to establish fully anaerobic conditions in the reactor. As it can be seen in the table, very large biomass concentrations were achieved under total feed flow rates of 450 mL/hr corresponding to approximately 0.5 hr^{-1} overall dilution rate, i.e., the same level as the maximum specific growth rate of the culture. Notice that the residual glucose was minimal in both cases, both in the reactor and the sedimentor part of the overall system.

The biomass in the exit stream from the plates was higher in the aerated than in the nonaerated situation due to a decreased plate separation efficiency caused by air bubbles traveling through the settler. In the nonaerated situation, very few air bubbles entered the plate region, and this resulted in better than 99% retention efficiency. Still CO_2 bubbles were apparent during the course of the fermentation, but they appear to have little or no effect on the precipitation efficiency of the settler. The concentration of ethanol was approximately the same in the reactor and in the exit streams from the reactor and the plates. It was higher in the nonaerated run versus the aerated one by approximately 30%. Based on the flow rate through the reactor and the ethanol concentrations at the exit of the settler, an overall productivity of 11 g of ethanol per hour per liter of fermentor volume was achieved with this design. It should be pointed out that no attempt whatsoever was made to optimize the

ethanol production rates in this system by controlling the level of dissolved oxygen, increasing the concentration of glucose in the feed or by other means.

Furthermore, the productivity can be increased by increasing the total throughput which can be easily accomplished by increasing the number of identical plates in the settler. This involves a rather straightforward scale-up process since the operation in each individual channel is independent from the others. Thus an n -fold increase in the number of channels in the settler will allow n times larger flow rate to be accommodated through the reactor with a similar increase in the overall productivity of the system. The reported ethanol concentrations in the nonaerated case correspond to a yield equal to 90% of the theoretical. It should be also mentioned that the reactor was operated for approximately 3 weeks without any fouling and significant wall growth occurring inside the reactor or in any parts of the plates that constitute the settler.

Another potential advantage of this reactor design is based on its selected properties for larger cell sizes. Small size cells are selectively removed in this high flow environment and they cannot establish an active culture because the rate at which they grow is significantly smaller than the total washout rate. The result is an increased resistance against small size contaminants. To test this hypothesis, a pure yeast culture that was growing in the reactor at steady state under conditions similar to those of Fig. 6 was cross inoculated with a substantial amount of Escherichia coli. The total dilution rate through the reactor was equal to 0.89 hr^{-1} with $D_p = 0.48 \text{ hr}^{-1}$. The relative numbers of E. coli and yeast cells were followed as a function of time, and results are reported in Fig. 7. They demonstrate the very rapid

decrease of the total numbers of e. coli in the system under the very high dilution rates. After about 10 hrs of operation, E. coli had declined to very low levels. Yeast, on the other hand, was not affected by the addition of the E. coli inoculum and remained at approximately the same levels. The run was continued under the same conditions for a long period of time and some of the data reported in Fig. 6 were collected from this experiment.

DISCUSSION

The results reported in the previous section support the original proposition that the new reactor can offer an interesting alternative for high cell density and high flow continuous fermentations. No attempt was made to explore the operating limits of the reactor. Certainly the attainable steady-state cell densities can be increased by further increasing the concentration of the growth-limiting substance in the feed medium. Also, the maximum flow rate depends on the design and flow characteristics through the precipitator. Larger flow rates are possible by further increasing the available cross sectional area for flow through the precipitator and by introducing some other modifications in the basic precipitator design. These increases in total flow rate will, of course, be accompanied by proportional increases in the overall system productivity.

One of the important consequences of the selection properties of the new design for larger cell sizes is the increased resistance of the reactor to small size contaminants. Some other advantages are discussed in this section. One possibility is to use this reactor with flocculating strains forming flocs several times larger than the component cells. These flocks could be easily retained in the reactor at even higher flow rates. Presently, cell retention in continuous flow fermentations with

flocculating strains is achieved by only withdrawing broth from the top of the reactor. With the proposed design, the total rate of withdrawal could be greatly increased due to the enhanced sedimentation of the larger flocs on the inclined plates with proportional increases in the total productivity of the process. Another possibility is to employ the new design for continuous fermentations involving product formation stationary cultures. Stationary cultures do not allow continuous operation. With the new design and minimal overflow, rate cells can be efficiently retained inside the reactor while product-bearing liquid is continuously withdrawn from the end of the precipitator, thus providing for a continuous operation of an essentially nongrowing culture with high productivities at the same time. For example the effective growth rate of the experiment in Table 2 is less than 0.08 hr^{-1} which is very slow compared to the glucose consumption rates.

Mixed culture systems involving populations competing for the same growth-limiting substrate are known to be unstable in a chemostat with constant flow. The population that grows faster under the operating conditions will dominate while the other population will wash out of the system. Several schemes for sustaining such cultures in coexistence, have been examined in the past including the provision for a temporal or spatial variation in the fermentation environment (8,9). However these conditions are rather difficult to maintain for a long time. Another possibility is suggested by the selection properties of the proposed reactor. This reactor could be employed to sustain two competitors in coexistence provided that the two populations consist of cells of quite different sizes and that the population with a smaller size grows faster. In this arrangement, the smaller yet faster growing population is withdrawn at a

faster rate through the precipitator unit of the integrated system. Therefore by properly balancing the two flow rates F_r and F_p , it could be possible to sustain the mixed culture in coexistence and establish a stable steady state. This possibility has been explored with a mixed culture consisting of a population of S. cerevisiae and E. coli. It was found that for constant feed rate and F_r , it was possible to go from E. coli dominating region, to a region of coexistence, and then on to a yeast dominating region, as the rate of liquid withdrawal through the precipitator, F_p , was increased, respectively. These studies, which are going to be reported in more detail along with a theoretical analysis in another publication, demonstrated that the two species E. coli and S. cerevisiae can be sustained in the combined fermentor-precipitator system despite the fact that they grow at significantly different growth rates.

The above results indicate that the new reactor could possibly be employed in order to reduce the plasmid instability problems which are frequently encountered with recombinant microorganisms. The sizes of these organisms are usually larger due to the large amounts of foreign protein that they contain. They also grow at smaller rates because of the extra load that their metabolic machinery is subjected to in order to produce the foreign protein. Therefore, an initially pure recombinant culture will quickly evolve into a mixed culture system which consists of different populations with different cell sizes and different growth rates, depending on the plasmid number of the recombinant cells. In one extreme situation, one could model this mixed culture as consisting of two populations, one of smaller size with no foreign plasmids and growing at the faster growth rate and another, larger in size, with foreign plasmids and growing at a smaller specific growth rate. This mixed culture system

is similar to the one examined of E. coli and S. cerevisiae and the results obtained with this system provide an indication as to the possibility of maintaining and even enhancing the number of recombinant cells in the proposed reactor. This, of course, would require that the flow rates through the reactor be finely balanced. Work with recombinant cultures is presently being contemplated in order to demonstrate experimentally this possibility for the new reactor design.

The major advantage of this design is the very good cell retention within the reactor, all the while keeping the benefits of a well-mixed cell culture at high flow rates. Overgrowth and fouling common to immobilization schemes do not appear to be a problem. The high throughput of liquid allows little accumulations of toxins, inhibitors, or some contaminants as found in other cell recycle schemes.

The potential for further productivity increases by optimization of the design, scale up, and operating conditions not attempted in this paper gives promise for the exploration and utility of enhanced sedimentation.

Acknowledgment

This research was supported in part by the Caltech Process Biocatalysis Program and by an NSF, Presidential Young Investigator Award (GS). Partial support through the Caltech SURF (Summer Undergraduate Research Fellowship) program (MP) is also appreciated. Much appreciation is given to E. Herbolzheimer and A. Acrivos for their work on enhanced sedimentation and discussing its possible applications with us.

List of Symbols

b	width of parallel plates of Fig. 1
C_o	density of suspension
D_r	dilution rate based on the F_r flow rate
F_p	rate of fluid removal through the plates
F_r	rate of fluid removal from the fermentor for level control
g	acceleration of gravity
H	height of suspension
Q_e	enhanced volumetric settling rate per unit depth
R	particle radius
V	Reactor volume
v_s	Stokes velocity
v_e	enhanced vertically settling velocity
θ	angle of side-arm from the vertical
Λ	ration of the sedimentation Grashof number to Reynolds number
μ_F	fluid viscosity
ρ_F	fluid density
ρ_p	particle density

REFERENCES

1. G. R. Cysewski and C. R. Wilke, Biotech. and Bioeng., 19, 1125 (1977).
2. A. G. Boycott, Nature, 104, 532 (1920).
3. A. Acrivos and E. Herbolzheimer, J. Fluid Mech., 92, 435 (1979).
4. E. Herbolzheimer and A. Acrivos, J. Fluid Mech., 109, 485 (1981).
5. T. J. Walsh and H. R. Bungay, Biotech. and Bioeng., 21, 1085 (1979).
6. G. Ponder, Quant. J. Exp. Physiol., 15, 235 (1925).
7. N. Nakamura and K. Kuroda, Keijo J. Med., 8, 256 (1937).
8. G. Stephanopoulos, A. Fredrickson and R. Aris, AIChE J, 25, 863 (1979).
9. G. Stephanopoulos and A. Fredrickson, Biotech. and Bioeng., 21, 1491 (1979).

Table 1

Medium Composition	
Component	Amount (per litre)
$\text{CaCl}_2 \cdot 2\text{H}_2\text{O}$	0.2 g
$\text{MgCl}_2 \cdot 6\text{H}_2\text{O}$	0.52 g
$(\text{NH}_4)_2\text{SO}_4$	12.00 g
H_3PO_4 , 85%	1.6 ml
KCl	0.12 g
$\text{CaCl}_2 \cdot \text{H}_2\text{O}$	0.09 g
NaCl	0.06 g
$\text{MnSO}_4 \cdot \text{H}_2\text{O}$	3.8 mg
$\text{CuSO}_4 \cdot 5\text{H}_2\text{O}$	0.5 mg
H_3BO_3	7.3 μg
$\text{NaMoO}_4 \cdot 2\text{H}_2\text{O}$	2 mg
NiCl	2.5 μg
$\text{ZnSO}_4 \cdot 7\text{H}_2\text{O}$	12 mg
$\text{CoSO}_4 \cdot 7\text{H}_2\text{O}$	2.3 μg
KI	1 mg
$(\text{FeSO}_4)(\text{NH}_4)_2\text{SO}_4 \cdot 6\text{H}_2\text{O}$	0.035 g
m-Inositol	125.0 mg
Pyridoxine-HCl	6.25 mg
Ca-D-Pantothenate	6.25 mg
Thiamine-HCl	5.0 mg
Nicotinic Acid	5.0 mg
D-Biotin	0.125 mg
KPhthtate	0.23 g
EDTA	0.1 g
Kphthlalate	0.2 g
Glucose	5 g

* Adjust to pH5 with KOH

Table 2

Results of Continuous Sedimentation				
	Aerated		No Aeration	
	Reactor	Plates	Reactor	Plates
Ethanol (g/l)	17	17	22	23
glucose (mg/l)	10	11	15	12
biomass (g/l)	47	4	47	0.7
μ (1/hr)	0.08		0.01	

Flow rates: $F_P = 430 \text{ ml/hr}$, $F_R = 20 \text{ ml/hr}$; $S_F = 50\text{g/l}$ glucose

$$\mu = D_R + \frac{x_P}{x_R} D_P$$

Figure Captions

Figure 1: Schematic illustration of the phenomenon of enhanced sedimentation.

Figure 2: Schematic of the new fermentor design for facilitated cell precipitation and recycle.

Figure 3: Experimental determination of the Stokes velocity of S. cerevisiae cells.

Figure 4: Top view of the settler part of the fermentor of Figure 2.

Figure 5: Steady-state cell size distributions at the entrance and exit streams of the settler of Fig. 4 for varying flow rates.

Figure 6: Steady-state cell densities and product concentrations for the fermentor-precipitator combination as a function of the reactor dilution rate ($D_r = F_r/V$; where F_r is the rate of culture withdrawal directly from the reactor).

Figure 7: Washout of the smaller-size population from a mixed culture of E. coli and yeast occurs at high flow rates.

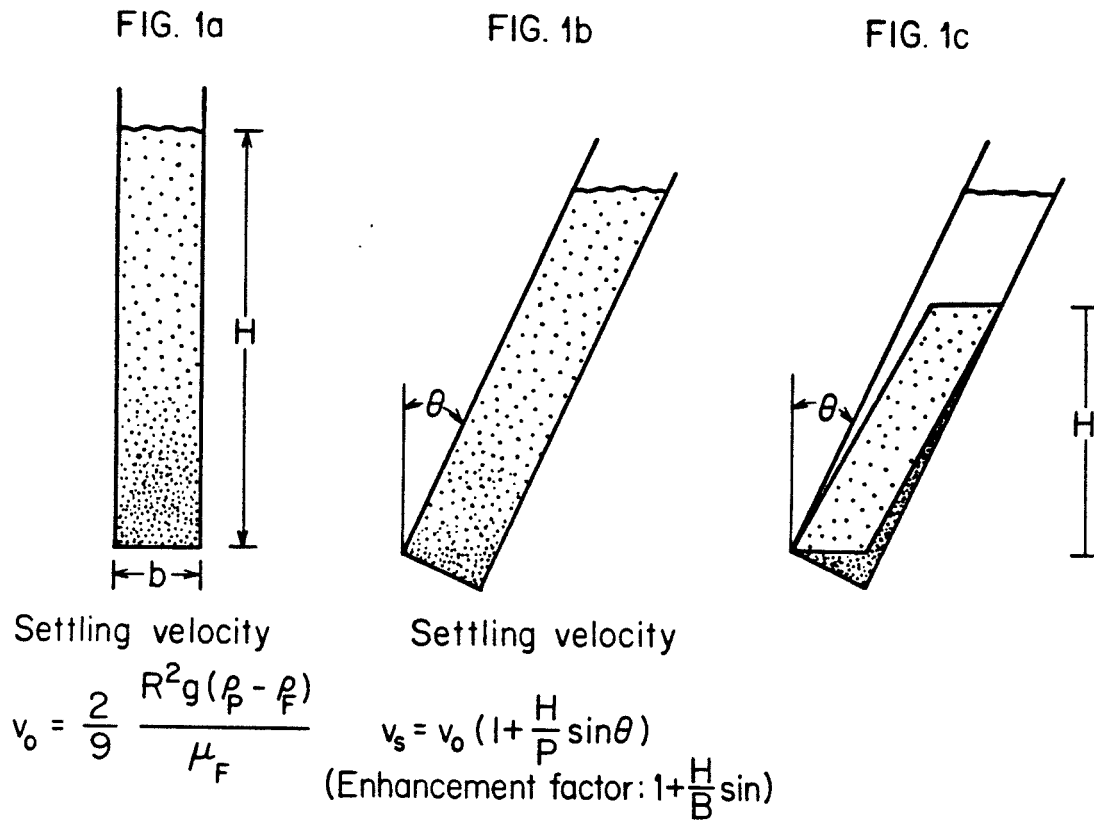


Figure 1: Schematic illustration of the phenomenon of enhanced sedimentation.

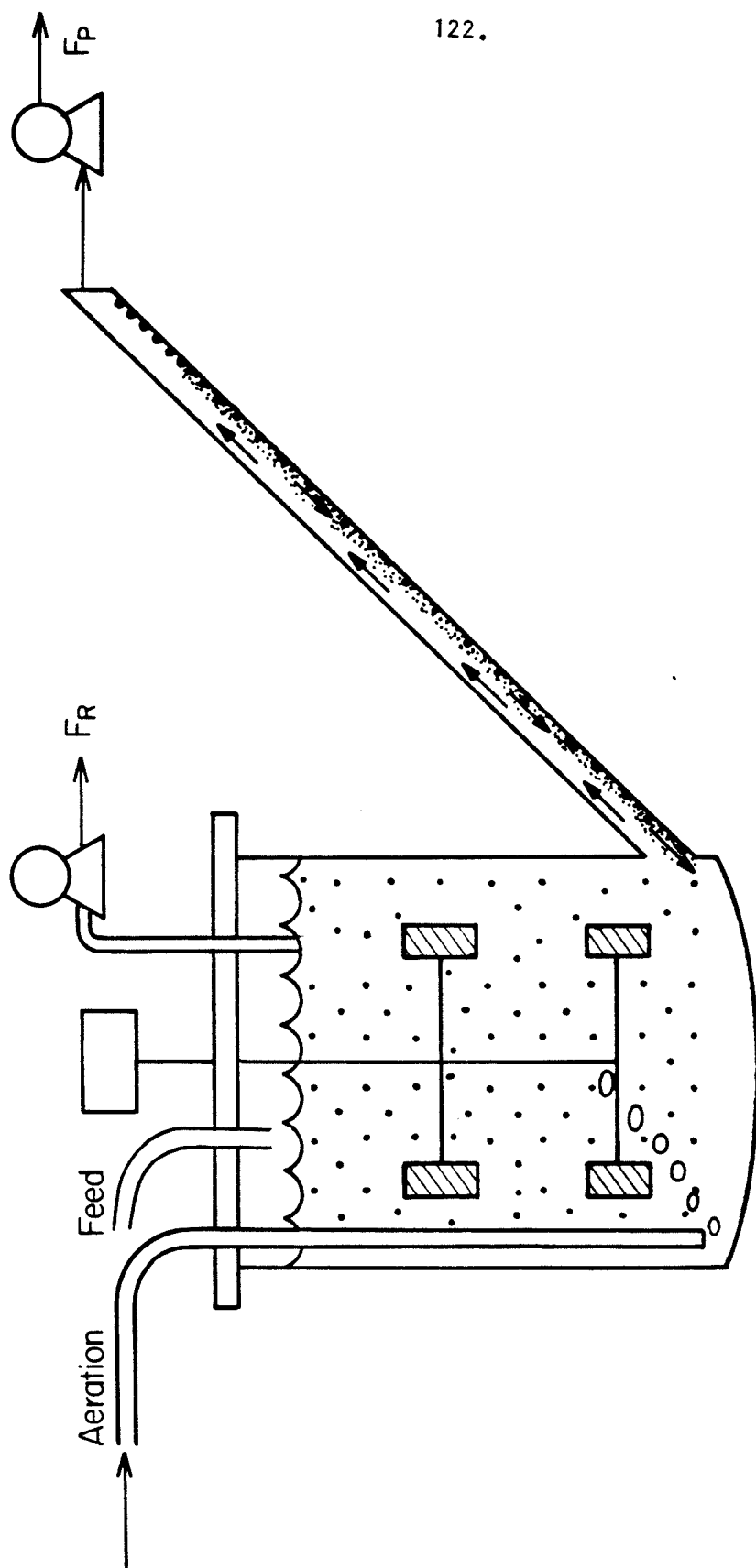


Figure 2. Schematic of the new fermentor design for facilitated cell precipitation and recycle. Reactor also contains probes for pH and temperature with controllers attached to a KOH addition line and a heater.

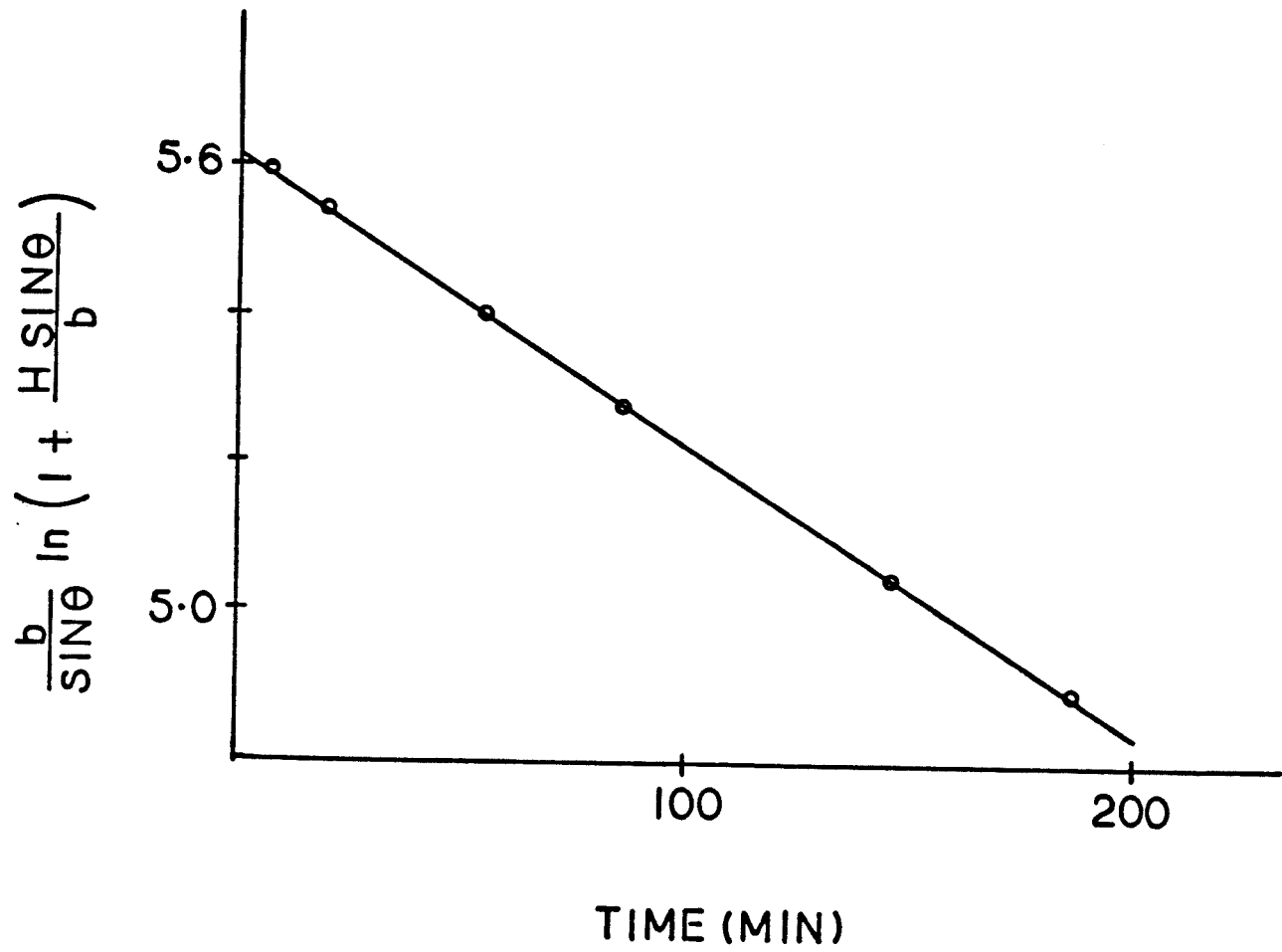


Figure 3: Experimental determination of the Stokes velocity of S. cerevisiae cells.

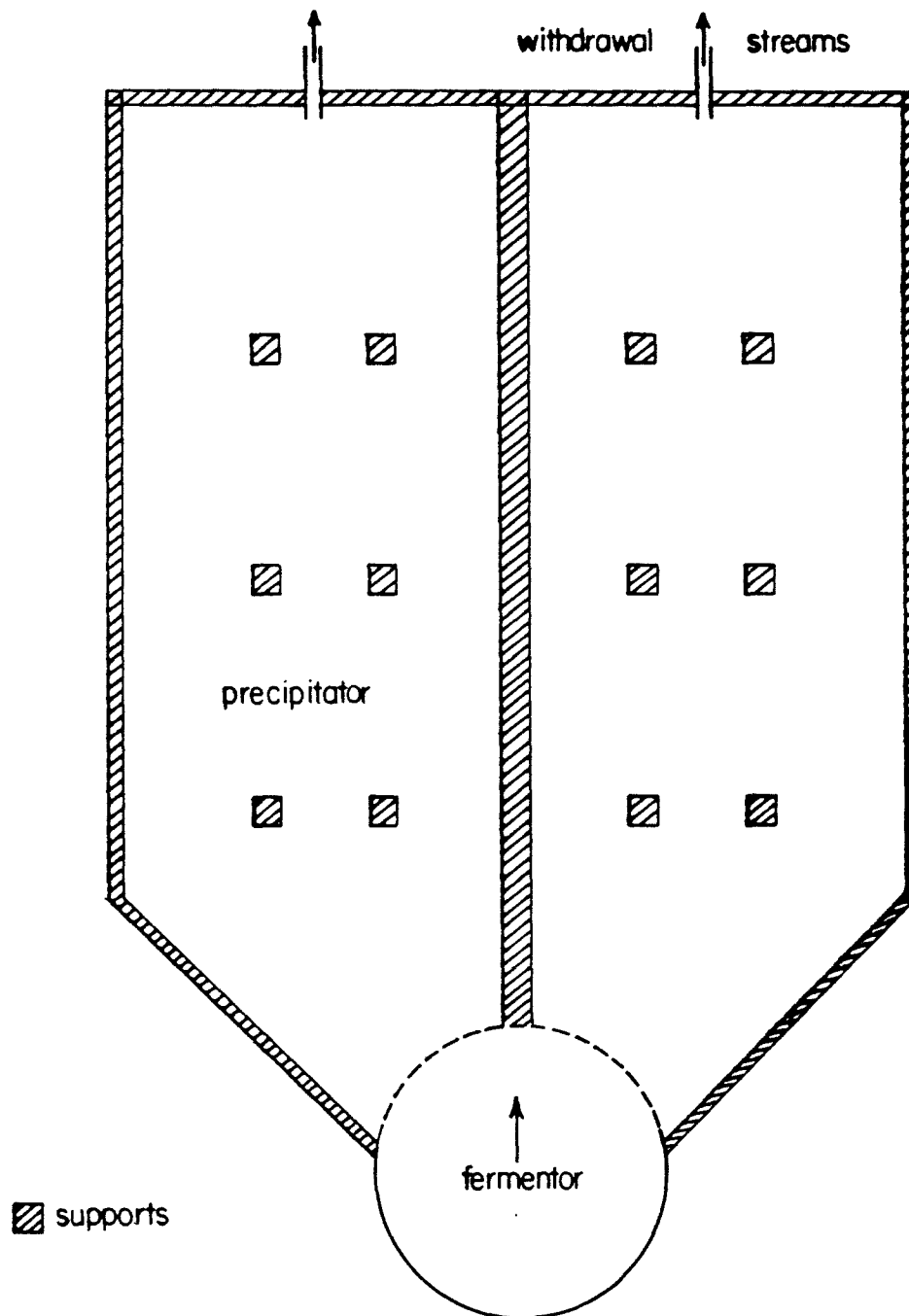
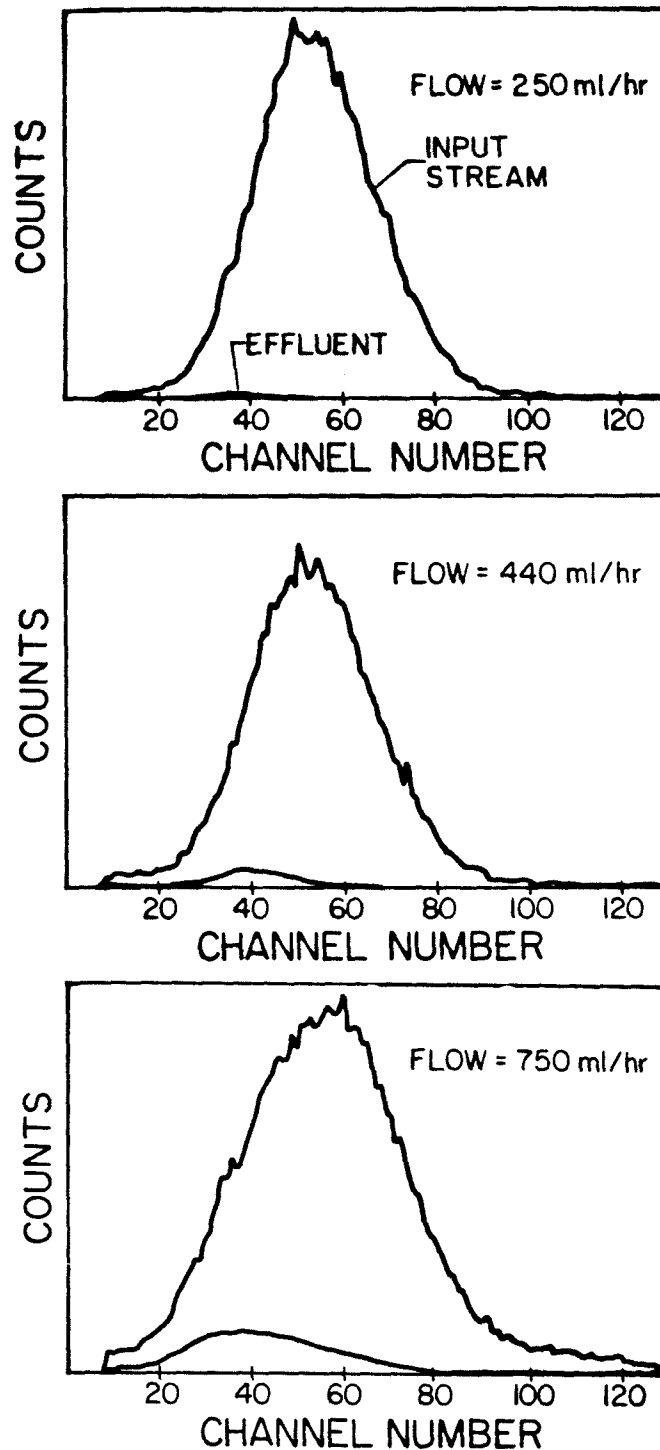


Figure 4: Top view of the settler part of the fermentor of Figure 2.



SIZE DISTRIBUTION OF INPUT AND EXIT STREAM
(CHANNEL 46 CORRESPONDS TO PARTICLE DIAMETER OF $4.1\mu\text{m}$)

Figure 5: Steady state cell size distributions at the entrance and exit streams of the settler of Fig. 4 for varying flow rates.

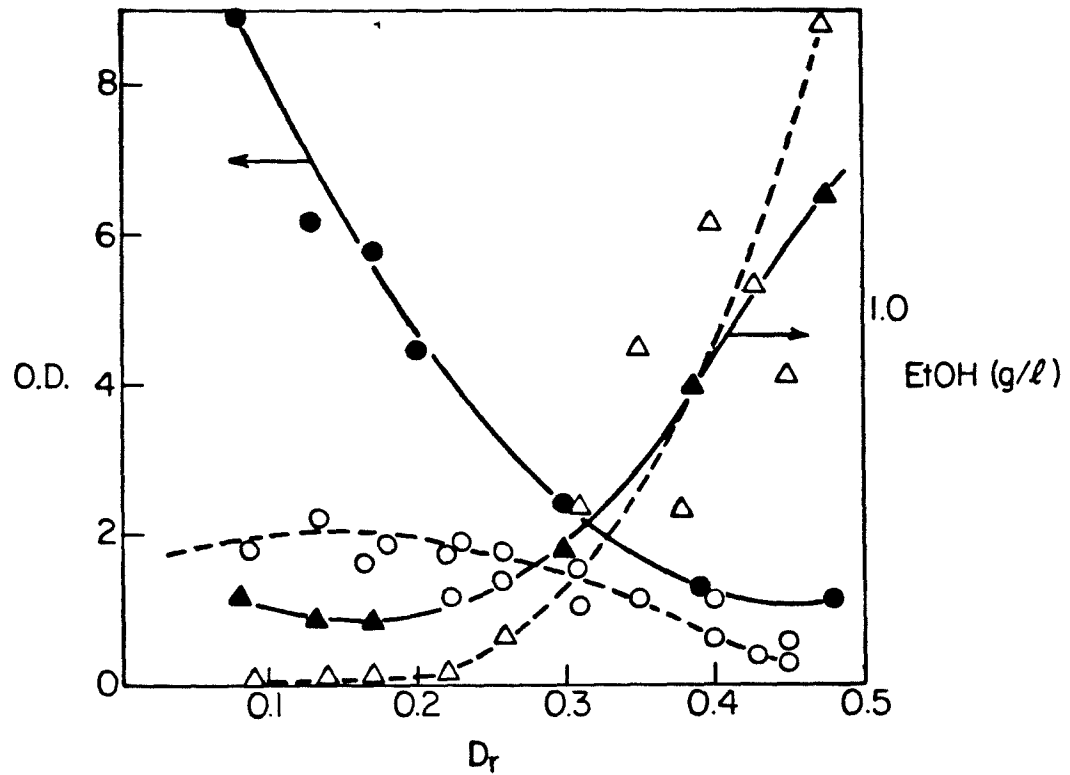


Figure 6. Steady state cell densities and product concentrations for the fermentor-precipitator combination as a function of the reactor dilution rate ($D_r = F_r/V$; where F_r is the rate of culture withdrawal directly from the reactor).
 ●, ▲: optical density and EtOH conc. for $D_p=0.4/\text{hr}$.
 ○, △: optical density and EtOH conc. for $D_p=0.0/\text{hr}$.
 ($D_p=0.0/\text{hr}$ is a typical chemostat)
 $S_F = 5 \text{ g/l glucose}$

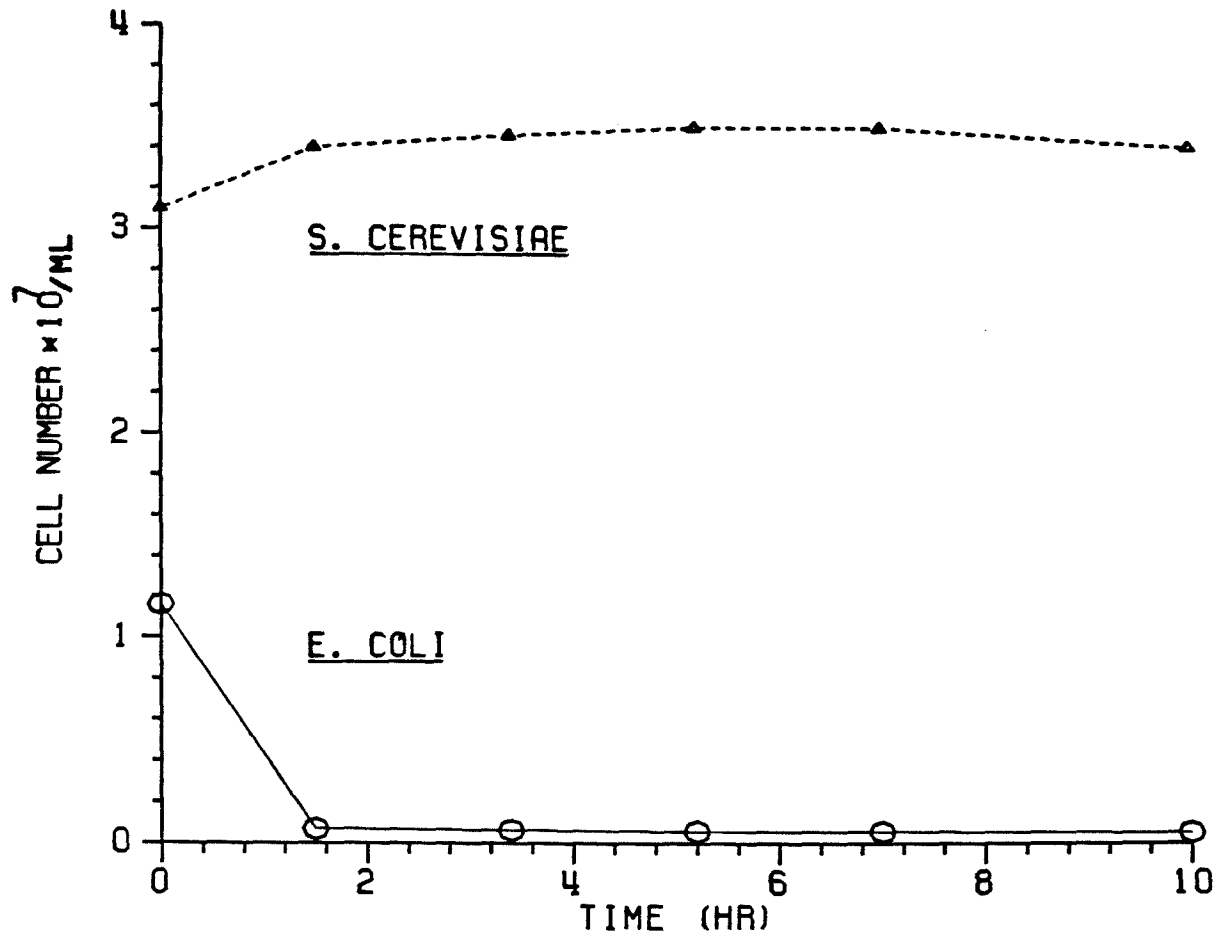


Figure 7. Washout of *E. coli* at high flow

Chapter 5.

Coexistence in a Recycle Reactor with Size-Selective Properties

originally prepared as *Stable Competitive Coexistence
in a Recycle Reactor with Size-Selective Properties*
by B.H. Davison, K.-Y. San, and G.N. Stephanopoulos

SUMMARY

A reactor with size-selective properties was found to allow a mixed culture of *Escherichia coli* and *Saccharomyces cerevisiae* to coexist under continuous culture conditions. The reactor consisted of a fermentor with an attached inclined side-arm to recycle the cells by enhanced sedimentation. The larger size yeast population was retained preferentially and recycled at high efficiencies while the smaller yet faster growing bacteria were removed through the side-arm. Stability analysis indicated that the coexistence of this system could be stable only if the net yeast removal rate through the side-arm as a function of the reactor yeast concentration was concave up. This would occur if growth continued in the side-arm or if settling efficiency decreased at higher cell densities. Another experimental system was devised to measure this net removal rate function. A negative removal rate (i.e., a net addition of yeast to the fermentor) was observed at low biomass indicating growth in the settler and explaining the stability of the coexistence steady state.

Introduction

A novel bioreactor was examined previously [Chapter 4] with high cell retention efficiencies under high flow rate conditions. The basic feature of this reactor was the introduction of an inclined side-arm at the side of a typical fermentor for the purpose of facilitating the precipitation of the suspended cells on the inclined surface, and thereby allowing cell-free liquid to be withdrawn at high flow rates from the reactor through the side-arm. Experimental studies with continuous fermentations of *S. cerevisiae* showed that very high cell density cultures could be retained in the reactor at total dilution rates exceeding by far the values allowed by the maximum specific growth rate of the culture. Furthermore, viable cells could be maintained under conditions of very low growth and ethanol was formed at high productivities that should be possible to increase further by a straightforward scale-up process of the side-arm settler.

With the new design the basic Stokes precipitation velocity is enhanced proportionally to the aspect ratio of the inclined settler. The Stokes velocity is, of course, proportional to the square of the cell diameter for dilute suspensions. There are two consequences of this fact: first, the new reactor is relatively ineffective for small cell-size bacterial fermentations (sizes on the order of $1\ \mu\text{m}$ equivalent diameter) while very good results are obtained with cell sizes larger than approximately $4\ \mu\text{m}$. Second, for a polydispersed microbial population, differences in the Stokes precipitation velocities can be magnified significantly to the point at which separation of the cell population on the basis of size is possible and retention of the larger-size cells in the reactor can be achieved.

In the latter case, critical to the type of culture established in the reactor is the net rate of cell removal in relation to the relative rates of growth of the various size populations in the fermentor. For a pure but polydispersed culture in

which all cells are growing at the same rate the reactor will be enriched in the larger size cells at sufficiently high side-arm withdrawal flow rates. For a mixed culture consisting of populations well separated with regard to cell size it is possible to use this reactor to selectively retain the population with the larger cells despite its possibly smaller rate of growth compared to that of the smaller cell population. This was demonstrated [Chapter 4] by washing out the faster growing but smaller size *E. coli* from a mixed culture with *S. cerevisiae* thus supporting the argument of increased resistance to small size contaminants in the new reactor operating at sufficiently high flow rates.

Another possibility suggested by the above studies is the stable coexistence under continuous flow conditions of microbial populations competing for the same rate-limiting nutrient. It has been shown by many workers that such coexistence is not possible in a well-mixed chemostat and the faster-growing species under the system conditions will eventually dominate the culture. If, however, the faster-growing organism is also of smaller size and thus can be preferentially removed from the reactor, then the possibility of coexistence arises by properly balancing the cell retention efficiencies for the two species with their corresponding growth and washout rates. In other words, the new reactor properly designed and operated could provide an environment where microbial competitors can coexist under continuous flow conditions.

This work investigated the above possibility with a mixed culture of *E. coli* and *S. cerevisiae* on glucose-limited medium. Experimental results showing coexistence are presented. Also, the stability of the mixed culture system in the modified chemostat environment is analyzed and conditions for stable coexistence are derived. This analysis assumes an unknown function for the net cell removal rate through the settler. Then perturbation eigenvalues are found for the linearized system. Necessary and sufficient conditions for stable

coexistence were found for the net removal rate function and experimentally verified.

These results offer another explanation to the observed species diversity in natural ecosystems despite apparent competitive interactions for a limited number of resources, namely, that other selection mechanisms are also in operation in addition to the one based on the rate of growth. Here the selection is based on size and occurs in different regions of the reactor system. Furthermore, a new apparatus is suggested for the stable propagation, or even the enrichment in the slower-growing population, of industrially important competing mixed cultures such as those resulting from plasmid segregation phenomena in cultures of recombinant microorganisms.

Materials and Methods

The reactor that was used for these studies has been described in detail elsewhere [Chapter 4] along with the basic hydrodynamic results needed for the design of the side-arm settler. A schematic of the reactor is shown in Fig. 1. The feed stream and aeration are supplied. The reactor contents can be withdrawn directly from the reactor through the level-control tube at a rate Q_R or through the side-arm at a rate, Q_P . In the latter case cells precipitate on the inclined surface at a rate enhanced by approximately 60 times over that of Stokes velocity for this reactor and fall by gravity back to the fermentation zone. The contents of the stream Q_R are the same as of the reactor while those of stream Q_P are depleted in the larger size cells. Controlling the two flows Q_R and Q_P independently offers an extra degree of freedom in fine-balancing washout rates and growth rates to meet a certain objective. In general, very large rates for Q_P yield a stream with the same contents as the reactor (no cell retention); intermediate rates would deplete the stream of larger size cells, and low flow rates yield a cell-

free medium. With the settler design used, a cell-free stream at a rate, Q_p , of 400 ml/hr could be withdrawn from the plates, while a rate of 700 ml/hr yielded 90% cell retention efficiency for a pure *S. cerevisiae* fermentation. A working volume of 900 ml was used in these studies.

E. coli strain B/R and *S. cerevisiae* strain ATCC #4126 comprised the mixed culture. Culturing, transferring and counting procedures have been reported before [Chapter 2]. Pure culture batch and washout studies have yielded a maximum specific growth rate of 0.6 hr^{-1} for *E. coli* and 0.45 hr^{-1} *S. cerevisiae*. Also the substrate saturation constant is much smaller for *E. coli* (5 mg/L) than for *S. cerevisiae* (50 mg/l) resulting in a specific growth rate for *E. coli* larger than that of the *S. cerevisiae* at all concentrations of the limiting nutrient. Furthermore, *E. coli* cells are much smaller than *S. cerevisiae* cells allowing for the easy discrimination between the two populations by the Coulter counting techniques, and also *E. coli* grow faster. These facts provide the necessary conditions for coexistence in the modified chemostat as presented in the introduction. Glucose-limited media were used in a phthalic acid buffer and at a composition similar to that reported earlier [Chapter 2].

Cell counts, optical densities, and glucose and ethanol concentrations were followed during the course of the fermentation by collecting samples from the two exit streams as well as directly from the reactor. Optical densities were measured spectrophotometrically (B&L Spec 21), glucose analyses of cell-filtered samples were performed with enzymatic kits (Sigma #15-UV), acetic acid and ethanol concentrations were measured by gas chromatography on Chromosorb 101. Viability tests of the sediment were performed by microscopic examination after treatment with methylene blue.

The reactor was inoculated with an actively growing culture and run in

batch culture until a significant biomass was achieved. Then the pumps (Masterflex) were started at the desired levels for the feed stream, Q_F , and plate withdrawal, Q_P . The pump for the reactor overflow, Q_R , was set faster than necessary so that it could also act as a level controller at the position of the exit tube. In operation the flow rates of streams Q_P and Q_R were measured directly and the feed stream calculated from the sum. A pH probe (Ingold) and controller (Chemtrix) were used with a base addition reservoir to control the pH at 4.0 for the pure yeast culture experiments and pH 5.0 for the mixed culture. The temperature was maintained at 30°C in the reactor by a heat exchanger and water bath. The plates due to their large surface area were probably nearer to room temperature (~22°C). When in operation, samples were taken and the reactor checked for leaks and contaminants. Air was sparged through the reactor at about 1.5 l/min. The reactor portion was kept well mixed with a magnetic stirrer.

Results and Discussion of Mixed Culture Experiments

Two separate sets of experiments with different glucose feed concentrations were carried out to study the stability behavior of the integral reactor sedimentor with *E. coli* and *S. cerevisiae*. Detailed descriptions on the experimental setup and procedure have been reported earlier (Chapter 4). As before, the concentration of each of the populations was monitored through cell counts by a Coulter Counter. Shown in Fig. 2 are the results of two different experiments with 5 g/l of glucose in the feed but with a different initial concentration of *E. coli*. As it can be seen, in both experiments the cell counts of both *E. coli* and *S. cerevisiae* at the end of the experiment stabilize for more than 20 hrs. Both experiments were shut down due to flocculation of the yeast when hundreds of cells clumped together and resulted in the domination of yeast in the reactor.

Two experiments at the same flow conditions with 1 gm/l glucose in the feed failed to establish a stable coexistence of the two populations. Each time *E. coli* was the dominant population. In experiments at high flow rates (Fig. 3), *E. coli* was washed out rapidly while yeast maintained a high density. It should be pointed out that *E. coli* experiences a dilution rate of D_T , Q_T/V_R , which here was in excess of its maximum specific growth rate while yeast sees an effective dilution rate of D_R , below its maximum specific growth rate.

Theory and Analysis

The dynamics of the above system with cell recycle as shown in Fig. 1 can be described by the following set of differential equations.

$$\dot{x}_1 = \mu_1(s)x_1 - \frac{(Q_T - Q_P)x_1}{V_R} - f(x_1, Q_P) \quad (1a)$$

$$\dot{x}_2 = \mu_2(s)x_2 - \frac{Q_T x_2}{V_R} \quad (1b)$$

$$\dot{s} = \frac{Q_T}{V_R}(s_f - s) - \frac{\mu_2 x_1}{Y_1} - \frac{\mu_2 x_2}{Y_2} \quad (1c)$$

where the subscripts 1 and 2 refer to the populations of *S. cerevisiae* and *E. coli*, respectively, x is the biomass concentration, s is the limiting substrate concentration. Q_T is the total flow rate into the reactor, Q_P is the flow rate of the side-arm and V_R is the reactor volume. In the above formulation, it is assumed that the specific growth rate of each of the populations is a function of the limiting substrate concentration alone.

Theoretical knowledge of exactly how a continuous settler would act on a polydispersed suspension is unknown. Thus for convenience all effects of the real side-arm are lumped into an undetermined function, f , as the net cell removal rate from the reactor proper. It is also assumed that there is no recycle for

the *E. coli* and that the removal rate of *S. cerevisiae* from the side-arm is a function of the side-arm flow rate and the cell concentration in the reactor only. Strictly speaking, the function $f(x_1)$ refers to the net removal rate of biomass at the interface between the fermentor and the side-arm. If it is assumed that there is no cell growth inside the side-arm, then once the cells once enter the side-arm they will either be removed from the side-arm through the exit stream or be recycled back into the fermentor. When cell growth does exist and case when the cell growth rate is larger than the removal rate, the function $f(x_1)$ may have different signs. If f is negative, a net amount of cells are being added to the fermentor from the side-arm.

In the following stability analysis, it will be assumed that $\mu_1(s)$ and $\mu_2(s)$ are both monotonic increasing functions of s , for example, a Monod type, and that the yields Y_1 and Y_2 are constant. It can be shown that if a steady state for the system described by Eqs. (1) does exist, the stability of such steady state will depend on the functional form of $f(x_1)$ alone for a fixed Q_P . The stability analysis is quite straightforward and is performed by employing linearized stability theory and applying the Routh test on the characteristic equation of the linearized system. Thus, if the steady state values of the above system for a given value of \tilde{Q}_T and \tilde{Q}_P are denoted by a tilde over the corresponding state variables, the linearized version of Eq. (1) is given by

$$\begin{pmatrix} \Delta \dot{x}_1 \\ \Delta \dot{x}_2 \\ \Delta \dot{s} \end{pmatrix} = \begin{pmatrix} W & 0 & \mu_{1s}(\tilde{s})\tilde{x}_1 \\ 0 & 0 & \mu_{2s}(\tilde{s})\tilde{x}_2 \\ \frac{1}{Y_1}\mu_1(\tilde{s}) & \frac{1}{Y_2}\mu_2(\tilde{s}) & Z \end{pmatrix} \begin{pmatrix} \Delta x_1 \\ \Delta x_2 \\ \Delta s \end{pmatrix} \quad (2)$$

with

$$W = \mu_1(\tilde{s}) - \frac{(Q_T - Q_P)}{V_R} - f_{x_1}(\tilde{x}_1)$$

$$Z = \frac{-\mu_{1s}(\tilde{s})\tilde{x}_1}{Y_1} - \frac{\mu_{2s}(\tilde{s})\tilde{x}_2}{Y_2} - \frac{Q_T}{V_R}$$

where Δx_1 , Δx_2 and Δs are the deviations of x_1 , x_2 and s from their steady state values and the subscript s refers to the derivative with respect to s . The characteristic equation of this linearized system is then given by

$$\lambda^3 + \lambda^2[-W-Z] + \lambda \left[ZW + \frac{\mu_2(\tilde{s})\mu_{2s}(\tilde{s})\tilde{x}_2}{Y_2} + \frac{\mu_1(\tilde{s})\mu_{1s}(\tilde{s})\tilde{x}_1}{Y_1} \right] - \frac{\mu_2(\tilde{s})\mu_{2s}(\tilde{s})\tilde{x}_2}{Y_2} W = 0 \quad (3)$$

where λ denotes the eigenvalues. The system is stable if all of the eigenvalues have negative real parts. It follows from the Routh criteria that we have to satisfy the following conditions. First it is necessary that all of the coefficients be positive. Second, if the first condition is satisfied, then it is necessary and sufficient that the following expression

$$-(W+Z)(WZ) - (Z) \left[\frac{\mu_2(\tilde{s})\mu_{2s}(\tilde{s})\tilde{x}_2}{Y_2} \right] - (W+Z) \left[\frac{\mu_1(\tilde{s})\mu_{1s}(\tilde{s})\tilde{x}_1}{Y_1} \right] \quad (4)$$

be positive and nonzero. Close examination of Eq. (3) reveals that the first condition requires W to be less than zero.

$$W = \mu_1(\tilde{s}) - (\tilde{Q}_T - \tilde{Q}_P) - f_{x_1}(\tilde{x}_1) < 0$$

or

$$\frac{f(x_1)}{\tilde{x}_1} < f_{x_1}(\tilde{x}_1) \quad (5)$$

Notice also that the expression in (4) will be positive and nonzero if the inequality (5) holds. Hence, one can conclude from the above analysis that the system governed by Eqs. (1) is stable if the inequality in Eq. (5) is satisfied.

In view of the importance of the recycle characteristics of the side-arm upon the stability of the system, a more detailed treatment on this subject will be presented.

It was shown above that the necessary and sufficient condition for stability of the mixed system was $\frac{f}{x_{1R}} < \frac{\partial f}{\partial x_{1R}}$, where x_{1R} is the reactor concentration of the larger species capable of settling and f is the net cell removal function from the reactor proper through the sedimentor. What curves might be expected for this function $f(x_R)$? Considering the settling characteristics of the cells as inert particles, two limiting cases are apparent. In the limit of a perfect 100% efficiency settler, $f(x_R)$ will equal zero throughout, presuming that a perfect settler can not be overloaded with particles. In the other extreme of a completely inefficient settler where no retention occurs (i.e., very high flow rates), $f(x_R)$ will equal $x_R Q_P$ and the reactor equations are equivalent to a chemostat with no settler.

In intermediate regimes, sedimentation theory indicates that the settler efficiency is independent of concentration; therefore f will equal $(1-\eta)Q_P x_R$ where η is the sedimentor efficiency. For a perfectly efficient settler η equals 1 and f equals 0. It is expected and was seen that at low flow rates the settler was 99% efficient. As flow rate increases, the size of the clarified top region will decrease and at some critical flow rate the efficiency, η , will fall from near unity. None of these possibilities will yield stability as in each case $\frac{f}{x_{1R}}$ equals $\frac{\partial f}{\partial x_{1R}}$. If there was a transition from $f = 0$ to $(1-\eta)x_R Q_P$ as x_R increased beyond some overload value, stability could appear in this concave region. This possibility is illustrated in Fig. 5.

But cells are not the inert particles demanded by this theory so there may be

other interactions that should be considered. First among these stabilizing interactions is growth; in addition there may be clumping, wall growth or fouling, and cell lysis. Clumping would act to increase the settler efficiency and have no effect on stability. Wall fouling, if minimal, should have no effect. If significant, the fouling would narrow the channel and thus the effective settler area, and so it would decrease the efficiency. This is a time-dependent phenomenon and its stability effect is unclear. This fouling should occur preferentially on the bottom plate where the dense sediment is already collecting. Wall growth is similar to fouling unless daughter cells are shed into the flow region and settle out. If wall growth is minimal this can be considered in the growth discussion below. Fouling and wall growth in this settler were minimal even in week-long runs. Lysis or the breakup of cells would decrease settler efficiency but should not occur under the low shear conditions in the settler.

Growth, if it occurs in the settler, allows the possibility of f being negative or the settler accomplishing a net addition of cells to the reactor. This would stabilize the equations proposed purely on transport characteristics shown earlier. Assuming that $f(x_R = 0)$ equals zero, these possible modified $f(x_R)$ are presented in Fig. 6. Some residual growth on cell storage materials should occur in the actively growing cells removed from the reactor. But this may not affect the measured biomass. In addition the cells may experience shock after removal from the well-mixed, low-residual sugar environment of the reactor with rapid sugar consumption to the cooler, low-substrate, high-ethanol and nonaerated sedimentor. Given a sufficiently long residence time the yeast should overcome whatever shock might occur and grow on the minimal residual substrate or the ethanol produced. The uncertainty due to these factors and in the absence of a clear theory for continuous settler operation and full knowledge of the cell cycle necessitates the experimental determination of

$f(x_R)$. The key element needed is the general shape of the curve and its sign so that a judgment may be made on the system stability.

Experimental Determination of $f(x_R)$

The function f may be visualized as the net flux across the junction between the reactor proper and the settling plates. In the integrated reactor-sedimentor system only the concentrations of the feed, reactor bulk, and effluent from the top of the plates can be sampled and measured. These measurements cannot determine f . A judgment can be made from these that f will be small relative to the system fluxes in an efficient settler. These difficulties can be resolved by redesigning the system in order to separate the reactor and settler functions.

An apparatus was assembled with a separate reactor and settler as shown in Fig. 7. The reactor operates as an ordinary chemostat providing a dense culture of actively growing cells. Aeration was 1 l/min, temperature was 30°C, and pH was controlled at 4 to reduce contamination. This culture will be the same steady state throughout the experiment with a total dilution rate of 0.2/hr and a 10 g/l glucose feed. Part of the reactor overflow will be pumped into a sterile stirred flask. Here it may be diluted with a buffered salt solution identical to the feed media and with minimal sugar (10 mg/l) and ethanol (1.5 g/l) added to match the steady state concentrations found in the reactor. This intermediate mixer is 30 ml in volume to minimize the holding time. As shown, the exit lines from the mixer are an air vent, a line to the settler, and a separate overflow line acting as a level controller. This configuration allows both the flow rate and the cell concentration to the settler to be varied independently from zero to the full reactor concentration and feed rate. Most importantly this is done without changing the state of the growing cells as would occur if the flow was controlled by changing the reactor dilution rate.

The settler, of course, is the heart of the experiment. A single channel was used, made of plexiglas and measuring 28" long by 4" wide and 1/4" separation. A sloped bottom was used to separate the inlet from the sediment collector and to aid in the sediment collection as shown in the inset of Fig. 7. This reduced the effective length to 26" with a working volume of 450 ml. The angle of inclination of the settler was fixed to achieve the same enhancement factor v_e/v_{Stokes} in the earlier reactor.

$$\begin{aligned}\frac{v_e}{v_{\text{Stokes}}} &= 1 + \frac{H}{b} \sin \theta = 1 + \frac{15.75''}{1/8''} \sin 33^\circ \\ &= 1 + \frac{26''}{1/4''} \sin \theta = 69\end{aligned}$$

yields

$$\theta = 40^\circ.$$

The effluent was controlled from the top and sediment collected in an unvented bottle connected to the lowest point of the plate by reducing tubes. The bottle is filled with sterile media without substrate. This salt solution must be used or the natural convection of different density solutions will dominate instead of solutions differing only in the amount of suspended cells. The sediment of suspended cells displaces the clear salt solution and collects in the bottle. The narrow, 1/8" or 1/4", connecting tube ensured mixing of the displaced cell-free solution with cells before entering the plates. This can be seen as a two-part system: the cells settle in the plate to the lowest point and enter the collector mouth. From there they remix and settle into the bottle. This was confirmed by observations that the collector mouth was well mixed and separation occurred lower in the collection tubes.

The pump was originally placed between the mixer and the plates, but back pressure changes when replacing the sediment or effluent collection bottles at low flow rates disturbed the plate stability (i.e. mixing of settled and clarified regions occurred) and eventually the pump was moved to the plate exit stream.

The inability to measure accurately and directly a sediment stream necessitated this collection cup approach. When a flow system of a certain cell concentration was begun, the system was allowed to stabilize for at least one plate residence time. The dynamics of enhanced velocity sedimentation allow rapid stabilization. Then cup samples were collected from the reactor and mixer overflows to determine the plate inlet concentration and timed samples were collected from the plate outlet and into a sediment bottle. The samples' volumes were measured and the samples centrifuged and filtered through 0.4 μm paper, and dried at 100°C for 4-5 hrs to determine the concentrations as gm Dry Wtg/l. The net cell removal rate is equal to flux of cells at the plate bottom or

$$f = x_m \cdot Q_p - \dot{S}$$

where x_m is the concentration of cells leaving the mixer and entering the plate, Q_p is the flow rate through the plates measured at the exit, and \dot{S} is the sediment collection rate calculated as the gm D.W. collected per the time that bottle was connected.

The sedimentor loss rate or the gm D.W./hr removed from the settler top effluent was calculated as $x_p \cdot Q_p$. x_p can be compared to x_m to give a measure of the settler efficiency η .

The experiments were performed at low flow rates from 20 to 86 ml/hr. A flow rate of 86 ml/hr in this settler gives a superficial velocity (Q_p/Area) of 14

cm/hr which is equivalent to the superficial velocity of the earlier integrated reactor at a flow rate of 430 ml/hr. This is compared to the Stokes velocity of 0.23 cm/hr measured in the previous chapter and the enhancement factor of 69 calculated earlier.

The averaged results of the samples are presented in Table I. Occasionally the collection of samples or changing of sediment bottles allowed backflow, disturbing the enhanced sedimentation within the plates, and the effluent concentration shot up until the system restabilized. These intermittent high x_p samples and the coincident \dot{S} values were discarded. An interesting observation was that the height of the clear zone from the plate top was independent of concentration and varied linearly with flow rate. Throughout the experiment the residual glucose was minimal at about 10 mg/l in the reactor, and at about 8 mg/l at the plate outlet. The ethanol varied from 1.0 to 1.4 g/l but was always comparable throughout the system. Acetic acid was negligible throughout (< 0.02 g/l) at these low sugar conditions and moderate dilution rate in agreement with the Crabtree effect. Thus inhibition and production of acetic acid, important in Chapter 3, can be neglected here.

It is quickly apparent that the magnitude of the two terms in f (equals $x_m Q_p - \dot{S}$) are comparable and there is a great sensitivity to error. Thus the results reported are the average of 4 to 6 samples each with a standard deviation of about ± 15 mg/hr. Some of the scatter was lessened by placing the pump at the plate exit and by replacing the 1/8" collection tube with a 1/4" diameter tube to avoid plugging of the collection channel at very low flow rates. From the data a plot of $f(x_R)$ was constructed for various Q_p (Fig. 8). At the maximum concentrations used, f is about zero for a Q_p of 40 to 86 ml/hr. At lower concentrations f becomes negative and more negative for the lower flow rates. This implies that the longer the residence time in the plates the more

growth can occur. The data at Q_p equals 20 ml/hr were marred by plugging of the collector due to the very low flow rates. At the lowest flow rates flocs could form and become large enough to block the outlet without being broken up.

The presence of a negative f at low x_R demonstrates that growth can occur in the plates, albeit at a slow rate. The slow rate is consistent with the minimal glucose levels at the plate inlet and outlet and with the plates operating at the nonoptimal ambient temperature. But growth and this $f(x_R)$ allow the stability criterion to be met. The magnitude is not important, for this stability criterion $f(x_R)$ must be concave up as shown in Fig. 7 and as required from the discussion earlier, once the assumption of continued growth in the plates is proven.

Conclusion

The experimental coexistence was shown and justified by theory and experiment. This demonstrates that the different physical characteristics of a mixed culture (size in this case) can be used to establish coexistence. Spatial nonuniformity, here the extreme case of a size selective settler, can accentuate the effect of these physical differences and allow coexistence in a competitive mixed culture where otherwise coexistence would not occur.

NOTATION

b	distance between plates in sedimentor
D	dilution rate = Q/V_R (hr^{-1})
D_T	total dilution rate = Q_T/V_R (hr^{-1})
D_R	reactor overflow dilution rate Q_R/V_R (hr^{-1})
f	net biomass removal rate from reactor through side-arm (mg/hr)
H	height of settler
Q_P	flow rate from settler (ml/hr)
Q_R	flow rate directly from reactor (ml/hr)
Q_T	total or reactor feed flow rate (ml/hr)
s	substrate (g/l)
sf	substrate concentration of chemostat feed (g/l)
\dot{S}	biomass sediment collection rate (mg/hr)
t	time (hr)
v_{Stokes}	Stokes settling velocity (cm/s)
V_R	reactor volume (l)
x_j	biomass concentration of species j (g/l); [$j=1$, <i>E. coli</i> ; $j=2$, <i>S. cerevisiae</i>]
x_m	biomass concentration in mixer (g/l)
x_P	biomass concentration in settler effluent (g/l)
x_R	biomass concentration in reactor (g/l)
Y_j	yield coefficient of species j per substrate consumed (g/g)
Δ	denotes a perturbation variable
μ_j	specific growth rate of species j (hr^{-1})
θ	angle of inclination of the settler
\sim	denotes a steady state

List of Figure Captions

Figure 1. Schematic of the new reactor design for facilitated cell precipitation and recycle. Reactor also contains probes for pH and temperature with controllers attached to a KOH addition line and a heater.

Figure 2. Coexistence at moderate D_R of *E. coli* and *S. cerevisiae* with 5 g/l glucose feed, $D_T=0.33/\text{hr}$ and $D_P=0.23/\text{hr}$. Fig. 2a High initial *E. coli*. Fig. 2b Low initial *E. coli*.

Figure 3. Washout of *E. coli* at high flow, $D_T=0.89/\text{hr}$, $D_P=0.48/\text{hr}$, and $s_f=5 \text{ g/l}$.

Figure 4. Possible curves for the Net Removal Rate, $f(x_R)$, from transport characteristics.

Figure 5. Possible curves for $f(x_R)$ if growth occurs.

Figure 6. Schematic of experimental apparatus to determine $f(x_R, Q_P)$.

Figure 7. Experimental Net Removal Rate, $f(x_R, Q_P)$.

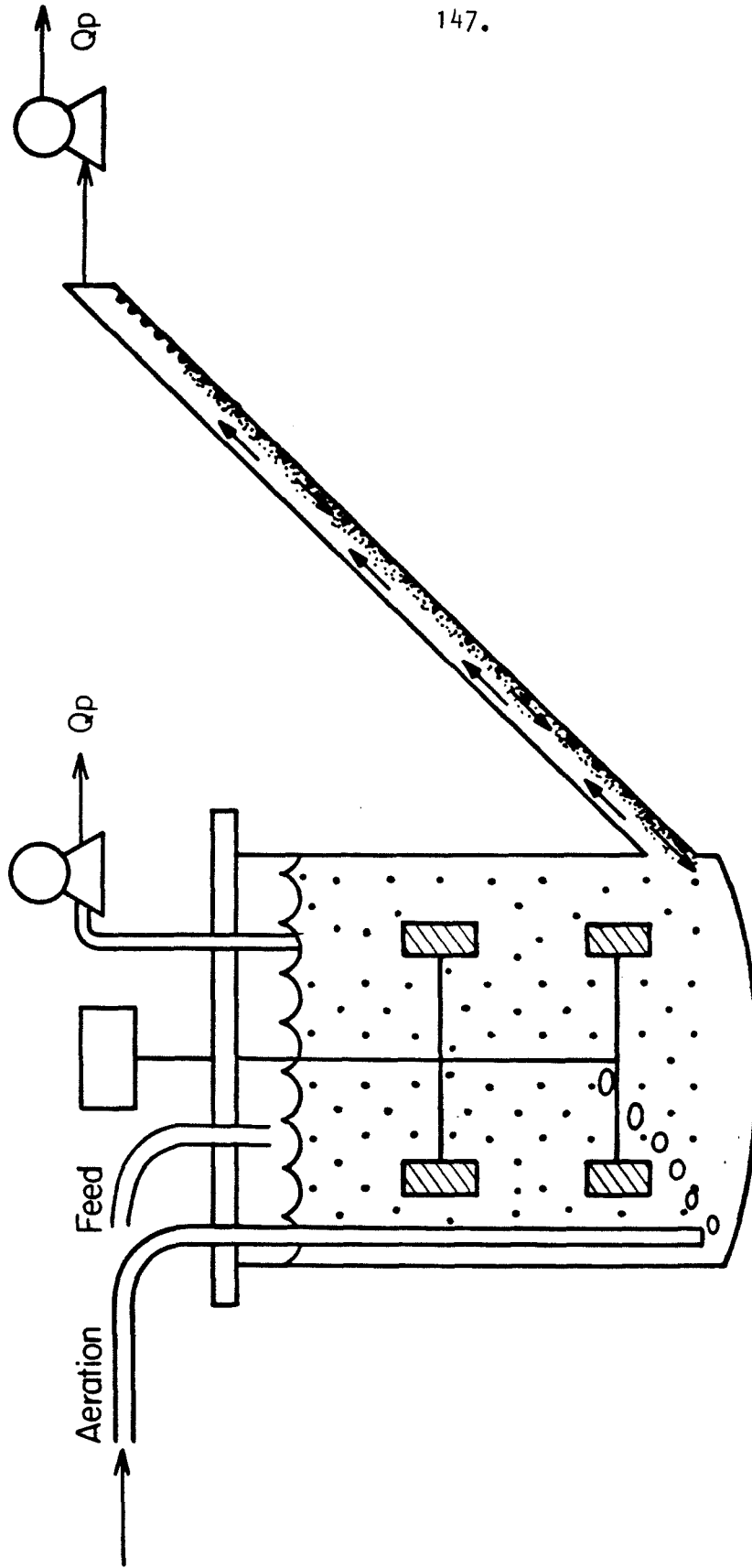


Figure 1. Schematic of the new fermentor design for facilitated cell precipitation and recycle. Reactor also contains probes for pH and temperature with controllers attached to a KOH addition line and a heater.

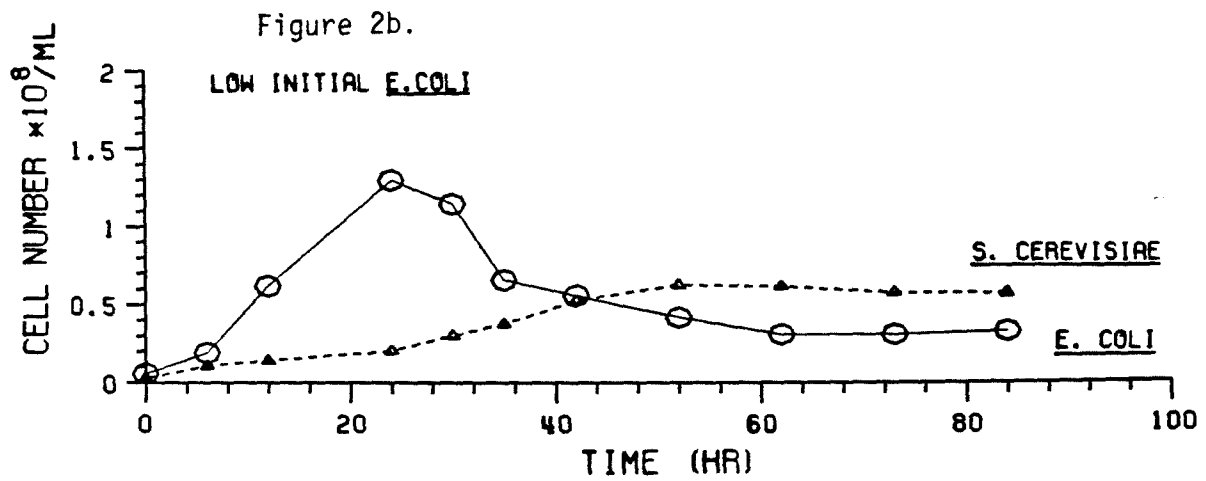
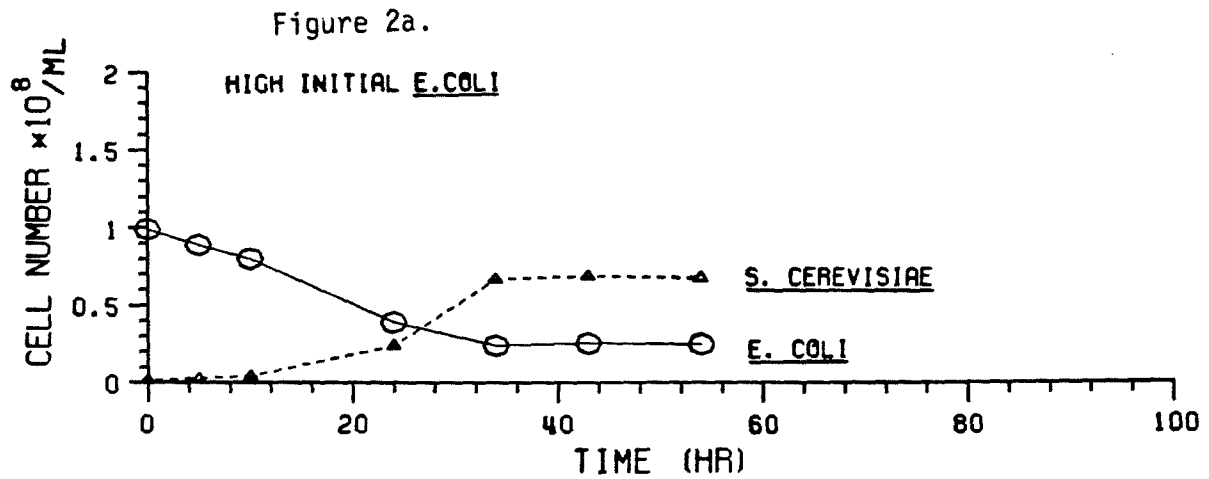


Figure 2. Coexistence at moderate D_R of *E. coli* and *S. cerevisiae* with 5 g/l glucose feed, $D_T=0.33/\text{hr}$ and $D_P=0.23/\text{hr}$.

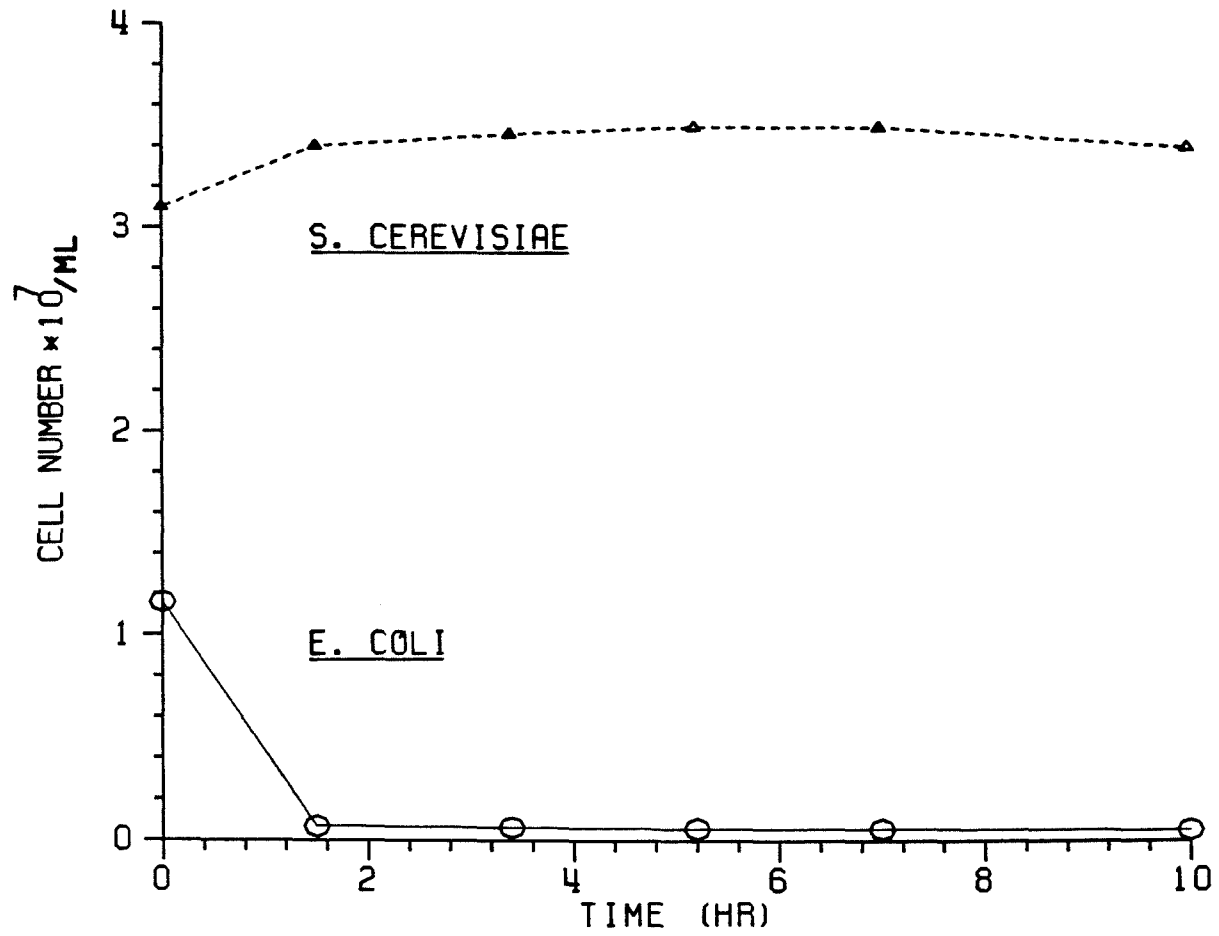


Figure 3. Washout of *E. coli* at high flow, $D_T=0.89/\text{hr}$, $D_P=0.48/\text{hr}$, and $s_f=5 \text{ g/l}$.

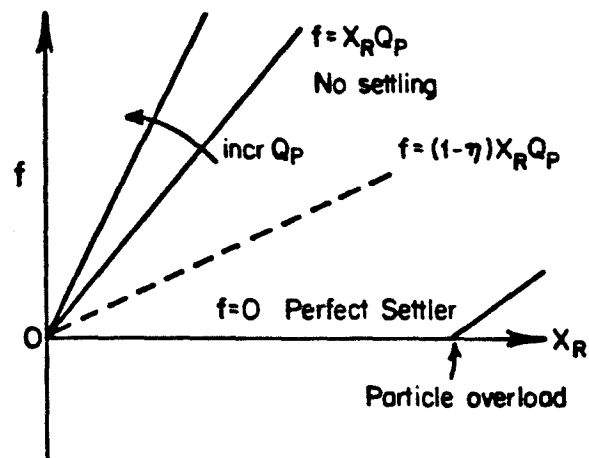


Figure 4. Possible curves for Net Removal Rate, $f(X_R)$, from transport characteristics.

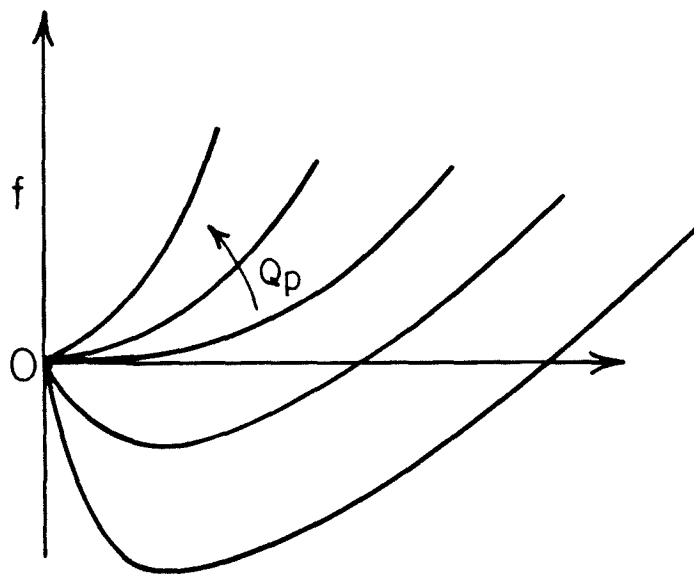


Figure 5. Possible curves for $f(X_R)$ if growth occurs.

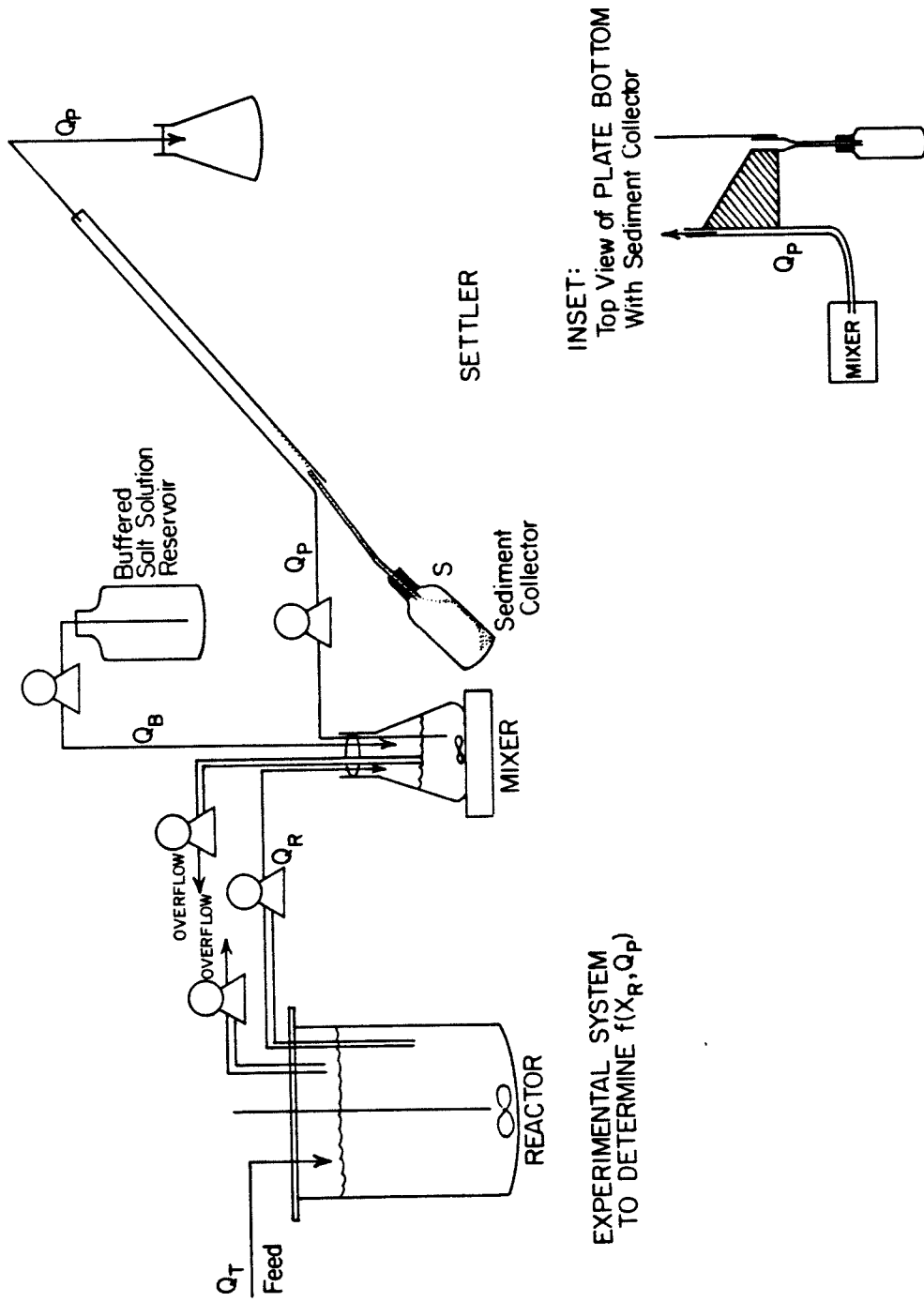


Figure 6. Schematic of experimental apparatus to determine $f(X_R, Q_P)$.

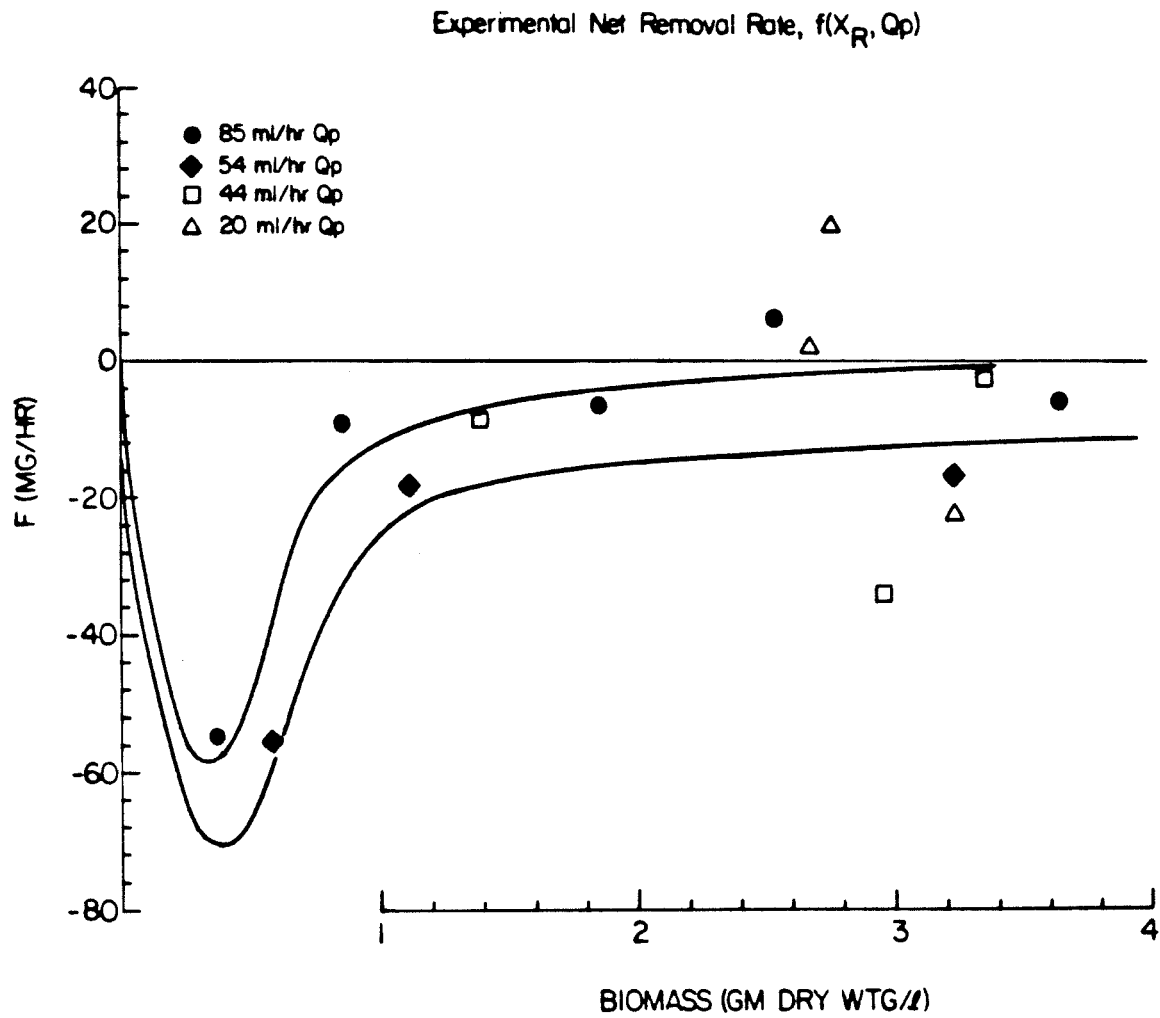


Figure 7. Experimental Net Removal Rate, $f(X_R, Q_p)$

Chapter 6.

Cross-Dominance and Dilution Rate in Two Mixed Culture Pairs

INTRODUCTION

This chapter returns to the pure culture and cross dominance experiments mentioned as preliminary results earlier- particularly in determining the μ_{\max} and K_s . These experiments are presented and discussed in more detail in order to illustrate some of the complexities and problems faced in performing mixed culture experiments. Notable among these was the search for a proper mixed culture and also the unexpected ability of *E.coli* to adapt slowly to increasingly acidic conditions.

The initial goal of my research was to create a persistent mixed culture using cyclic flowrates (or dilution rates). Stephanopoulos et al.[1979] have theoretically studied the stability of various systems using these suggestions. Cyclic inputs can lead to stable periodic trajectories of coexistence [Stephanopoulos et al., 1979b]. The organisms must have crossing substrate saturation curves. Then coexistence is achieved by cycling the dilution such that one is favored for a while, and then the other population is favored, or it is achieved by periodic harvesting of a portion of the reactor. The cycle time and the magnitude of the dilution range or harvest volume are operating parameters necessary to determine the stability numerically.

This goal appeared promising from the pure culture batch and continuous experiments. But this approach was eventually abandoned as intransigent for reasons reported below.

Materials and Methods

The materials and methods used were reported earlier (Chap 2.). In brief: the media were a defined glucose media for yeast reported earlier and a lactic acid media reported here. The quantities for the *Spirillum* enrichment media are for 1. l distilled water: 1.25g (NH₄)₂SO₄, 0.5g MgSO₄*7(H₂O), 0.002g MnSO₄, 0.01g NaCl, 0.02g CaCl₂, 1.77g K₂HPO₄*3(H₂O), 0.335g KH₂PO₄, 0.2mg EDTA, 2.3mg FeSO₄, 0.125 lactic acid, and neutralized with KOH to pH 7.

The primary measure of the biomass was by optical density at 660 nm. A correlation was established for the deviation from linearity of the total absorbance and biomass by testing dilution of the samples. Complete batch growth on 1 gm/l glucose gave final absorbances of about 0.400 and 0.450 for *S. cerevisiae* and *E. coli*, respectively. The absorbance of *S. cerevisiae* is linear throughout this range, while *E. coli* deviates above A=0.200 to a maximum deviation of 10%.

The Coulter Counter was used to give a direct count of particles and their size distribution in a sample. Both sample and background counts were taken.

The metabolites were measured using enzymatic test kits. 2 mls of sample were filtered within three minutes of removal and frozen to await enzymatic testing. The numerical calibrations for glucose and ethanol were checked and found accurate. The lowest concentrations detectable by this method are 20 μ M glucose and 2 μ M ethanol (4.0 mg glucose and 0.1 mg EtOH).

The batch experiments were performed in 125 ml Erlenmeyer flasks with cotton plugs in a rotary shaker. All batch runs were performed in parallel with three or four identical flasks and the results averaged. The chemostat used for *E. coli* and *Scerevisiae* system was a modified version of the New Brunswick Bioflow system. There was a pH probe, controller, and magnetic stirrer For the

Sp. metamorphum and the *E. coli* a blown glass chemostat was used with a 450 ml volume. Phosphate buffer in the media maintained the pH near 7 and mixing was provided by the aeration. In both, the level was maintained by overflow; temperature was controlled with a water bath.

The reactor was sterilized, filled, and inoculated with an actively growing culture. The reactor was run batch while biomass increased to near the expected steady state value. Flow rates were checked by measuring the overflow. Samples were taken about every residence time: the absorbance measured and a filtrate frozen for glucose and ethanol analysis. A steady state was assumed if both the biomass and glucose concentrations were constant within 5% for three samples. It was discovered in the first runs that constant biomass alone did not indicate a steady state. Samples were also diluted with electrolyte and run through the Coulter Counter at the appropriate settings.

Mixed Cultures

The common stable mixed cultures such as yogurt and predation involve some sort of mutualism. Most other mixed systems are unstable in a conventional CSTR. The creation of stable coexistence by varying operating conditions for an otherwise unstable mixed culture will increase the possible usable mixed cultures and their applications dramatically. Competition is studied as the cleanest interaction and the least stable under constant conditions. Exploring the interactions and dynamics of mixed cultures will help develop strategies for stable coexistent operations with uses and problems for which current pure culture techniques may be inapplicable.

E. coli - *Sp. metamorphum* System

The first system studied was *Escherichia coli* and *Spirillum metamorphum* on lactic acid. These had been shown to have crossing substrate saturation curves [Jannasch, 1967]. The literature sizes (*E. coli* is a 2 μm by 1 μm rod and *Sp. metamorphum* is 6 by 1 μm bent rod) indicated that the Coulter Counter would be able to distinguish between them. Under pure batch growth, the two cultures when mixed gave a bimodal peak which could be analyzed into separate populations.

Batch studies were performed first. *E. coli* on lactic acid is relatively independent of temperature between 25 and 37°C., while *Sp. metamorphum* grows weakly at 37°C and best at 30°C. A phosphate buffer was used to control pH. The effect of pH between 7.1 and 7.8 was studied for each. A pH of 7.3 was chosen since *E. coli* did slightly better at the lower pH; while the *Spirillum* did better at the higher values. At shaker settings above 100 rpm *Sp. metamorphum* does not grow. From microscopic observation of damaged cells it

appeared that the shear was too great. *E. coli* was unaffected by the increased agitation and aeration; this indicated no shear and sufficient aeration at 100 rpm. Throughout the experiments it was noted that *Sp. metamorphum* is a weak organism: given to long lags and very susceptible to shocks and contamination. The batch experiments gave μ_{\max} of 0.41/hr and 0.12/hr for *E. coli* and *Sp. metamorphum*, respectively. With the literature K_s values this system would have crossing specific growth curves.

Under the limited growth conditions in the chemostat, most organisms are smaller than in exponential growth. The *Spirillum* became much smaller- about 3 μm long. Now mixtures of the two population formed a unimodal size distribution and were unseparable with the Coulter Counter. Colonies for plate counts on nutrient agar or lactic acid media agar were practically indistinguishable. Another unique media for easy and accurate plate counts of both species were not known. For separate plate counts Eosin Methylene Blue agar is specific for *E. coli* but a media specific for *Spirillum* was not known.

A system of *Spirillum serpens* and *E. coli* on asparagine was briefly explored; but the preliminary growth results were not promising and the size differential between the species was even less than above.

This system with crossing substrate saturation curves was taken from the literature. For convenience and accuracy a Coulter Counter was planned to be used to separate the populations. This would also eliminate the two-day lag in seeing results from plate counts. The batch runs of *E. coli* and *Sp. metamorphum* were promising with respect to both the μ_{\max} and the sizes. But under continuous culture the size separation disappeared. The inability of the Coulter Counter to distinguish the populations combined with the experimentally still undetermined K_s values and the recalcitrant nature of *Spirillum* growth made

choosing a new system more attractive than attempting to make do with the *Spirillum-E. coli* system.

***E. coli* - *Saccharomyces cerevisiae* System**

E. coli and *Saccharomyces cerevisiae* were chosen as the replacement pair. Both are common, well-studied organisms, especially when grown on glucose, our chosen substrate. Their cell volumes are quite separated. *E. coli* is a 2 by 1 μm rod and *S. cerevisiae* is a 5 to 8 μm sphere. Furthermore, literature data indicated that with proper adjustments of the cultivation conditions a crossing of the specific growth rate curves could be achieved. The table below summarizes some literature values for growth. [Shehata and Marr,1971; Leuenberger,1972]

Table I Monod Growth Constants

	μ_{\max}	K_s	T_{opt}	pH_{opt}
	hr^{-1}	M glucose	$^{\circ}\text{C}$	
<i>E. coli</i>	0.8	10^{-6}	37	7
<i>S. cerevisiae</i>	0.5	10^{-4}	30	6

It can be noticed from the table that the K_s values are widely separated for the two species. On the other hand, the μ_{\max} values, which are sensitive to pH and temperature, are rather close. The *E. coli* are more sensitive to pH than the yeast. Therefore the strategy in creating crossover was to operate at 30 $^{\circ}\text{C}$ and a low pH to give the yeast a larger μ_{\max} . The positions of K_s should not be

reversed since the difference is two orders of magnitude. These attempts were successful as shown below.

A second possible complication with the new system of *S. cerevisiae* and *E. coli* was the possible interference of the metabolic products of the two organisms on glucose. *S. cerevisiae* produces ethanol and *E. coli* produces acetic acid. *S. cerevisiae* exhibits the "Crabtree" effect; in brief, a fermentative metabolism is used at high substrate levels while a slower but more efficient respiratory metabolism functions at low substrate. However, this is no problem since, if there is inhibition due to product formation, the ethanol production will only occur at high dilution rates where the yeast already should dominate by pure competition alone. In contrast, acetic acid production will be greatest at low dilution rates where *E. coli* should dominate. Therefore the products may affect the quantitative results but not the crossing substrate saturation curves at low substrate concentrations.

Results and Discussion

Batch Experiments

For *E.coli* and *S.cerevisiae* sufficient aeration is provided by shaking at 150 rpm, below 80 rpm growth is affected. No shear effects were noted for either at 150 rpm.

The initial batch experiments for both species at pH 4.0, 4.5, 5.0, and 5.5 showed that pH decreased rapidly during growth for both and that *E.coli* stopped all growth below pH 4.0. These preliminary experiments indicated that the desired pH, for which the maximum growth rate of *S. cerevisiae* is greater than that of *E.coli*, lay between pH 4 and 5. The next attempt to control the flasks' pH was by measuring the pH of each sample and adding the base needed to restore the pH with a sterile micropipet. With sampling every hour and using this stepwise base addition, pH could only be maintained to within 0.5.

Below pH 5.5 the phosphate buffer in the media is ineffective and most common buffers in this range are organic acids which are readily metabolizable by *E.coli*. The use of phthalic acid as a possible buffer was investigated. In the defined media, without glucose but with 5 or 1 gm of Potassium Phthalate neither *E.coli* at pH 7 nor *S. cerevisiae* at pH 6 grew at all. In succeeding experiments using $10^{-3}M$ and $10^{-2}M$ phthalate buffer with a much reduced stepwise base addition, the pH was maintained within ± 0.2 and ± 0.05 , respectively. There was no apparent effect on growth from the phthalic acid in any of the experiments. The only difference was a much better agreement among the parallel runs, due to the stable pH. From this point on all batch flasks were run with phthalate buffer.

The batch growth experiments are summarized in Table II. Typical runs for

each are shown in Fig. 1. It is clear that *S. cerevisiae* is insensitive to pH between 4 and 5, while *E.coli* is very sensitive. It is important to note that, while pH 4.0 stops the growth of *E.coli*, the bacteria remain viable. In both batch and chemostat experiments growth stopped at pH 4.0 but would resume when the pH was restored to a higher value. The maximum growth rates on glucose at pH 4.5 are 0.42/hr and 0.31/hr for *S. cerevisiae* and *E.coli*, respectively.

Complete analysis of some batch runs indicates that ethanol production is not directly growth-associated. A maximum of 0.32 gm ethanol/l was achieved during a batch on 1 gm/l glucose. This agrees with the "Crabtree" effect- a dual fermentative and respiratory pathway with a varying degree of respiration depending on the sugar concentration.

S. cerevisiae will not grow on acetic acid and *E.coli* will not grow on ethanol as the sole substrates in the defined media. This eliminates commensalism, where one lives off the other's products as a possible stabilizing interaction.

Next the possible inhibition effects of these products on the other organism were explored. The maximum yield of these products is theoretically one mole for every mole of glucose. Since 1 gm glucose/l is used, we chose 0.5 gm/l of ethanol or acetic acid to be in excess of this maximum for our inhibition studies. Acetic acid in any concentration up to the maximum had no effect on the growth of *S. cerevisiae* on glucose. Yeast growth on glucose is then independent of acetic acid (Table IIc). As expected, ethanol does inhibit *E.coli*, but not at low concentrations. There is no appreciable effect below 0.05 gm/l ethanol and only a slight effect up to 0.2 gm/l (Table II d or see Chap. 3, Fig.2). During respiratory growth of yeast negligible alcohol will be formed. During fermentative (high sugar) growth alcohol is formed and some inhibition may occur. The experimental yield of about 0.32 gm ethanol per gm glucose in batch growth indicates that

the ethanol inhibition of *E. coli* will be minor if at all.

It was discovered in batch and chemostat runs that care must be taken to ensure that the organisms are sufficiently acclimated to the culture conditions from the refrigerated stock cultures. At least 12 successive generations or three flasks were grown before initiating the experiments. If the acclimation was not sufficient, for example, the yeast grew qualitatively correct but at half its maximum growth rate and with a different yield.

Continuous Experiments

Some of the pure continuous culture runs of *E. coli* are recorded in Table IIIb. In all the steady states achieved the sugar concentration was at the very lower limit of the enzyme kit. The K_s must be in the range of 4 to 8 mg/l glucose. The small increase of biomass with D can be explained. The Monod model, used above for illustration, assumes a constant yield (Y) and no maintenance (m). For a steady state biomass this gives

$$x = (s_f - s)Y.$$

But maintenance is important in substrate limited systems. Just simply including a constant maintenance term gives

$$x = (s_f - s) \left(\frac{1}{Y} + \frac{m}{D} \right)$$

where m is gm glucose/gm biomass-hr. Then at very low s , as D increases the biomass will increase. As discussed before this change in model will not affect the desired or expected results.

The observed steady states for *S. cerevisiae* are reported in Table IIIa. As with *E. coli* the sugar concentration was low; but the yeast values are all

consistently higher than for *E. coli*. From these K_s is estimated at about 30 mg/l glucose, still significantly larger than the K_s of *E. coli*. As seen above, maintenance appears to be important at low growth rates. As D increases, a slight increase in biomass was observed followed by a decrease to washout. Ethanol production was qualitatively as expected from the literature and the Crabtree effect. Negligible alcohol levels were found at low D and low sugar and higher levels at the higher dilution rates. The ethanol levels observed were all below that needed to inhibit *E. coli*.

Typical population size distributions for yeast and *E. coli* were shown in Chapter 2, Fig. 2.

The organisms, especially *E. coli*, grew better in continuous rather than in batch culture. This is probably due to the more stable conditions (substrate, aeration, and, most importantly, pH) which allow a better adaptation. This caused a problem. At pH 4.5 *E. coli* completely dominated over established cultures of *S. cerevisiae* at several dilution rates up to and including 0.4/hr. Obviously the μ_{max} of *E. coli* had increased. This was counteracted by lowering the pH further. During the last run the pH was lowered to 4.3 while still at $D=0.4$ and with *E. coli* winning. The high concentration of *E. coli* washed out while the yeast increased from a negligible residual population. This run became contaminated before complete dominance of the yeast was attained. The new condition was successful in lowering the μ_{max} of *E. coli* below that of the yeast. The next continuous run was at pH 4.3. *E. coli* was inoculated to a steady state *Saccharomyces* culture. At $D=0.14$, observed by the Coulter Counter, two separate inoculums of *E. coli* washed out of the system. The ethanol concentration was less than 10 mg/l, below that needed to inhibit *E. coli*. Before the third *E. coli* inoculum, the dilution rate was lowered to 0.07/hr. *E. coli* dominated within two days. After increasing to $D=0.22$, both populations initially dropped. The *E. coli*

continued washing out. The *S. cerevisiae* were increasing again when a contaminant appeared. The time course of this last run is shown in Fig. 2.

Contamination occurred in most runs of over two weeks' duration. This was alleviated by increased positive pressure, improved sampling technique involving purging the sample line, and the use of redundant sterile filters in the media and air streams.

At pH 4.3 there is cross dominance between *E.coli* and *S. cerevisiae* on glucose. Dominance can be predicted in advance by setting the dilution rate with low D favoring *E.coli* and high D favoring *S.cerevisiae*. The question remained whether that dominance can be switched at will back and forth between regimes with just the dilution rate in a long run.

The next experiments tested for a forced coexistence caused by cycling of the dilution rate. The chemostat was inoculated with one organism and run with a step change between two dilution rates. Each organism was favored by one of the dilution rates. These dilution rates were chosen equidistant to the critical crosspoint dilution; then equal time would be spent at each of the two rates. When the second species was added, if the second species increased then it was moving toward a state where it would persist in the system; or equivalently, there is a steady state for that organism in this cycling system despite competition. The experiment would then be repeated, reversing the organisms but with the same cycle. If the second organism also increased from its initial inoculum, it was moving so that it would persist, too. If both organisms would persist in the system then there must be a stable coexistent steady state. This use of a small inoculum into an existing cycling culture allows the demonstration of coexistence for those organisms without waiting for the system to stabilize into some limit cycle. If the runs can be extended longer without contamination,

they will indicate what form this forced coexistence will take. In the extreme of a very long switching time, a largely complete changeover between steady state populations is expected. As the switching time decreases, the magnitude of these cycles would decrease and the coexistence may be lost. Eventually when the changes are so rapid that the dilution rate is essentially constant at the average, the coexistence must be lost.

When these experiments were performed with an oscillation period of about a day, used in order to make obvious the population shifts it became apparent that the *E.coli* became increasingly acid-tolerant and eventually over a week or two came to dominate at all D. Whether this was due to continued adaptation or by mutation under strong selection pressures is unclear. No stable sustained oscillations in cell number were achieved by using D as the forcing function.

This was especially frustrating as the crossing substrate saturation curves had been clearly demonstrated. But due to the changing μ_{\max} of *E.coli* a forced persistence of the mixed culture caused by flowrate variations was deemed impossible to demonstrate in a long experiment and unconvincing in a short experiment because of the irreproducibility. Oscillations of pH were then explored (successfully as seen in Chap. 2). This avoided *E.coli* adaptation by changing the selection pressure drastically within every cycle. The best bacteria at pH 5 were the wild type and the acid-tolerant organisms would lose. In addition, small incremental changes would not be preserved due to the large pH shift. By contrast with D shifts the selection pressure was constant to increase μ_{\max} at pH 4.3 and a slightly more acid-tolerant bacteria would be preserved and come to dominate at all D.

REFERENCES

- Jannasch, Holger W. (1967). "Enrichments of Aquatic Bacteria in Continuous Culture," *Archiv fur Mikrobiologie*, **59**, 165.
- Leuenberger, Hans Georg W. (1972) "Cultivation of *Saccharomyces cerevisiae* in Continuous Culture: II. Influence of the Crabtree Effect on the Growth Characteristics of *S. cerevisiae* Grown in a Glucose Limited Chemostat," *Arch. Mikrobiol.*, **83**, 347.
- Shehata, T.E., and Allen G. Marr. (1971). "Effect of Nutrient Concentration on the Growth of *Escherichia coli*". *J. Bacteriology*, **07**, 210.
- Stephanoloulos, G., Fredrickson, A., Aris, R. (1979). "Growth of Competing Microbial Populations in CSTR with Periodic Varying Inputs," *AIChE J.* **25**, 863.
- Stephanopoulos, G., Fredrickson, A. (1979). "Effect of Spatial Inhomogeneities on the Coexistence of Competing Microbial Populations," *Biotechnology and Bioengineering*, **21**, 1491.

Table II**Summary of Batch Growth Experiments**

(all experiments on 1 gm/l glucose at 30 °C)

Table IIa.		μ_{\max} vs. pH with no pH control					
		<i>initial pH</i>					
		4.0	4.5	5.0	5.5	6.0	6.5
<i>E.coli</i>		0	$0.3 \pm .1 \ddagger$	$0.55 \pm .1$	$0.51 \pm .05$	$0.57 \pm .01$	$0.50 \pm .05$
<i>S.cer.</i>		$0.40 \pm .01$	$0.41 \pm .01$	$0.40 \pm .01$	$0.42 \pm .01$	$0.39 \pm .01$	$0.38 \pm .02$
		\ddagger standard deviation among four flasks					

Table IIb		μ_{\max} with pH control			
	<i>Conditions</i>			<i>Growth Rates (hr⁻¹)</i>	
	<i>Phthalic buffer</i>	<i>Stepwise Base Addition</i>	<i>pH</i>	μ_{\max}	μ on EtOH produced
<i>E.coli</i>	no	yes	5.0	$0.48 \pm .05$	-
<i>S.cer.</i>	$10^{-3}M$	yes	5.0	$0.31 \pm .05$	0.10
<i>E.coli</i>	$10^{-3}M$	yes	4.5	$0.18 \pm .05$	-
<i>E.coli</i>	$10^{-2}M$	yes	4.5	$0.31 \pm .02$	-
<i>S.cer.</i>	$10^{-2}M$	yes	4.5	$0.42 \pm .03$	0.14

Table IIc		Growth of <i>S. cerevisiae</i>			
		on glucose with Acetic Acid inhibition			
<i>Conditions</i>		<i>(pH4.5, 10⁻²M buffer, base add.)</i>			
<i>Acetic acid</i>	<i>(gm./l)</i>	<i>0.01</i>	<i>0.05</i>	<i>0.20</i>	<i>0.50</i>
μ_{\max}	<i>(hr⁻¹)</i>	<i>0.40</i>	<i>0.42</i>	<i>0.41</i>	<i>0.41</i>

Table II d		Growth of <i>E. coli</i>		
		on glucose with Ethanol inhibition		
<i>Conditions</i>		<i>(pH4.5, 10⁻²M buffer, base add.)</i>		
<i>Ethanol</i>	<i>(gm./l)</i>	<i>0.05</i>	<i>0.20</i>	<i>0.50</i>
μ_{\max}	<i>(hr⁻¹)</i>	<i>0.29</i>	<i>0.25</i>	<i>0.10</i>

Table III**Summary of Steady States from Continuous Experiments**

(all experiments on 1 gm/l glucose at 30 °C)

Table IIIa. Steady States of <i>S. cerevisiae</i>				
	averaged values	pH 4.5		
	D	Biomass	Glucose	EtOH
	(hr ⁻¹)	Abs(660nm)	mg/l	mg/l
Run # 3		washout		
Run # 4	0.11	0.492	18.	2
Run # 7	0.08	0.464	35.	4
Run # 8	0.15	0.431	35.	2
Run # 9	0.18	0.475	22.	2
	0.33	0.344	38.	0.014
	averaged values		pH 4.3	
Run # 11	0.42	0.115	500.	108
Run # 12	0.14	0.430	36.	2

Table IIIb. Steady States of E. coli			
	averaged values	pH 4.5	
	D	Biomass	Glucose
	(hr ⁻¹)	Abs(660nm)	mg/l
Run #4	0.16	0.501	6.0
Run #5	0.21	0.466	8.
Run #6	0.26	0.493	8.
Run #7	0.08	0.446	8.
	0.24	0.531	10.
Run #10	0.33	0.528	4.

List of Figure Captions

Figure 1a. Typical Batch Run of *E. coli* - $\ln(\text{Abs})$ and Acetate

Figure 1b. Typical Batch Run of *S. cerevisiae* - $\ln(\text{Abs})$ and EtOH

Figure 2. Mixed Continuous Culture of *E. coli* and *S. cerevisiae* at pH 4.3 and various D.

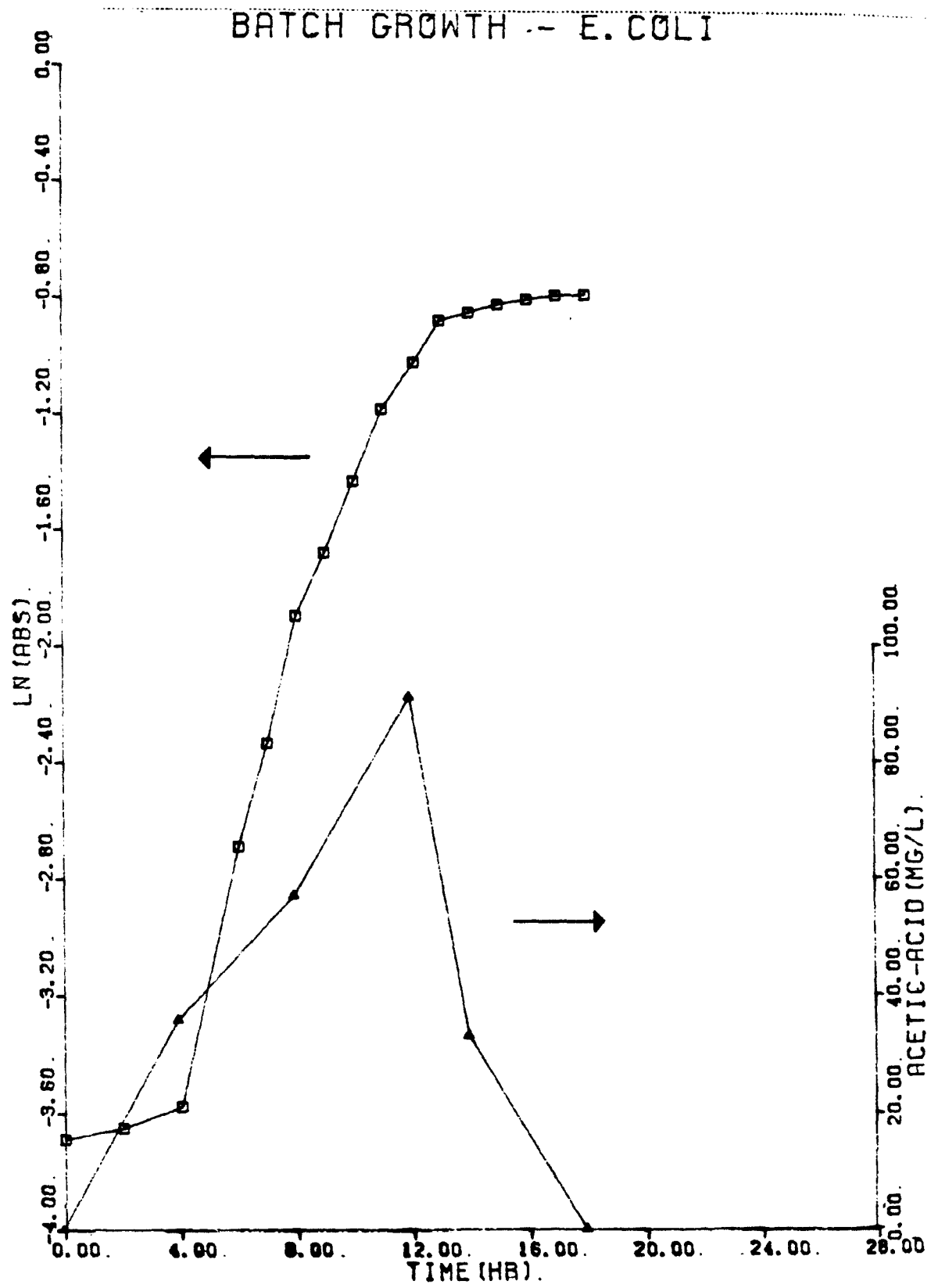


Figure 1a.

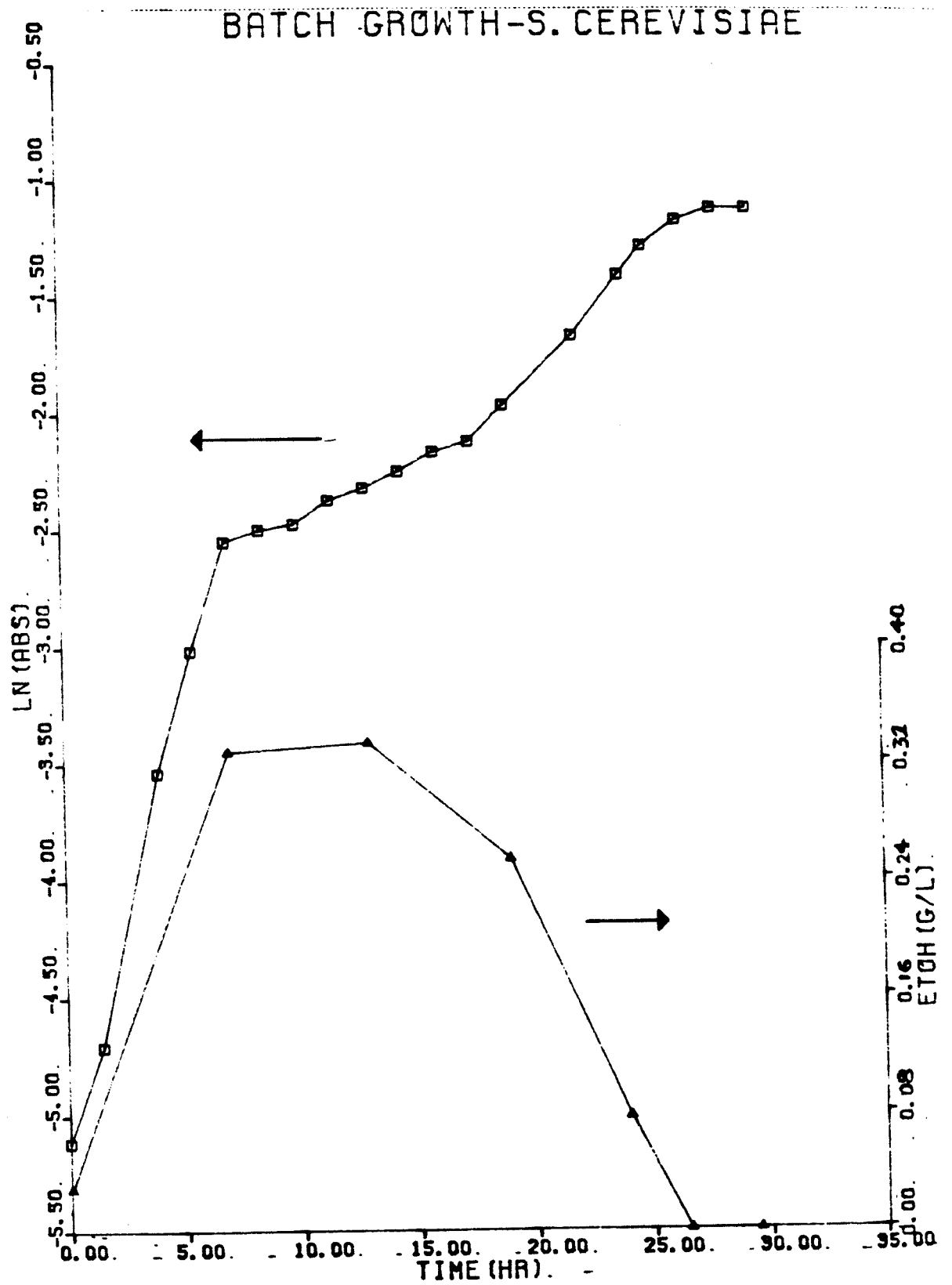


Figure 1b.

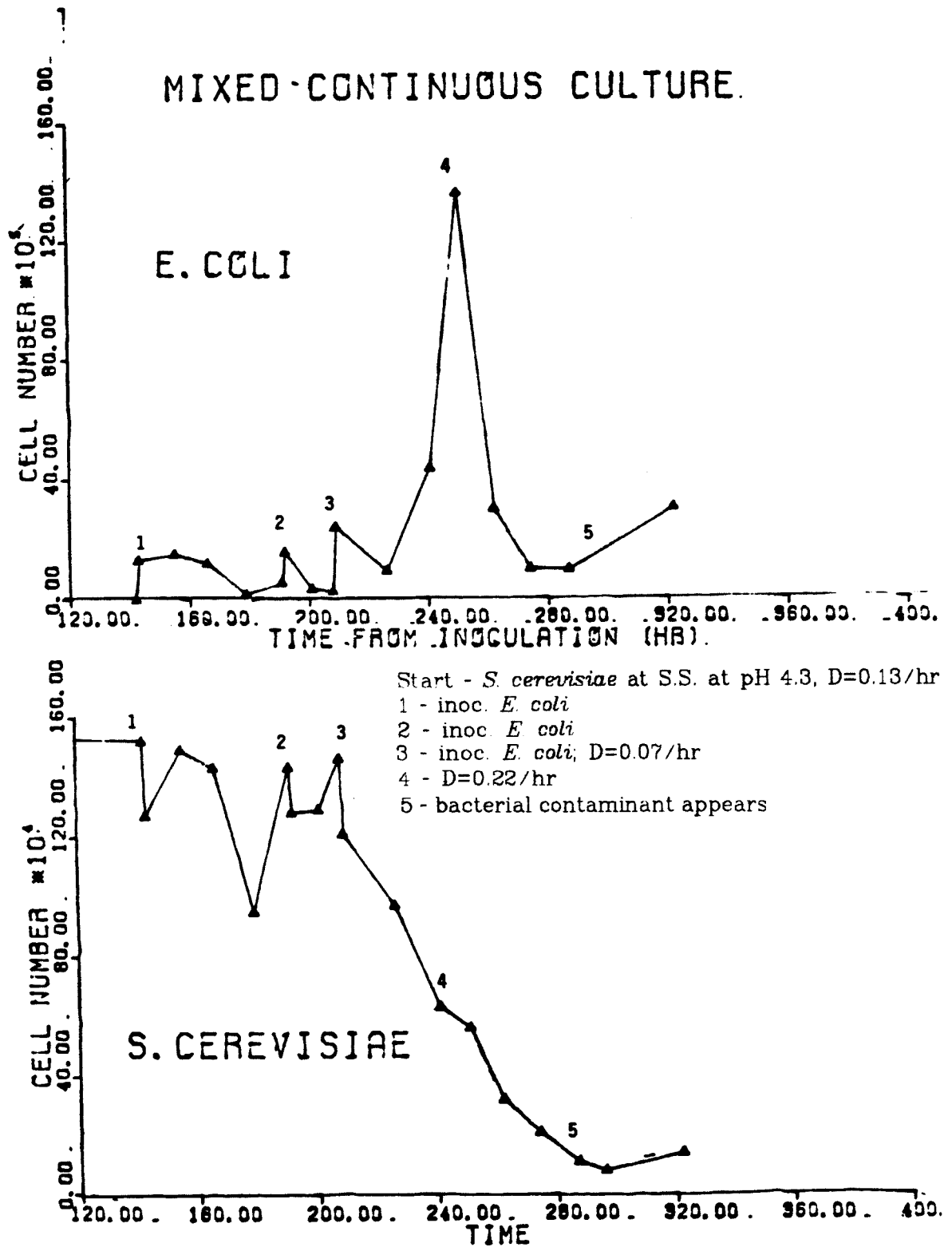


Figure 2.

Chapter 7.

Conclusions and Future Work

Conclusions

1. A mixed culture of *E. coli* and *S. cerevisiae*, that was unstable during pure competition under constant well-mixed conditions as expressed in the Competitive Exclusion Principle, was made to persist indefinitely by the use of time-varying conditions (such as pH oscillations), or the addition of other interactions (such as inhibition), or the design of spatially nonuniform reactors (such as the side-arm settler).
2. pH oscillations can allow a stable coexistent cycle.
3. Temporal variations are a possible explanation for microbial diversity in the environment.
4. Some mixed cultures may be stabilized by temporal variations.
5. Inhibition effects can cause stable coexistence under constant conditions.
6. Stability of inhibition/competition systems can be predicted from pure culture data.
7. Enhanced sedimentation can be used successfully for cell recycle with a chemostat for high density, high flow fermentations with observed productivities up to 11 g ethanol/l-hr.
8. Size selective cell recycle by enhanced sedimentation can allow coexistence of yeast with the faster growing bacteria. This stability can be explained by the demonstrated continued growth of yeast in the side arm settler.
9. A well-defined mixed culture can be used to predict, test and explain stability and coexistence for interactions using pure culture data.

Future Work

1. Acetate inhibition at low pH and not at pH 7 may be governed by the appearance of the protonated form, HAc, since the pK_a is 4.7. This could be tested by determining K^I at various pH and comparing to the amounts of Ac^- and HAc.
2. The transient response to pH shock can be modeled and measured to study the dynamics of adaptation to new environments.
3. More optimization of the side-arm settler-fermenter should be performed both in design (notably baffles to prevent air from entering the fermentor) and in operating conditions.
4. The settler could be used at high efficiency and high flow to examine *in vivo* the limits to the ethanol product rate in *S. cerevisiae*.
5. Since plasmid free cells grow faster, examination of differences between plasmid expressing cells and plasmid-free revertants of both yeast and *E. coli* may find conditions using temporal variations or size segregation that may allow persistence of the plasmid in continuous culture.

Appendix A - Coulter Counter Programs and Calibration Equations

A very useful summary of the theory and operation of the Coulter Counter with a multichannel analyzer (MCA) can be found in **Coagulation in Continuous Particle Size Distributions: Theory and Experiments**, Appendix B, PhD. thesis by James Hunt (C.I.T., 1980).

Calibration Equations (from Hunt, 1980)

The first step in calibration is to determine the log base, b , of the electronic system. The voltage jump is proportional to the particle volume, d_p^3 . $i = \log_b d_i^3 + \text{constant}$ for a particle with diameter d_i appearing in the MCA channel i . With two particles of d_i and d_j in channels i and j , respectively, the constant is eliminated and

$$b = \left(\frac{d_i}{d_j} \right)^{3/(i-j)}.$$

For this system $b=1.04$. With a known b and a known calibration particle of diameter d_c in channel c , any other particle in channel i can be evaluated by

$$d_i = d_c b^{(i-c/3)}.$$

Calibration particles from Duke Scientific were used.

Computer Programs for Particle Size Analysis

The pertinent Pascal programs and their functions are listed below:

1. COULTER.PAS - transfer of data from MCA to computer, in essence COULTER tells the CP/M computer how to act like a teletype. Representative data files are also included.
2. COULPLOT.PAS - plotting routine for the Baush and Lomb #dmp-29.
3. BRIAN.PAS - a counting program, BRIAN will subtract one data file (say the background) from another and then will sum all counts between any two designated channels.

The programs follow.

```

(
    A) TYPE COULTER.PAS
(
    PROGRAM COULTER;
(
    {COULTER -- reads in the data inputted from the coulter counter}
    {
        and dumps it into a file with the time and date.
    }

(
    CONST      B_STATUS = $22;    {status port of Serial B}
               B_DATA = $23;    { data port of Serial B}

(
               TxRDY = 7;        {transmitter end of character bit}
               RxRDY = 6;        {output data available bit}

(
               BELL = $07;

(
    TYPE      FILE_NAME = STRING;

(
               TIME_OF_DAY = RECORD
(
                   YEAR : 1982..2000;
                   MONTH : 1..12;
                   DAY : 1..31;
                   HOUR : 0..23;
                   MINUTE : 0..59;
                   SECOND : 0..59;
                   END;

(
               MONTH_NAME = ARRAY[1..12] OF STRING[11];

(
    VAR      F : TEXT;
            F_NAME : FILE_NAME;
            F_RESULT : INTEGER;
            TIME : TIME_OF_DAY;
            M_NAME : ^MONTH_NAME;
            IN_CHAR : CHAR;
            RCV_CHAR : CHAR;
            CH : CHAR;
            I, J : INTEGER;
            DATA_SET : ARRAY[1..1025] OF CHAR;

(
            {**** found in CRT2.ERL ****}
(
            EXTERNAL PROCEDURE CONOUT(OUTCHAR : CHAR);

(
            {**** found in LAB.ERL ****}
(
            EXTERNAL PROCEDURE READ_CLOCK(VAR NOW : TIME_OF_DAY);

(
    PROCEDURE MONTHS;
    BEGIN {Months of the year}
    INLINE ($09 / ' JANUARY ' /
(
        $0A / ' FEBRUARY ' /
(
        $07 / ' MARCH ' /
(
        $07 / ' APRIL ' /
(
        $05 / ' MAY ' /
(
        $06 / ' JUNE ' /
(
        $06 / ' JULY ' /
(
        $08 / ' AUGUST ' /
(
        $0B / ' SEPTEMBER ' /
(
        $09 / ' OCTOBER ' /
(
        $0A / ' NOVEMBER ' /
(
        $0A / ' DECEMBER ' )

```

```

END;

(
FUNCTION GETC : CHAR;
BEGIN
  REPEAT UNTIL TSTBIT(INP[B_STATUS],R×RDY);
  GETC:=CHR(INP[B_DATA] & $7F)
END;

(
BEGIN
  M_NAME:=ADDR(MONTHS);
  REPEAT
    WRITELN;
    WRITE('Enter the name of data file to be sent: ');
    READLN(F_NAME);  WRITELN;
    ASSIGN(F,F_NAME);
    REWRITE(F);
    IF IORESULT=255 THEN
      WRITELN('**** Error creating ',F_NAME,
              ' -- Disk directory probably full')
  UNTIL IORESULT<>255;

  WRITELN;
  WRITELN('Turn dial to READOUT on the Multi-Channel Analyzer.');
```

WRITELN(CHR(BELL));

```

  FOR I:=1 TO 1025 DO
    BEGIN
      CH:=GETC;
      IF (CH=CHR($7F)) OR (CH=CHR($00)) THEN    {convert DEL & NUL characters}
        CH:=' ';                                {to spaces}
      DATA_SET[I]:=CH
    END;

    {write out the time and the data set to disk}
    READ_CLOCK(TIME);
    WITH TIME DO
      BEGIN
        WRITE(F,' ':14,'The date is : ');
        WRITE(F, DAY:2, M_NAME^[MONTH], YEAR:4);
        WRITE(F,' ':5, HOUR:2, ':');
        IF MINUTE <= 9 THEN
          WRITE(F,'0', MINUTE:1, ':');
        ELSE WRITE(F, MINUTE:2, ':');
        IF SECOND <= 9 THEN
          WRITELN(F,'0', SECOND:1)
        ELSE WRITELN(F, SECOND:2);
      END;

  FOR J:=1 TO 1025 DO
    BEGIN
      WRITE(F, DATA_SET[I]);
      WRITE( DATA_SET[I])
    END;

  WRITELN(F);
  CLOSE(F,F_RESULT);
  IF IORESULT=255 THEN
    WRITELN('**** Error creating ',F_NAME,' -- Disk probably full');
  WRITE(CHR(BELL))
END.

```

A>TYPE A23C.DAT

The date is 23/ 4/83 3:36:13

000000	000000	000000	000000	000011	010810	010899	010713	010238	003921
009322	008423	007886	006893	006219	005375	004811	003915	003324	002821
002180	001808	001376	001035	000884	000696	000562	000484	000403	000304
000326	000267	000261	000262	000228	000290	000247	000267	000258	000295
000283	000326	000321	000388	000410	000446	000489	000525	000575	000631
000648	000707	000741	000769	000772	000790	000770	000773	000733	000726
000662	000672	000631	000573	000527	000472	000439	000408	000392	000355
000353	000296	000268	000247	000192	000204	000163	000185	000154	000131
000122	000130	000106	000094	000096	000096	000073	000099	000069	000061
000060	000070	000055	000059	000063	000051	000059	000061	000041	000035
000042	000029	000027	000033	000028	000031	000030	000020	000032	000044
000014	000020	000018	000015	000015	000015	000018	000021	000009	000018
000020	000015	000014	000008	000013	000010	000013	000011		

A>TYPE A24B.DAT

The date is 24/ 4/83 3:26:47

000000	000000	000000	000000	000042	016509	016749	016823	016290	015737
014929	013828	012650	011723	010529	009191	007952	006817	005621	004773
003893	003062	002302	001733	001371	000983	000764	000535	000381	000232
000204	000202	000152	000137	000132	000123	000128	000100	000112	000092
000108	000103	000113	000115	000126	000125	000147	000148	000174	000162
000154	000162	000155	000178	000155	000178	000163	000156	000167	000174
000147	000151	000152	000151	000137	000160	000201	000177	000200	000176
000205	000226	000202	000196	000186	000197	000176	000183	000179	000186
000175	000157	000157	000153	000126	000124	000125	000093	000093	000059
000289	000078	000058	000050	000058	000042	000034	000028	000025	000017
000016	000014	000018	000015	000010	000015	000015	000011	000014	000009
000007	000008	000008	000012	000005	000007	000009	000009	000009	000001
000002	000005	000006	000006	000004	000006	000005	000002		

A>TYPE A28E.DAT

The date is 28/ 4/83 8:33:59

000000	000000	000000	000000	000052	016862	016765	016358	015820	015267
014145	013301	012016	010779	009558	008621	007312	006052	005013	004054
003173	002530	001941	001388	001061	000717	000537	000397	000238	000043
000175	000138	000128	000134	000105	000089	000084	000078	000069	000070
000096	000100	000107	000087	000094	000118	000112	000109	000113	000147
000127	000163	000160	000182	000187	000201	000211	000232	000246	000210
000243	000246	000214	000239	000236	000246	000256	000212	000234	000221
000212	000211	000227	000226	000232	000213	000214	000234	000239	000242
000228	000269	000279	000260	000253	000284	000263	000297	000260	000263
000281	000263	000260	000237	000242	000250	000228	000180	000182	000172
000159	000158	000149	000139	000116	000097	000095	000080	000064	000061
000043	000054	000051	000033	000052	000027	000026	000026	000025	000026
000021	000013	000010	000012	000014	000015	000012	000011		

```

( A) TYP. CO ULPLOT .PAS
( COULPLOT.PAS
( PROGRAM BRIAN;
( { $I PLOTLIB.TYP }
(
( VAR PLOT_RES : RESOLUTION;
( I : INTEGER;
( IDRESULT : INTEGER;
( NOTRERUN : BOOLEAN;
( PLOTITLE : BOOLEAN;
( TITLE : STRING;
( INFILE : TEXT;
( F_NAME : STRING;
( X_LABEL : STRING;
( Y_LABEL : STRING;
( ANSWER : STRING;
( PLOTAXIS : BOOLEAN;
( AUTO : BOOLEAN;
( RECTANGLE : BOOLEAN;
( RIGHTAXIS : BOOLEAN;
( COUNT : INTEGER;
( X, Y : R_VECTOR;
( X_SCALE : REAL;
( Y_SCALE : REAL;
( X_MAX : REAL;
( Y_MAX : REAL;
( YYMAX, XXMAX : REAL;
( FACTOR : REAL;
( DUMMY : REAL;
( YDIV : REAL;
( CHAR_SCALE : STRING;
( CHARI : CHAR;
( TITLE_LENGTH : REAL;
( TITLE_START : REAL;
(
( { $I PLOTLIB.EXT }
(
( PROCEDURE ASK_QUESTION;
( BEGIN
( WRITE('Input the data file to be plotted : ');
( READLN(F_NAME);
( WRITELN(' WANT TO PLOT AXIS-- YES OR NO');
( READLN(ANSWER);
( PLOTAXIS:=FALSE;
( IF (ANSWER = 'YES') THEN PLOTAXIS:=TRUE;
( IF (PLOTAXIS) THEN
( BEGIN
( RIGHTAXIS:=FALSE;
( WRITELN(' WANT TO PUT Y-AXIS ON LEFT HAND SIDE?');
( READLN(ANSWER);
( IF (ANSWER='NO') THEN RIGHTAXIS:=TRUE;
( WRITELN(' INPUT LABEL FOR Y_AXIS');
( READLN(Y_LABEL);
( IF (NOT RIGHTAXIS) THEN
( BEGIN
( WRITELN(' INPUT LABEL FOR X_AXIS');
( READLN(X_LABEL);
( RECTANGLE:=FALSE;
( WRITELN(' WANT TO PLOT A RECTANGULAR BOX?');
( READLN(ANSWER);
( IF (ANSWER='YES') THEN RECTANGLE:=TRUE
( END;
(
( END;

```

```

      END;
      PLOTITLE:=FALSE;
      WRITELN(' WANT TO PLOT TITLE? IF YES THEN PUT IN PEN #3');
      READLN(ANSWER);
      IF ( ANSWER ='YES') THEN PLOTITLE:=TRUE;
      IF (PLOTITLE) THEN
        BEGIN
          WRITELN(' INPUT TITLE OF PLOT');
          READLN(TITLE)
        END;
      AUTO:=FALSE;
      WRITELN('DO YOU DESIRE AUTOSCALING BY THE PROGRAM?');
      READLN(ANSWER);
      IF (ANSWER = 'YES') THEN AUTO:=TRUE;
      IF ( NOT AUTO) THEN
        BEGIN
          WRITELN(' INPUT X_MAX');
          READLN(X_MAX);
          WRITELN(' INPUT Y_MAX');
          READLN(Y_MAX);
          WRITELN(' INPUT SHRINKING_FACTOR');
          READLN(FACTOR)
        END;
      END;

      PROCEDURE AUTOSCALE;
      VAR
        X1,X2 : REAL;
        XFACT : REAL;
        I,J : INTEGER;
        DUMMY : REAL;
      BEGIN
        X1:=YYMAX;
        WRITELN(' THE MAXIMUM VALUE FOR Y IS ',YYMAX);
        XFACT:=1.0;
        I:=0;
        WHILE (X1 > 10.0) DO
          BEGIN
            I:=I+1;
            XFACT:=XFACT*10.0;
            X1:=X1/10.0
          END;
        CHARI:=CHR(ORD('0')+I);
        YYMAX:=ROUND(X1+0.5);
        IF ( (X1/YYMAX) < 0.7) THEN
          BEGIN
            DUMMY:=TRUNC(X1);
            DUMMY:=(X1-DUMMY)*10;
            DUMMY:=(ROUND(DUMMY+0.5))*0.1;
            YYMAX:=(TRUNC(X1))+DUMMY
          END;
        Y_MAX:=XFACT;
        FACTOR:=Y_MAX;
        WRITELN(' SCALE FACTOR IS ', Y_MAX);
        X_MAX:=128
      END;

      BEGIN
        REPEAT
          ASK_QUESTION;
          ASSIGN(INFILE,F_NAME);
          RESET(INFILE);

          READLN(INFILE);
          READLN(INFILE);

```

```

YYMAX:=0.0;

FOR I:=1 TO 128 DO
  BEGIN
    READ(INFILE,COUNT);
    X[I]:=I;
    Y[I]:=COUNT;
    DUMMY:=COUNT;
    IF ( YYMAX ( DUMMY) THEN YYMAX:=DUMMY
  END;

IF (AUTO) THEN AUTOSCALE;
X_SCALE:= 11.0/X_MAX;      {scaling for the plot}
Y_SCALE:= 7.0/(Y_MAX*YYMAX);

FOR I:=1 TO 128 DO
  BEGIN
    X[I]:=X[I]*X_SCALE;
    Y[I]:=Y[I]*Y_SCALE
  END;

PLOT_RES:=LOW_RES;
PLOT_BEGIN(LARGE);

PEN_SPEED(2); {4 inches/second}
WHILE (PLOTAXIS) DO
  BEGIN
    PLOTAXIS:=FALSE;
    YDIV:=YYMAX/5;
    IF (RIGHTAXIS) THEN
      BEGIN
        AXIS(12.0,1.0,
              7.0,90,
              0.0,YYMAX,YDIV,
              Y_LABEL ,LABEL_BELOW);
        PLOT(11.86,7.4,UP);
        PLOT_STRING('X 10',90,0.105);
        PLOT(11.75,7.8,UP);
        CHAR_SCALE:=CONCAT(' ',CHAR1);
        PLOT_STRING(CHAR_SCALE,90,0.105);
        PLOT(1.0,8.0,UP);
        PLOT(12.0,8.0,DOWN);
        PLOT(1.0,1.0,UP)
      END
    ELSE
      BEGIN
        AXIS(1.0,1.0,
              7.0,90,
              0.0,YYMAX,YDIV,
              Y_LABEL ,LABEL_ABOVE);
        PLOT(1.25,7.4,UP);
        PLOT_STRING('X 10',90,0.105);
        PLOT(1.14,7.8,UP);
        CHAR_SCALE:=CONCAT(' ',CHAR1);
        PLOT_STRING(CHAR_SCALE,90,0.105)
      END;

    IF (NOT RIGHTAXIS) THEN
      AXIS(1.0,1.0,
            11.0,0,
            0.0,X_MAX,20.0,
            X_LABEL ,LABEL_BELOW);
    IF (RECTANGLE) THEN
      BEGIN
        PLOT(1.0,8.0,UP);
        PLOT(12.0,8.0,DOWN);

```

```

        PLOT(12.0, 1.0, DOWN);
        PLOT(1.0, 1.0, UP)
    END;

    END;

    PEN_SPEED(4); {16 inches/second}
    NEW_PEN(2);
    PLOT(1.0, 1.0, RE_ORIGIN);
    LINE(128, X, Y, SOLID, POINT);

    IF (PLOTITLE) THEN
        BEGIN
            NEW_PEN(3);
            TITLE_LENGTH:=(7/8)*0.28*(LENGTH(TITLE));
            TITLE_START:=(11.0-TITLE_LENGTH)/2.0+1.0;
            PLOT(TITLE_START, 7.50, UP);
            PLOT_STRING(TITLE, 0, 0.28)
        END;
    PLOT_FINISHED;

    WRITELN(' Want to repeat the plotting program?');
    READLN(ANSWER);
    NOTRERUN:=FALSE;
    IF ( ANSWER = 'NO') THEN NOTRERUN:=TRUE;
    UNTIL ( NOTRERUN );
END.

```


A) TYPE BRIAN.PAS

PROGRAM BRIAN;

```

VAR   IORESULT : INTEGER;
      IO1, IO2, IO3, IO4 : INTEGER;
      INFILE, INFILE2 : TEXT;
      RESULT : TEXT;
      SUMFILE : TEXT;
      SUMNAME : STRING;
      RESULT_FILE : STRING;
      FILE1, FILE2 : STRING;
      UPPERBOUND : INTEGER;
      LOWERBOUND : INTEGER;
      A, B, C : INTEGER;
      ANSWER : STRING;
      BACK : BOOLEAN;
      SUM : REAL;
      CORR : REAL;
      LOOP : BOOLEAN;
      I, J, K : INTEGER;
      NUMBER : INTEGER;

```

```

BEGIN
  WRITELN(' WANT TO SUBTRACT DATA FILE FROM BACKGROUND?');
  READLN(ANSWER);
  BACK:=FALSE;
  IF ( ANSWER ='YES') THEN BACK:=TRUE;
  IF (BACK) THEN
    BEGIN
      WRITELN(' INPUT DATA FILE');
      READLN(FILE1);
      WRITELN(' INPUT FILENAME FOR BACKGROUND');
      READLN(FILE2);
      WRITELN(' INPUT FILENAME FOR RESULT');
      READLN(RESULT_FILE);
      ASSIGN(RESULT, RESULT_FILE);
      REWRITE(RESULT);
      ASSIGN(INFILE2, FILE2);
      RESET(INFILE2);
      READLN(INFILE2);
      READLN(INFILE2);
      WRITELN(RESULT);
      WRITELN(RESULT);

      ASSIGN(INFILE, FILE1);
      RESET(INFILE);
      READLN(INFILE);
      READLN(INFILE);
    END;

```

NUMBER:=0;

```

IF (BACK) THEN
  BEGIN
    FOR I:=1 TO 128 DO
      BEGIN
        READ(INFILE, A);
        READ(INFILE2, B);

```

```

C      C:=A-B;
      IF ( C < 0 ) THEN C:=0;
      NUMBER:=NUMBER+1;
      WRITE (RESULT, C:8);
C      IF (NUMBER > 9) THEN
      BEGIN
C          WRITELN(result);
          NUMBER:=0
      END;
      END;
C      CLOSE (RESULT, IORESULT);
      CLOSE (INFILE, IO1);
      CLOSE (INFILE2, IO2);
C      END;
      WRITELN(' DO YOU WANT TO SUM BETWEEN TWO BOUND?');
      READLN(ANSWER);
      LOOP:=FALSE;
      IF ( ANSWER='YES' ) THEN LOOP:=TRUE;
      IF (LOOP) THEN
C          BEGIN
          WRITELN(' INPUT DATA FILE TO BE SUMMED');
          READLN(SUMNAME);
          ASSIGN(SUMFILE, SUMNAME);
          RESET(SUMFILE);
          READLN(SUMFILE);
          READLN(SUMFILE);
          WRITELN(' INPUT LOWER AND UPPER BOUND');
          READLN(LOWERBOUND, UPPERBOUND);
          LOWERBOUND:=LOWERBOUND-1;
          UPPERBOUND:=UPPERBOUND-1;
          SUM:=0;
          FOR I:=1 TO LOWERBOUND DO
              BEGIN
                  READ(SUMFILE, J)
              END;
          FOR K:=LOWERBOUND TO UPPERBOUND DO
              BEGIN
                  READ(SUMFILE, J);
                  IF ( J > 1000 ) THEN
                      BEGIN
                          CORR:=25*(J/1000)*(J/1000)/8;
                          CORR:=CORR+J
                      END
                  ELSE CORR:=J;
                  SUM:=SUM+CORR
              END;
          WRITELN(' THE TOTAL SUM IS ', SUM)
      END;
      END.

```

Appendix B

Floquet Analysis

This is a brief summary of the basic theory and equations. Suppose the dynamics of the system are described by the nonlinear vector equation:

$$\frac{d\mathbf{w}(t)}{dt} = \mathbf{h}(\mathbf{w}(t), u(t))$$

where $\mathbf{w}(t)$ is the state vector and $u(t)$ describes the periodic inputs to the system. $u(t)$ has a period τ .

Let $\mathbf{w}^*(t)$ denote a forced τ -periodic solution to the differential equation for an input $u^*(t)$. The Jacobian matrix along the solution is $\mathbf{J}(t)$:

$$\mathbf{J}(t) = \frac{\partial \mathbf{h}(\mathbf{w}^*(t), u(t))}{\partial \mathbf{w}}$$

Then, from Floquet theory, the periodic solution will be stable with regard to small perturbations if all the eigenvalues of $\mathbf{P}(\tau)$ have moduli less than unity; where the matrix $\mathbf{P}(\tau)$ is the solution to the initial value problem:

$$\frac{d\mathbf{P}(t)}{dt} = \mathbf{J}(t) \mathbf{P}(t)$$

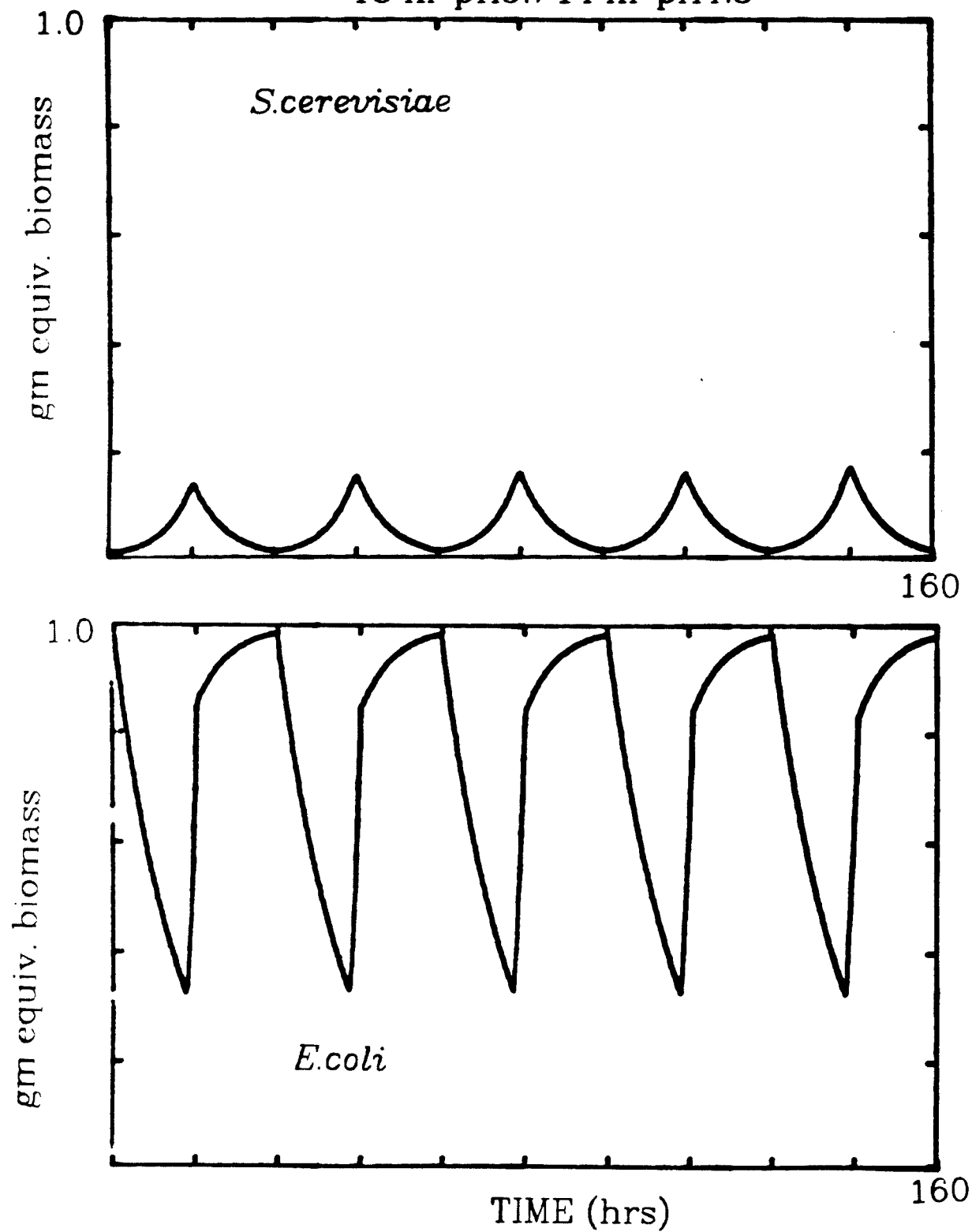
$$\mathbf{P}(t=0) = \mathbf{I}$$

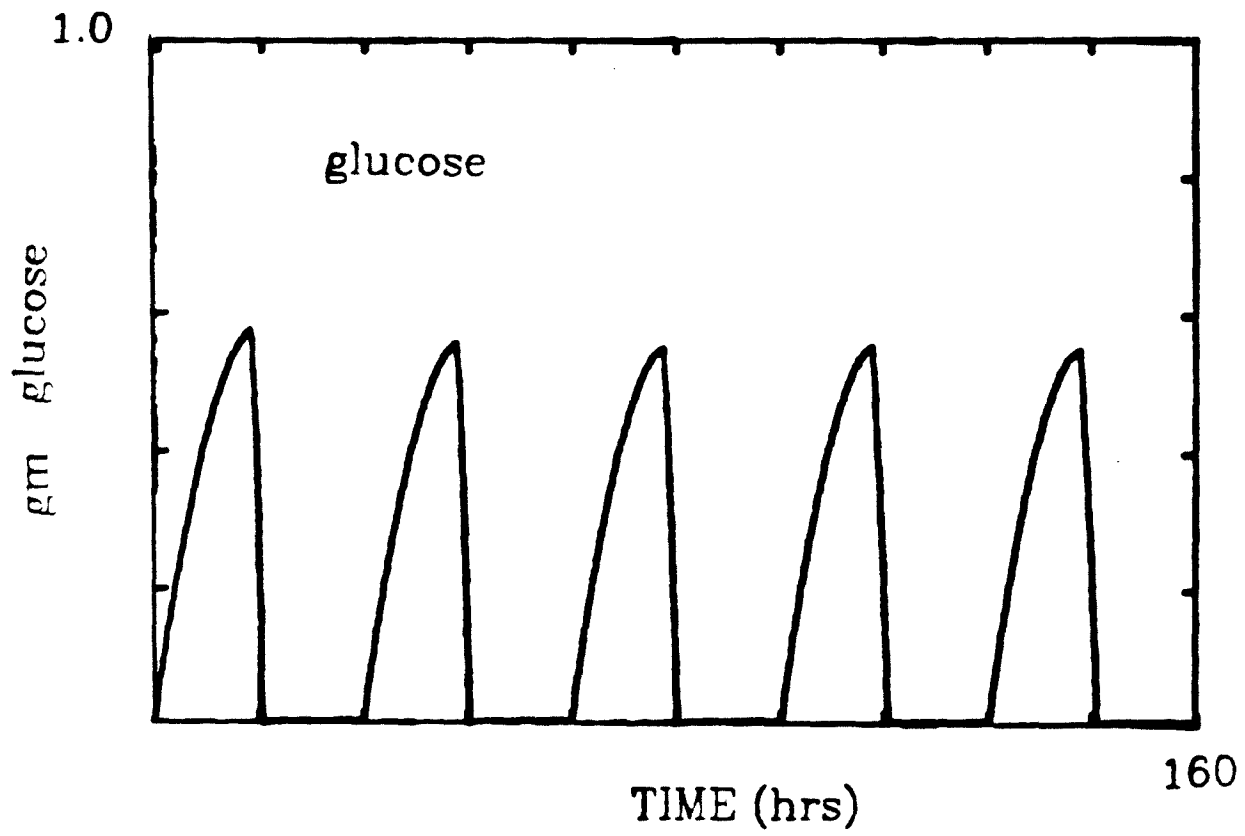
where \mathbf{I} is the identity matrix.

Appendix C

pH Oscillations Computer Simulation

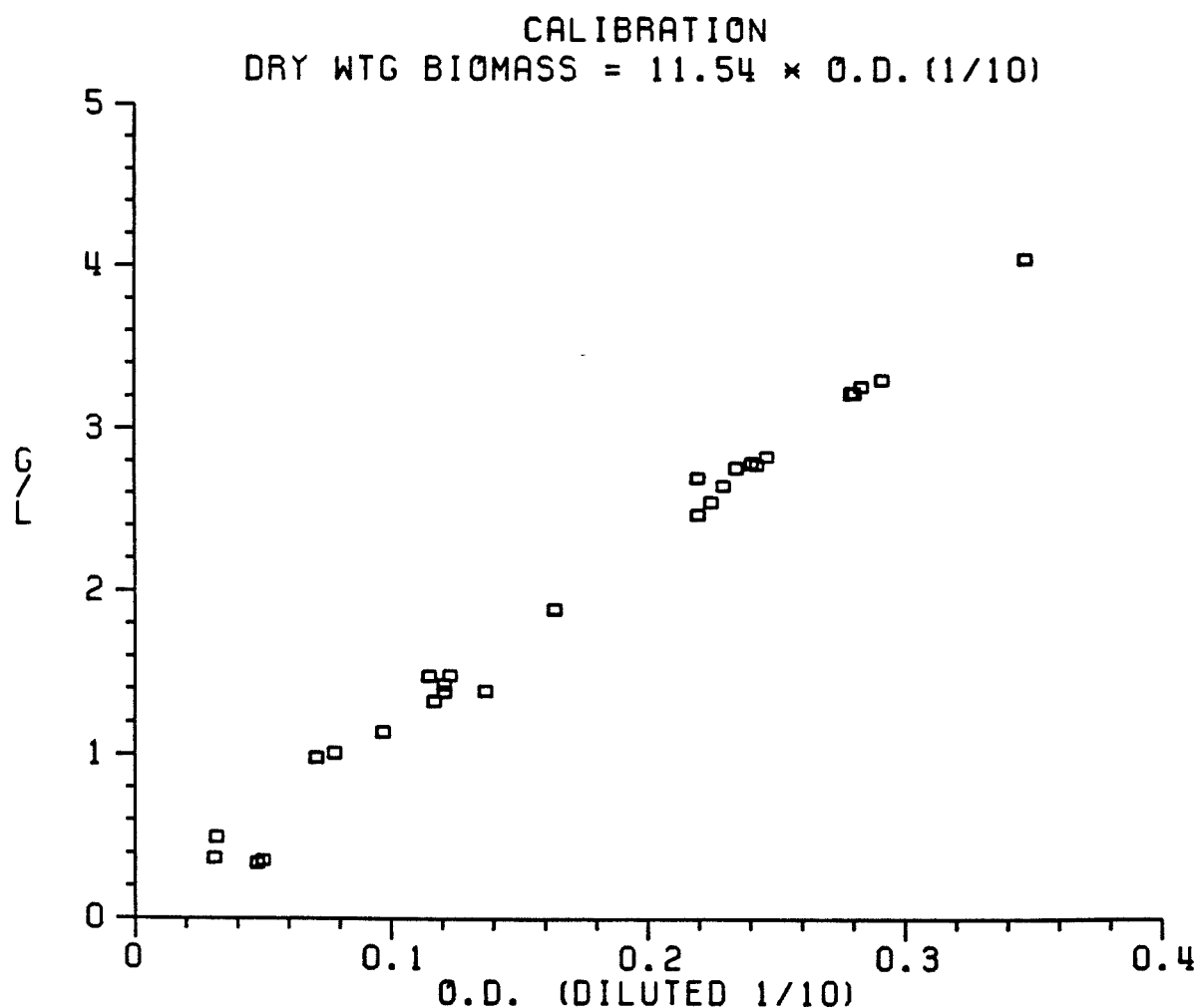
18 hr pH5./14 hr pH4.3





Appendix D

A calibration was made from the many Dry Weight measurements taken in Chapter 5. At each Dry Wtg. sample the Optical Density, diluted ten-fold, was measured at $\lambda = 660$ nm on a B&L Spectrophotometer. The data is plotted below and yield a straight line through the origin with a slope of 11.54. Then for *S. cerevisiae* throughout this thesis, g Dry Wtg./l = $11.54 \times \text{O.D.}$



Appendix E

The length of the clarified zone in a continuous enhanced sedimentation settler, such as used in Chapters 4 and 5, is a function of flowrate. The figure below, constructed from data taken during the determination of $f(x_m, Q_p)$ in Chapter 5, shows that the length z is linear in Q_p . It is possible to extrapolate that for clarification in this settler, the maximum possible flowrate is 128 ml/hr. In addition it was observed that z was independent of the biomass concentration from zero to 5 g D.W./l.

